Determining the effects of Pab1 acetylation at K131 on stress granule dynamics in *Saccharomyces cerevisiae*

Sangavi Sivananthan

Thesis submitted to the University of Ottawa in partial fulfillment of the requirements for the MSc degree in Biochemistry

MSc. Biochemistry specializing in Human and Molecular Genetics

Department of Biochemistry, Microbiology, and Immunology
Faculty of Medicine
University of Ottawa

Abstract

Under environmental stress, such as glucose deprivation, cells form stress granules - the accumulation of cytoplasmic aggregates of repressed translational initiation complexes, proteins, and stalled mRNAs. Recent research implicates stress granules in various diseases, such as neurodegenerative disease, but the exact regulators responsible for the assembly and disassembly of stress granules are unknown. Studies detect post-translational modifications on core stress granule proteins. One modification is lysine acetylation, in which a substrate is regulated by a lysine acetyltransferase (KAT) and lysine deacetylase (KDAC). My project deciphers the impact of lysine acetylation on an essential protein found in stress granules, poly(A) binding protein (Pab1) in *Saccharomyces cerevisiae*. In this work, I demonstrated that acetylation mimic of Pab1-K131 reduces stress granule formation upon glucose deprivation, and other stressors such as ethanol, raffinose, and vanillin. A potential KDAC that might be facilitating this role is Rpd3. Further, electromobility shift assay studies suggest that acetylation mimic of Pab1-K131 negatively impacts poly(A) RNA binding. This work will be useful when exploring therapeutic options when combating diseases linked to stress granules.

Acknowledgements

I would like to thank my supervisor, Dr. Kristin Baetz, for giving me the opportunity to work on this project in her lab. Her continuous support in my MSc. studies, her patience, motivation, and immense knowledge made this project possible.

I would like to thank the former Research Associate, Dr. Sylvain Huard, who constantly showed guidance when I had any questions along the way.

I would like to thank our Post Doc, Dr. Jessica Gosse, who constantly showed guidance near the end of this project.

I would like to thank my Thesis Advisory Committee, Dr. Jocelyn Côté and Dr. Micheal Downey, for their continuous support and encouragement throughout the project. I offer sincere appreciation for the learning opportunities and troubleshooting any problems I may have faced.

I would like to thank all Baetz Lab members, Dr. Eugene Fletcher, Dr. Jessica Gosse, Elizabeth Walden, Sarah Laframboise, and Lauren Deneault who have not only given moral support, but also provided scientific support whenever needed.

Lastly, I would like to thank the funding resources to this project: Canadian Institute of Health Research (CIHR).

Table of Contents

Title Page	**i**
Abstract	**ii**
Acknowledgements	**iii**
Table of Contents	**iv**
List of Abbreviations	**vii**
List of Figures	**x**
1.0 Introduction	**1**
1.1 Stress Granule Formation	**2**
1.1a mRNA cycle –Stress Granules vs P-bodies.	**2**
1.2 Cellular Consequence of Stress Granule Formation	**5**
1.2a Stress Granules and Disease	**6**
1.3 Pab1 in Stress Granules	**7**
1.4 Regulation of Stress Granule Assembly and Disassembly	**8**
1.5 Lysine Acetylation	**9**
1.5a KAT and KDACs in Saccharomyces cerevisiae	**10**
1.5b Lysine Acetylation and Stress Granule Dynamics	**11**
1.6 Acetylation of Pab1	**12**
2.0 Materials and Methods	**15**
2.1 Yeast strains, plasmids, primers, and media	**15**
2.2 Strain growth and stress assessment	**15**
2.3 Fluorescence microscopy	**16**
2.4 Quantitative western blotting	**17**
2.5 Dot assays	**18**

2.6 Time course **18**

2.7 GST purification **19**

2.8 Affinity Purification **21**

2.9 Electrophoretic mobility shift assay **22**

3.0 Results **24**

3.1 Pab1-K131 mutation impacts glucose deprived stress granule formation **24**

3.2 Pab1-*K131 mutations do not impact protein levels* **26**

3.3 PAB1-K131Q impacts stress granule formation upon ethanol, raffinose, and vanillin **27**

3.4 Genetic screening identifies KAT/KDAC regulating Pab1 acetylation sites **30**

3.5 KDAC Rpd3 mutant impacts glucose deprived stress granule formation **33**

3.6 Purification of Pab1 RRM1-RRM2 fragments **36**

3.7 Binding of eIF4G1-HA to Pab1 RRM1-RRM2 domain is not impacted by Pab1-K131 mutations **38**

3.8 Preliminary results suggest Pab1-K131Q RRM1-RRM2 reduces the binding to poly(A) mRNA **41**

4.0 Discussion **44**

4.1 Acetylation mimic of PAB1-K131Q-GFP reduces stress granule formation of a subset of environmental stresses. **44**

4.2 Identification of KAT/KDACs impact stress granule formation upon acetylation mimic. **45**

4.3 Molecular mechanisms of Pab1-K131 acetylation **47**

5.0 Conclusion **50**

6.0 References **51**

7.0 Contributors/Collaborators **64**

8.0 Appendices **65**

Supplemental Figure 1: Microscopy pictures of KAT/KDAC mutants upon glucose depleted conditions **65**

Supplemental Figure 2: *eaf1Δ* and *gcn5Δ* does not affect stress granule formation upon K131 acetylation **67**

Supplemental Figure 3: Co-immunoprecipitation's difficulty showing the binding of eIF4G1 to Pab1-K131 mutants **69**

Supplemental Figure 4: pGEX-4T-1 vector **71**

Supplemental Figure 5: Pab1 and mutants predicted protein structures **72**

Table 1: Strains used in this study **73**

Table 2: Plasmids used in this study **76**

Table 3: Oligonucleotides used in this study **77**

9.0 Curriculum Vitae **84**

List of Acronyms and Abbreviations

+ Glucose	Media containing glucose
- Glucose	Media without glucose
°C	Degree in Celsius
%	Percentage
AMP	Adenosine Monophosphate
BF	Bright Field
BSA	Bovine serum albumin
Co-IP	Co-immunoprecipitation
DNA	Deoxyribonucleic Acid
DTT	Dithiothreitol
E. coli	*Escherichia coli*
EDTA	Ethylenediaminetetraacetic acid
EGTA	Egtazic acid
EMSA	Electrophoretic mobility shift assay
g	Grams
G418	Kanamycin
GFP	Green Fluorescent Protein
GNAT	Gcn5 related N-acetyltransferase
h	Hours
HEPES	4-(2-hydroxyethyl)-1-piperazineethanesulfonic acid
HIS	Histidine
IPTG	Isopropyl ß-D-1-thiogalactopyranoside
KAT	Lysine Acetyltransferase
KCl	Potassium chloride
KDAC	Lysine Deacetylase
KH_2PO_4	Monopotassium phosphate
KOAc	Potassium acetate
mCHIP	Modified chromatin immunoprecipitation
$MgCl_2$	Magnesium chloride
MgOAc	Magnesium acetate
min	Minute
mL	Millilitre
mm	Millimetres

mM	Millimolar
M	Molar
mRNA	Messenger ribonucleic acid
NaCl	Sodium chloride
Na_2HPO_4	Disodium phosphate
NaOAc	Sodium acetate
nM	Nanomolar
nm	Nanometer
NP-40	Ethoxylated nonylphenol
OD_{600}	Optical Density at 600 mm
Pab1	Poly(A) Binding Protein 1
PCR	Polymerase chain reaction
PB	Processing Bodies
PBS	Phosphate buffered saline
PBS-T	Phosphate buffered saline tween
pH	Potential hydrogen
PMSF	phenylmethylsulfonyl fluoride
PTM	Post-translational modification
RNA	Ribonucleic acid
rpm	Revolution per minute
RRM	RNA recognition motif
SC	Synthetic Completion media without glucose
S. cerevisiae	*Saccharomyces cerevisiae*
SCD	Synthetic Completion media with glucose
SDS	Sodium dodecyl sulfate
SDS-PAGE	Sodium dodecyl sulfate polyacrylamide gel electrophoresis
SG	Stress granule
TBE	Tris/Borate/EDTA buffer
Tris-HCl	Trisaminomethane hydrochloride
Triton X-100	Octylphenol ethoxylate
URA	Uracil
V	Voltage
v/w	Volume by weight
WCE	Whole cell extract

WT	Wild Type
v/v	Volume by volume
YP	Yeast peptone
YPD	Yeast peptone dextrose
µg	Microgram
µL	Microlitre
µm	Micrometer
µM	Micromolar

List of Figures

Figure 1: Schematic representation of stalled mRNA cycle. **3**

Figure 2: Schematic representation of lysine acetylation. **10**

Figure 3: Formation of stress granules are reduced in *PAB1-K131Q-GFP* expressing cells. **13**

Figure 4: Glucose deprived stress granule formation is reduced in *PAB1-K131Q-GFP* mutant strain. **25**

Figure 5: K131 mutants regulate glucose deprived stress granules independently of Pab1 protein levels. **26**

Figure 6: *PAB1-K131Q-GFP* impacts stress granule formation upon ethanol, raffinose, and vanillin treatment in *Saccharomyces cerevisiae*. **28**

Figure 7: Systematic genetic screening of single, double, and triple KAT/KDAC mutants **31**

Figure 8: *rpd3Δ* affects stress granule formation **35**

Figure 9: Molecular mechanism of Pab1-K131 acetylation **37**

Figure 10: K131 mutants do not impact eIF4G binding upon glucose deprivation **40**

Figure 11: Preliminary data indicate Pab1-K131Q RRM1-RRM2 reduces binding to poly(A) mRNA **42**

1.0 Introduction

When exposed to environmental stress, eukaryotic cells utilize a variety of cellular mechanisms to remodel their pathways to specifically respond to stress and increase survival. One cellular stress response is the formation of cytoplasmic RNA-protein aggregates, or stress granules (SG), which develop under a variety of stress conditions. Stress granules are composed of messenger RNA (mRNA), poly(A) binding proteins and other proteins, including those implicated in signaling. However, the composition of stress granules varies upon different stressors (Kedersha et al., 1999, Buchan et al., 2008a). Not only is the formation of SG required for cellular survival against various environmental challenges, but they are a hallmark for disease progression of many neurodegenerative diseases and cancers (Arimoto et al., 2008, Nonhoff et al., 2007, Fournier et al., 2013, Thedieck et al., 2013). For each stress condition, distinct stress-activated signaling pathways regulate stress granule formation and disassembly; however, the molecular details of these pathways remain largely unknown. Numerous studies showed that lysine acetyltransferase (KAT) and deacetylases (KDAC) are signaling axis regulating stress granule formation. Large scale acetylome studies detected acetylation sites on many proteins found in stress granules, including the poly(A) binding protein – Pab1 (Brook et al., 2012, Smith et al., 2002, Henriksen et al., 2012, Mitchell et al., 2013). Our lab systematically mutated known sites of lysine acetylation on Pab1 and identified one site, K131, essential for stress granule formation upon glucose deprivation. As K131 is a conserved site found in many eukaryote poly(A) binding proteins, lysine acetylation at this position could be a conserved mechanism to control stress granule dynamics. In this thesis, I explore the potential impact of lysine acetylation at the site of K131 in regulation of stress granules upon glucose deprivation.

1.1 Stress Granule Formation

1.1a mRNA cycle –Stress Granules vs P-bodies.

Under normal conditions, messenger RNA (mRNA) is matured in the nucleus and undergoes multiple modifications such as 3' polyadenylation and 5' cap. Once mRNAs are exported out of the nucleus, translation of the mRNA begins. However, upon environmental stress, the translation of mRNA is stalled and shuttled in cytoplasmic ribonucleoprotein particles (Anderson and Kedersha, 2006). These cytoplasmic ribonucelo-protein particles are either Processing Bodies (p-bodies or PB) or Stress granules (SG) (Figure 1). P-bodies have degradation machinery and it was hypothesized that mRNA goes to the PB for mRNA decay (Sheth and Parker, 2003, Shah et al., 2013, Luo et al., 2018). Opposite is true for stress granules, where mRNA goes to be protected. Despite their different impact on mRNA, SG and PB biology are highly connected. Stress granules shuttle mRNA between themselves and processing-bodies (Youn et al., 2019). Due to physical association between SGs and PBs, stress granules are proposed to function as a triage site: store mRNA during stress, direct mRNA towards PB for degradation, or cytoplasm for translation once stress is uplifted (Hoyle et al., 2007, Buchan et al., 2008, Buchan et al., 2010).

Translation is regulated by the phosphorylation state of eIF2α. During inhibition of translation due to stress, the phosphorylation of eIF2α stabilizes the eIF2-GDP complex and thus prevents translation (Knutsen et al., 2015). Phosphorylation of eIF2α has been associated with SG formation; however, SGs can also be induced independent of phosphorylation of eIF2α. For example, they can also be induced through the inactivation of translation factors such as eIF4A or eIF4G (Mokas et al., 2009).

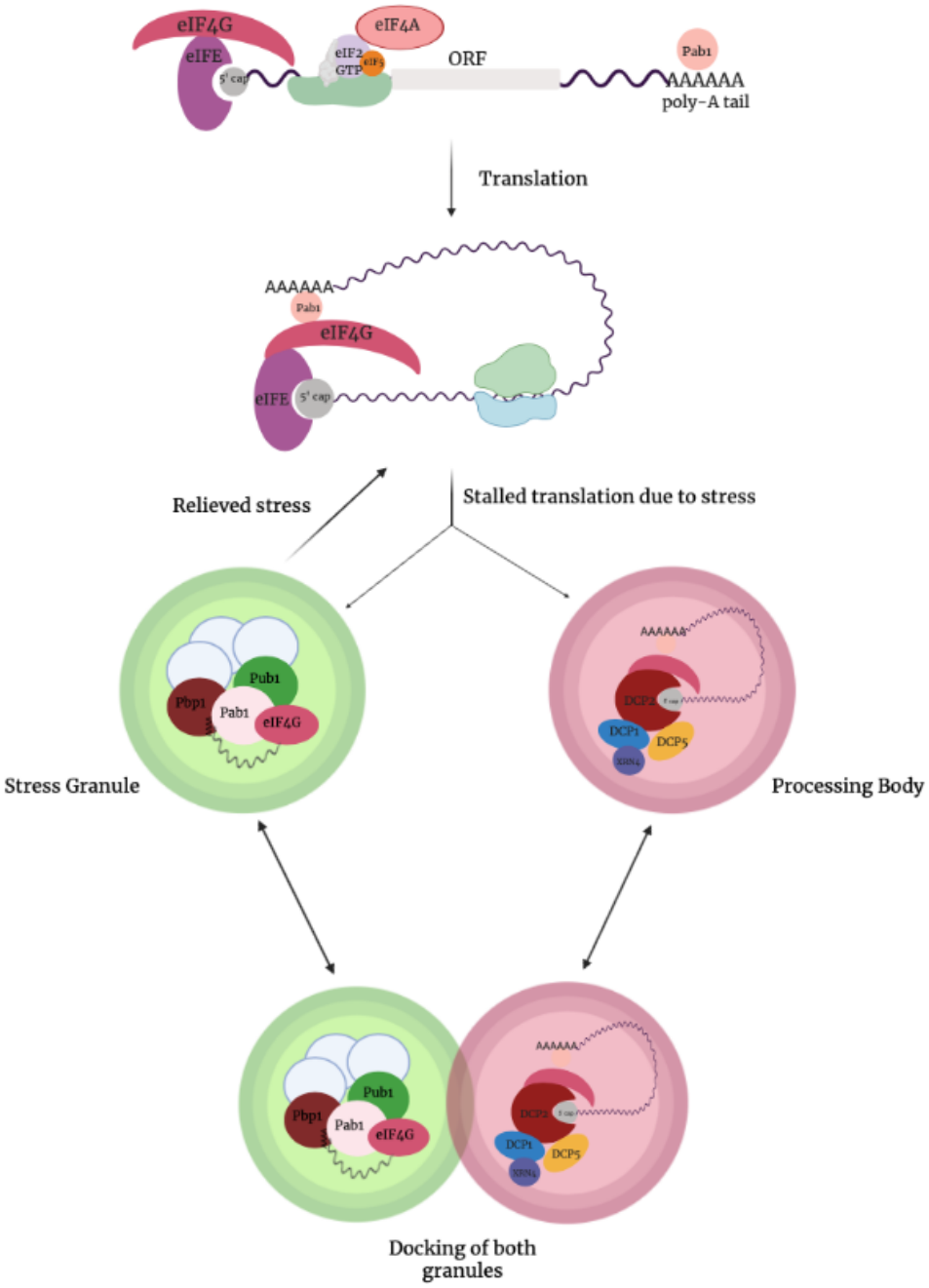

Figure 1*: Schematic representation of stalled mRNA cycle.* Stress granule is in green. Processing body is in pink. Known proteins and signaling pathways seen in granules are shown.

Stress granules are a type of cytoplasmic ribonucleoprotein particle that develop upon environmental stress. They contain translationally stalled mRNA and sequester various signaling pathways and other proteins for protection (Swisher and Parker, 2010, Buchan and Parker, 2009). Moreover, stress granules reserve cellular energy as the repressed mRNAs can

go back to translation as soon as the stressor is removed (Decker and Parker, 2012, Buchan and Parker, 2009). They were first discovered in the cytoplasm of tomato cells upon heat shock (Nover et al., 1983). Moreover, stress granules are seen in several organisms, such as mammalian and yeast cells (Kedersha et al., 1999, Buchan et al., 2008a). RNA compositions in stress granules were characterized through differential centrifugation, immunoprecipitation, and in situ hybridization (Khong et al., 2018, Jain et al., 2016, Namkoong et al., 2018). The type of RNA being sequestered depends on intrinsic properties of the RNA, such as RNA binding domains, intrinsically disordered regions, codon sequences, and their ability to engage in interactions with other molecules (Feric et al., 2016, Wang et al., 2018). The mRNAs are only sequestered in stress granules for a short period of time, typically less than minute (Mollet et al., 2008). Stress granule disassembly associates with recovery of mRNA; however, full disassembly is not required for recovery (Loschi et al., 2009).

Stress granules are a non-membrane bound organelle that represent liquid droplets that form spontaneously by liquid-liquid phase separation (Brangwynne, 2013, Elbaum-Garfinkle et al., 2015). These liquid-liquid phase separations can be driven by high concentrations of core SG proteins containing intrinsically disordered regions through electrostatic and hydrophobic protein-protein interactions (Lin et al., 2015, Nott et al., 2015, Wright and Dyson, 2015). Stress granules are comprised of two phases: an unstable outer shell due to weak dynamic interactions, and a more stable inner core (Jain et al., 2016).

There are several known yeast core proteins associated in stress granules, such as Pab1, Pbp1, Pub1, Lsm12, Ngr1, and Ded1 (Hoyle et al., 2007, Buchan et al., 2008, Swisher and Parker, 2010, Hilliker et al., 2011). Stress granules also sequester many housekeeping proteins and translation initiation factors – eIF4E, eIF4G, eIF4A, eIF3, and eIF2 (Anderson and Kedersha, 2009, Yang et al., 2014).

Stress granules form upon a variety of environmental stressors, such as glucose deprivation, oxidative stress, and UV radiation (Anderson and Kedersha, 2006). Pab1 is one of the essential proteins required to protect mRNA in stress granules during glucose deprivation (Hoyle et al., 2007). Different stress granules will be assembled depending on the type of stressor. For example, upon glucose deprivation, stress granules contain eIF4E, eIF4G, and Pab1. However, upon heat-shock, stress granules also contain the 40S ribosomal subunit and eIF3. Pub1 and Pbp1 are also required for the formation of glucose deprived stress granules, but not for the formation of heat-shocked SGs (Buchan et al., 2008, Buchan et al., 2010).

1.2 Cellular Consequence of Stress Granule Formation

It has been proposed that stress granules are a triage site for mRNA translation, storage, or degradation (Hoyle et al., 2007, Buchan et al., 2008, Buchan et al., 2010). Upon stress, mRNA undergoes a rapid polysome assembly that involves specific proteins and signaling pathways that determine its fate (Anderson and Kedersha, 2008). One role of SG is the protection of mRNA from degradation. PBs are assembled with key enzymes for RNA degradation, while SGs are assembled with essential components of translational machinery that could continue with mRNA translation once stress is uplifted (Stoecklin and Kedersha, 2013).

Another biological role stress granules partake is an increase in efficiency of certain cellular processes due to high local concentration of components in stress granules. For example, stress granules can promote the interactions of mRNA with translation factors, enhancing the formation of translational initiation factors (Buchan et al., 2008b). Moreover, stress granules limit the interactions of sequestered components from the cytosol affecting

biological interactions and reaction rates. For example, stress granules sequester TOR, RACK1 signalling pathway components which have broad effects in cell physiology (Protter and Parker, 2016). SGs also sequester specific proteins and signaling pathways. For example, stress granules negatively regulate apoptotic responses upon sequestering specific proteins required for the signaling pathway. This prevents cell death during stressful events (Arimoto et al., 2008).

1.2a Stress Granules and Disease

Normally, stress granules are dynamic and reversible, but multiple mutations can either increase or decrease stress granule formation, leading to accumulation of aggregates containing components seen in stress granules. These stress granule-like aggregates are seen in conditions such as neurodegenerative diseases (Li et al., 2013, Ramaswami et al., 2013). For example, it has been shown that stress granules are seen in patients with Alzheimer's disease. These stress granules contain an accumulation of S6 protein specific to Alzheimer's disease that appears to play a protective role (Castellani et al., 2011). Another example is mutations seen in proteins that affect autophagy, such as p62, obtineurin, or ubiquillin-2, which leads to neuro- or muscular degenerative diseases (Cipolat Mis et al., 2016, Protter and Parker, 2016). Despite numerous studies on stress granules, the regulation of the assembly and disassembly of these structures remain poorly defined. Given that SGs have been implicated in a wide variety of diseases it is important to determine the molecular mechanisms regulating the formation and disassembly of stress granules, as these may reveal novel potential therapeutic targets.

1.3 Pab1 in Stress Granules

During 3' polyadenylation, poly(A) binding protein (Pab1) binds to the poly(A) tail to stabilize the mRNA by preventing deadenylation and degradation (Sachs et al., 1987). Later, Pab1 binds to the 5'cap in a closed-loop conformation to further stabilize the mRNA to promote translation (Sachs et al., 1997, Tarun and Sachs, 1997, Wells et al., 1998, Amrani et al., 2006, Safaee et al., 2012).

Pab1 is an essential poly-(A) binding protein. Normally, Pab1 is required for efficient mRNA export and quality control in the nucleus; however, under stressful conditions Pab1 protects mRNA from degradation by inhibiting deadenylase activity (Brune et al., 2005). Pab1 plays an important role in stress granules. It is important to note that Pab1 is found in both yeast and mammalian stress granules, and therefore used as a marker to detect these dynamic organelles (Swisher and Parker, 2010). Although deletion of *PBP1* did not dramatically affect the formation of stress granules, a strain lacking the Pab1 protein reduces the formation of stress granules (Swisher and Parker, 2010). It has been proposed that Pab1 is essential for stress granules because it might promote the transition of mRNA from p-bodies to stress granules (Swisher and Parker, 2010).

Pab1 contains 4 RNA recognition motifs (RRM) linked to a carboxy-terminal domain and a proline domain (Yao et al., 2007) (Figure 3A). The C-terminal domain is important for the binding of Pan3, Ccr4 activity, binding of Erf and other regulatory proteins for translation (Mangus et al., 2004, Kuhn and Wahle, 2004, Webster et al., 2018, Zhang et al., 2013). The proline domain is important for Pab1-Pab1 interactions and Ccr4 deadenylation (Yao et al., 2007, Webster et al., 2018). These RNA recognition motifs are highly conserved and are critical for the mRNA protection (Zhang et al., 2013). Although the motifs have many functions, the first and second RNA recognition motifs are involved in poly(A)-binding

(Deardorff and Sachs, 1997). Meanwhile, the third and fourth RNA recognition motifs are involved in U-rich regions located adjacent to the poly(A) tail (Mullin et al., 2004). RRM1, RRM4, and proline domain interactions are critical for circularization of mRNA for translation (Brambilla et al., 2017). RRM1 is also important for the binding of Xpo1/Crm1 to export out of the nucleus (Brune et al., 2005). Compared to all the domains, only RRM4 is important for export of mRNA, while the other domains are important for deadenylation (Yao et al., 2007). Moreover, RRM2 mediates the RNA binding (Deo et al., 1999). In yeast, the RRM2 motif is also required for binding of eIF4G to Pab1 (Gallie, 2014). This is believed to be important for forming a closed-loop structure before translation.

1.4 Regulation of Stress Granule Assembly and Disassembly

In addition to stalled mRNA translation, assembly and disassembly of SGs can be affected by protein-protein interactions. For example, Pbp1 or Pub1 promote stress granule formation but are not required for the assembly. This suggests that redundancy of interactions contribute to stress granules forming under different conditions by different interactions (Protter and Parker, 2016). Another example is seen with G3BP1 and G3BP2, which can self-interact and interact with RNA binding proteins under oxidative stress, but not under osmotic stress (Tourriere et al., 2003, Solomon et al., 2007). This shows that there are specific cellular conditions that promote certain protein interactions that affect SG formation.

RNA-RNA interactions may play a critical role in the formation and composition of stress granules. For example, RNA can form large assemblies that show overlap with stress granule transcriptome, suggesting that RNA-RNA interactions could define the RNA composition in stress granules (Van Treeck et al., 2018). Once stress has been uplifted, smaller

stress granules fuse together and eventually disperse, but the mechanism of how it dissessembles is unknown (Kedersha et al., 2000).

In addition to stalled mRNA translation, stress granules can be regulated through other signalling pathways including post-translational protein modifications, such as phosphorylation, acetylation, methylation, and glycosylation. For example, phosphorylation of eIF2α promote SG formation, while phosphorylation of G3BP reduces the assembly of stress granules (Wek et al., 2006, Tourriere et al., 2001). Modifications on HDAC6 deacetylase affect ubiquitin metabolism which in turn affects stress granule formation (Kwon et al., 2007). Methylation also has an effect on stress granule assembly, which is necessary for localization of stress granule components (De Leeuw et al., 2007, Goulet et al., 2008). Proteins with O-GlcNAc sites for glycosylation also enhance stress granule formation (Ohn et al., 2008).

1.5 Lysine Acetylation

Lysine acetylation is a global post-translation modification that is involved in various of cellular processes (Drazic et al., 2016). Lysine acetyltransferases (KAT) add an acetyl moiety to lysine residues, (Polevoda and Sherman, 2002, Galdieri et al., 2014), while lysine deacetylases (KDAC) catalyze the removal of an acetyl moiety (Bernstein et al., 2000) (Figure 2). The addition and removal of acetyl moiety revoke or create positive charges of the lysine residue, altering the interactions these modified proteins may have.

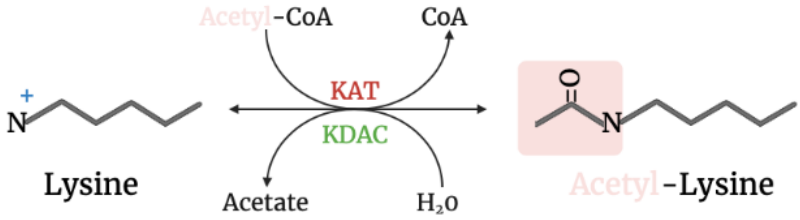

Figure 2*: Schematic representation of lysine acetylation.* Blue represents charges on molecules. Pink represents acetyl moiety. Red represents lysine acetyltransferase (KAT), and green represents lysine deacetyltransferase (KDAC).

Like all post-translational modifications, lysine acetylation has been implicated in regulating many cellular process including protein activity, stability, localization, and interactions (Yang and Seto, 2008, Glozak et al., 2005, Xiong and Guan, 2012). Lysine acetylation was first seen on histone proteins and has been extensively studied in the regulation of the conversion between DNA heterochromatic and euchromatic states and transcriptional regulation (Oliver and Denu, 2011, Peserico and Simone, 2011). Due to their role with histones, KATs and KDACs were first called Histone acetyltransferases (HATs) and Histone deacetylases (HDACs). However, more are known about their involvement in non-histone modifications as well. With new techniques emerging in the mass spectrometry field, lysine acetylation has emerged as a global phenomena not limited to only histones or nuclear proteins.

1.5a KATs and KDACs in Saccharomyces cerevisiae

There are 9 KAT proteins that have been confirmed *in-vivo* activity in *Saccharomyces cerevisiae:* Esa1, Sas3, Eco1, Elp3, Hat1, Hpa2, Rtt109, Sas2, and Gcn5 (Smith et al., 1998, Takechi and Nakayama, 1999, Toth et al., 1999, Wittschieben et al., 1999, Kleff et al., 1995, Angus-Hill et al., 1999, Scholes et al., 2001, Ehrenhofer-Murray et al., 1997, Grant et al., 1997). KAT enzymes can be classified into 3 families: Gcn5 related N-acetyltransferase (GNAT), MYST and CBP/p300. GNATs consist of Gcn5, Hat1, Elp3, Eco1, Hpa2 (Roth et

al., 2001). This is the largest superfamily and is involved in many cellular processes. MYST consists of Sas2, Sas3, and Esa1 (Aka et al., 2011). GNAT and MYST superfamilies' share a sequence motif for an essential acetyl-CoA binding domain (Lafon et al., 2007). CBP/p300 family consists of Rtt109, Taf1, Spt10 (Steger et al., 1998, Roth et al., 2001, Lee and Workman, 2007). This family does not contain any similar sequences with GNAT nor MYST superfamilies.

There are 10 KDAC proteins in *S.cerevisiae* that are also grouped into 3 categories. Class I consists of Rpd3, Hos1, and Hos2. Class II consists of Hda1, and Hos3 (Gregoretti et al., 2004). Both Class I and Class II are zinc dependent KDACs. Finally, the remaining Class III proteins consist of Sirtuins (Sir2, Hst1, Hst2, Hst3, and Hst4) (Smith et al., 2002). This class uses NAD^+ as a co-activator (Shore, 2000).

1.5b Lysine Acetylation and Stress Granule Dynamics

It has been shown that both KAT and KDACs co-localize in stress granules, suggesting their potential implication in regulation (Sadoul et al., 2011, Kwon et al., 2007). For example, in 2013, Buchan and colleagues determined that KAT mutant *gcn5Δ* and KDAC mutant *hst1Δ* resulted in increased stress granule formation under non-stressed conditions in yeast (Buchan et al., 2013). Our lab determined that mutants of the NuA4 KAT complex had a decreased stress granule formation upon glucose deprivation, but NuA4 did not impact SG formation upon heat shock nor ethanol stresses (Rollins et al., 2017). Further, our lab systematically screened all deleted mutants of non-essential KAT and KDAC proteins and suggested that mutants of Gcn5, Rpd3, and Hos3 increase stress granule formation under non-stress conditions.

KAT-interactome studies determined that Esa1 co-purifies Pab1, Pbp1, Lsm12, and Pbp4 and that both Pab1 and Pbp1 are *in vitro* acetylation of NuA4 (Mitchell et al., 2013). Further acetylome studies have determined that stress granule proteins are acetylated *in vivo*, including Pab1 (Brook et al., 2012, Henriksen et al., 2012, Mitchell et al., 2013).

1.6 Acetylation of Pab1

Given mass spectrometry studies that have determined that core stress granule proteins are acetylated (Protter and Parker, 2016, Kuechler et al., 2020, Kwon et al., 2007) and the impact of KAT and KDAC mutants on stress granule dynamics (Buchan et al., 2013, Rollins et al., 2017), one intriguing hypothesis is that acetylated stress granule proteins contribute to SG dynamics. Given the critical role of Pab1 in stress granule formation, and the numerous acetylation sites identified on this protein, our lab is interested in determining if Pab1 acetylation impacts stress granule dynamics.

Mass spectrometry identified lysine acetylation sites on Pab1, including K7, K504, K164, K131, and K288 (Brook et al., 2012, Smith et al., 2002, Henriksen et al., 2012, Mitchell et al., 2013). Our lab tested four acetylation sites, K7, K131, K288, K504, making either acetylated mimics (K-Q) or non-acetylated mimics (K-R) (Figure 3B). Importantly, the K131 site conserved across species is found in RRM2, the Pab1RRM pivotal for RNA and eIF4G binding (Melamed et al., 2013, Deo et al., 1999, Gallie, 2014). Arginine (R) residue replaces lysine as a non-acetylated mimic due to its close positively charged side chain structure. Glutamine (Q) residue replaces lysine as an acetylated mimic due to an uncharged side chain with similar structure of acetylated lysine (Kamieniarz and Schneider, 2009). *PAB1-K131Q-GFP* mutants with plasmids expressing *Pab1-GFP* have decreased formation of glucose

deprived stress granules (Figure 3B and BC). Here I seek to decipher the biological impact of Pab1 acetylation at K131.

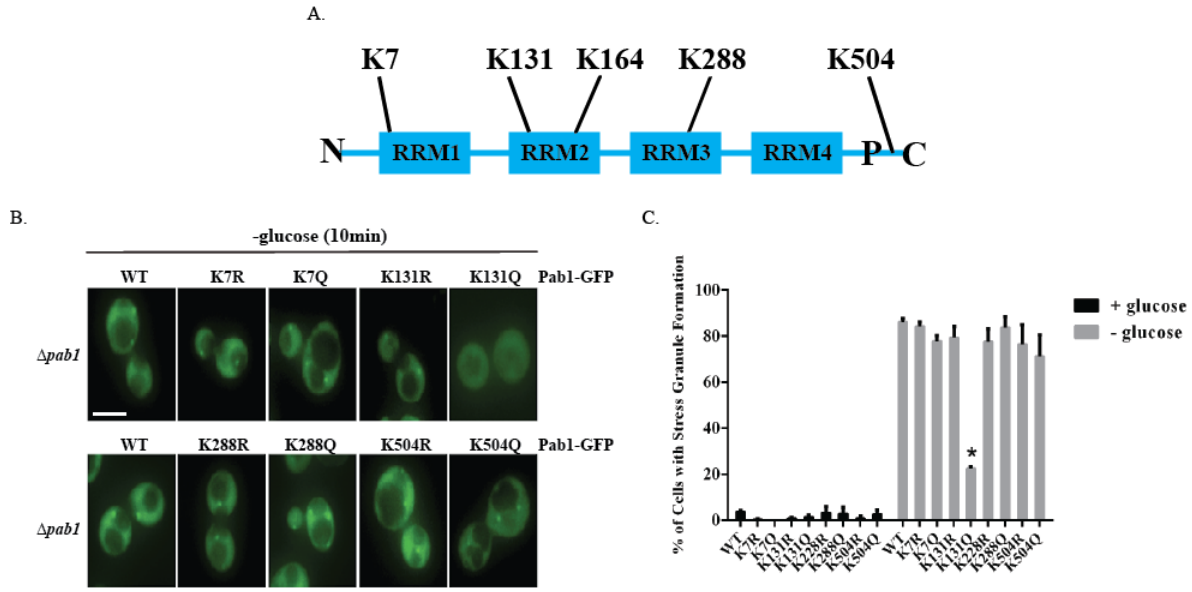

Figure 3*: Formation of stress granules are reduced in PAB1-K131Q-GFP expressing cells*. A) A graphical representation of Pab1 protein that includes the RNA recognition motifs and known acetylation sites B) *pab1Δ* cells were transformed with *PAB1-GFP::URA::CEN* (WT YKB4033), or the indicated mutations *PAB1-K7R-GFP* (YKB4037), *PAB1-K7Q*-GFP (YKB4038), *PAB1-K131R-GFP* (YKB4035), *PAB1-K131Q-GFP* (YKB4036), *PAB1-K288R-GFP* (YKB4039), *PAB1-K288Q-GFP* (YKB4040), *PAB1-K504R-GFP* (YKB4041), *PAB1-K504Q-GFP* (YKB4042). Strains were cultured in SCD-URA media at 30°C and exponential-phase cells were subjected to 10 minutes of glucose deprivation and immediately assessed for *PAB1-GFP* foci (stress granule). C) Quantification of the percentage of cells with stress granule formation after 10 minutes of glucose deprivation. Results are the average of three biological replicates, a minimum of 100 cells per replicate were scored, error bars indicate SEM. *$p<0.05$ determined using a two-way ANOVA test.

Hypothesis and Aims

The overall objective of this study is to understand the molecular mechanism regulating the assembly and disassembly of stress granules by acetylation mimics of Pab1 at K131. My working hypothesis is that acetylation of Pab1-K131 inhibits the formation of glucose deprived stress granule formation and that this site must be deacetylated for the formation of glucose deprived stress granules. To test this working hypothesis I performed series of aims:

Aim 1 - To characterize the impact of Pab1-K131 acetylated state on the formation of stress granules to a variety of environmental stress I performed a series of live microscopy and western blot analysis experiments.

Aim2 – To identify the potential KAT(s)/KDAC(s) modulating the acetylation state of Pab1-K131 I conducted a genetic screen.

Aim 3 – To decipher the molecular mechanisms by which Pab1-K131 acetylation impacts glucose deprived stress granule formation I tested a series of hypothesis using both affinity purification and EMSA studies.

2.0 Materials and Methods

2.1 Yeast strains, plasmids, primers, and media

Strains, plasmids, and primers used in this study are listed in Table 1, Table 2, and Table 3, respectively (see appendix). Strains were created by modification of chromosomal genes through PCR and homologous recombination (Longtine et al., 1998). Integrated mutants via CRISPR/Cas9 were created by Sylvain. Yeast cultures were grown at 30ºC at 200 rpm in either YPD medium (w/v 1% yeast extract, 2% peptone, 2% dextrose), YP medium (w/v 1% yeast extract, 2% peptone), SCD medium (w/v 0.67% yeast nitrogenous base without amino acids, 0.2% amino acid dropout mix, 2% dextrose), or SC medium (w/v 0.67% yeast nitrogenous base without amino acids, 0.2% amino acid dropout mix).

2.2 Strain growth and stress assessment

Yeast transformed with GFP tagged plasmids were grown in SCD-URA media and GFP tagged integrated mutants were grown in YPD media that was prepared using standard methods.

For glucose deprivation, cultures were grown in YPD or SCD-URA media until mid-log phase (OD_{600} ~0.5-0.8) and centrifuged at 3000rpm for 3 minutes at room temperature prior to being resuspended in the same glucose deprived media. Cells were grown at 30ºC and harvested for analysis following experiment specific incubation times.

For 20 nM ethanol, 3% glycerol, 2% raffinose, and 30 nM vanillin stressors, cells were collected as for glucose deprivation. However, cells under 20 nM ethanol, 3% glycerol, and 2% raffinose stress were resuspended in YP media, whereas cells under 30 nM vanillin stress were resuspended in YPD media. Cells were grown at 30ºC for 30 minutes and harvested for analysis.

For temperature stress, cells were collected as for glucose deprivation and resuspended in YP media. However, cells were grown at indicated temperatures for 30 minutes and harvested for analysis.

2.3 Fluorescence microscopy

Microscopy was completed using a Leica DMI 6000 microscope equipped with Hamamatsu Orca AG camera, Sutter DG4 light source, Ludl emission filters wheel with Chroma bandpass emission filters (Leica Microsystems GmbH, Wetzler Germany).

Cells were grown in 25 mL of YPD or SCD-URA media as indicated until mid-log phase. Cultures were centrifuged at 3000rpm for 3 minutes at room temperature. Pellet was washed twice with indicated media and centrifuged again. Following centrifugation, cells were resuspended in 100 µL of SCD media. 15 µL of cells were spotted onto a glass plate and live imaged immediately. Following live-cell imaging under non-stressed conditions, cells were exposed to glucose deprivation for 10 minutes as previously described. Following incubation, the treated cultures were harvested and imaged as described above. Z-stacked images (0.2 µm across 7µm) were obtained using Volocity 4.3.2 (Perkin Elmer) using a 63x objective without binning and 3 seconds exposure for GFP fluorescence .

Microscopy experiments were completed in triplicate and each replicate consisted of at least 100 cells. Number of total cells and number of cells that form stress granules were determined by manual counting of stacked images. From these values, the percentage of cells that form stress granules was determined. Statistics was completed using an online t-test calculator by GraphPad Prism (GraphPad T test calculator). ANOVA was utilized, with a p-value of <0.05 representing statistical significance.

2.4 Quantitative western blotting

Yeast strains were grown overnight in YPD and diluted into 100 mL cultures to an OD_{600} 0.1. Cells were harvested at mid-log phase and whole cell extracts of glucose replete and glucose depleted cultures were collected as previously described. The cell pellets were mixed with 2x the pellet volume of lysis buffer (100mM HEPES (pH 8.0), 20 mM MgOAc, 300 mM NaOAc, 10% glycerol, 10 mM EGTA, 0.1 mM EDTA, protease inhibitor [Sigma]), and lysed using bead beating for 1 minute 6 times with equal volume of 0.5 mm glass beads (Fisher). Whole cell extracts were collected by centrifugation and protein was quantified using a Bradford assay. A standard curve for each protein was performed to determine the optimal amount of protein to be loaded. 30 µg of protein with 2x Laemmli dye (1M Tris-HCl (pH 6.8), 60% glycerol, 12.5% SDS, 9.3% DTT, 0.06% bromophenol blue) were boiled at 95°C for 10 min and separated by SDS-PAGE using the 10% TGX Stain-Free™ Acrylamide Kit (Bio-Rad) at 180V. Following electrophoresis, acrylamide gels were activated using the Bio-Rad Chemidoc™ XRS system (Bio-Rad) and ImageLab software 5.2 (Bio-Rad) before being transferred onto nitrocellulose membrane (Bio-Rad). Proteins were transferred onto a nitrocellulose membrane using the Bio-Rad Semi-dry trans-blot turbo™ Transfer system (Bio-Rad) for 7 minutes. Total proteins were visualized under UV light at 302 nm. Blocking was performed with 5% of non-fat milk powder dissolved in PBS-T (8% NaCl, 0.2% KCl, 1.42% Na_2HPO_4, 0.24% KH_2PO_4, and 1% Tween) for 1 hour. The membranes were incubated overnight at 4°C with 1:5000 anti-GFP primary antibody (Sigma-Aldrich) in 5% milk PBS-T. Next day, blots were washed with PBS-T three times, incubated with 1:5000 goat-anti-mouse secondary antibody (Bio-Rad) for 2 hours, then washed with PBS-T three times. Lastly, blots were developed with Clarity Western ECL substrate (Bio-Rad) and protein bands were visualized with the Bio-Rad Chemidoc™ XRS system using the equipment chemiluminescent

setting. Relative protein abundance was quantified using ImageLab Software and each band was normalized to the total protein signal of the lane then calculated relative to the wild type signal of the protein. This was done with 3 biological replicates.

2.5 Dot assays

Cultures were grown to mid-log in YPD before being diluted to an OD_{600} 0.1. Three 10-fold serial dilutions (0.01, 0.001, 0.0001) of 5 µL of the serial dilutions were spotted onto the indicated plates. The plates were incubated for 24 hours at the appropriate temperatures. Images of dot assays were taken using the Bio-Rad Chemidoc™ XRS system under epi-white light illumination and ImageLab Software.

2.6 Time course

Cells were grown in 25 mL of YPD or SCD-URA media as indicated until mid-log phase. Cultures were centrifuged at 3000rpm for 3 minutes at room temperature. Pellet was washed twice with indicated media and centrifuged again. Following centrifugation, cells were resuspended in 100 µL of SCD-URA media. 15 µL of cells were spotted onto a glass plate and live imaged immediately. Following live-cell imaging under non-stressed conditions, cells were exposed to glucose deprivation for 20, 30, 60, 90 minutes as previously described. Following incubation, the treated cultures were harvested and imaged as described above. Z-stacked images (0.2 µm across 7 µm) were obtained using Volocity 4.3.2 (Perkin Elmer) using a 63x objective without binning and 3 seconds exposure for GFP fluorescence.

Microscopy (equipment previously mentioned) experiments were completed in biological replicates of three and each replicate consisted of at least 100 cells. Number of total cells and number of cells that form stress granules were determined by manual counting of

stacked images. From these values, the percentage of cells that form stress granules were determined. Statistics for each experiment was completed using GraphPad Prism 6.0. ANOVA was utilized, with a p-value of <0.05 representing statistical significance.

2.7 GST purification

The DNA encoding Pab1 RRM1-RRM2 was cloned into EcoRI and NotI restriction sites of pGEX-4T-1 plasmid (Figure S4) and PCR confirmed by GenScript (GenScript Biotech Corporation, USA). DNA sequences created by GenScript found in Table 3 in the appendix.

Wild type Pab1 RRM1-RRM2 (692 base pairs; additional amino acids underlined, lysine residue at 131 in bold):

5′EFMADITDKTAEQLENLNIQDDQKQAATGSESQSVENSSASLYVGDLEPSVSEAHLYDIF
SPIGSVSSIRVCRDAITKTSLGYAYVNFNDHEAGRKAIEQLNYTPIKGRLCRIMWSQRDPSL
RKKGSGNIFI**K**NLHPDIDNKALYDTFSVFGDILSSKIATDENGKSKGFGFVHFEEEGAAKEA
IDALNGMLLNGQEIYVAPHLSRKERDSQLEETKAHYTNLYVKN*AA′3

Pab1-K131R RRM1-RRM2 (692 base pairs; additional amino acids underlined, lysine residue to arginine residue at 131 in bold):

5′EFMADITDKTAEQLENLNIQDDQKQAATGSESQSVENSSASLYVGDLEPSVSEAHLYDIF
SPIGSVSSIRVCRDAITKTSLGYAYVNFNDHEAGRKAIEQLNYTPIKGRLCRIMWSQRDPSL
RKKGSGNIFI**R**NLHPDIDNKALYDTFSVFGDILSSKIATDENGKSKGFGFVHFEEEGAAKEA
IDALNGMLLNGQEIYVAPHLSRKERDSQLEETKAHYTNLYVKN*AA′3

Pab1-K131Q RRM1-RRM2 (692 base pairs; additional amino acids underlined, lysine residue to glutamine residue at 131 in bold):

5′EFMADITDKTAEQLENLNIQDDQKQAATGSESQSVENSSASLYVGDLEPSVSEAHLYDIF
SPIGSVSSIRVCRDAITKTSLGYAYVNFNDHEAGRKAIEQLNYTPIKGRLCRIMWSQRDPSL
RKKGSGNIFI**Q**NLHPDIDNKALYDTFSVFGDILSSKIATDENGKSKGFGFVHFEEEGAAKEA
IDALNGMLLNGQEIYVAPHLSRKERDSQLEETKAHYTNLYVKN*AA′3

The constructs were transformed into chemically competent BL21 *Escherichia coli* cells for protein expression. This was achieved by transferring 1 µL of plasmid into 50 µL of

competent BL21 *E.coli* cells, and incubated on ice for 30 min. The cells are then incubated at 42°C for exactly 90 seconds, and rapidly put back in ice for 1-2 minutes. Next, 950 µL of LB media (v/w 1% tryptone, 0.5% yeast extract, 1% sodium chloride) was added to the cells and incubated for 30 minutes on ice, then 1 hour at 37°C. The cells are spun down at 3000rpm for 3 minutes, resuspended in LB media, and transferred onto LB + 1 µg/mL ampicillin (Amp) plates and incubated at 37°C.

Bacterial cultures were grown overnight at 37°C in 50mL of LB + Amp media. The cultures were inoculated to OD_{600} 0.1 in 100 mL LB + Amp media and incubated at 37°C until OD_{600} 0.5-0.6. The cultures were induced with 0.25 mM IPTG for 2 hours at 37°C. The culture was spun down at 3000rpm for 3 min, washed with 1xPBS, and spun down again prior to weighting the pellet. The cells were re-suspended with 2.5 mL/g of freezing buffer (1xPBS, 1mM EDTA, 1mM EGTA, and 1 mM PMSF), and froze at -80°C. The samples were thawed and 2.5 mL/g of freezing buffer with an addition of 15 mM DTT, 0.5% Triton X-100 was added, followed by sonication (Misonix Sonicator 3000 550W, Cole Parmer, Canada) 4 times for 30 seconds, with 1 minute resting period on ice. The samples were spun down at 4000rpm for 20 min. Glutathione Sepharose 4b (Life Technologies) was washed in washing buffer (1x PBS, 0.1% NP-40, 0.5 M NaCl, 1 mM DTT, 1 mM EDTA, 1 mM EGTA, and 1 mM PMSF). 500 µL of glutathione sepharose and the samples' supernatants were batch bonded in a closed column for 2 hours at 4ºC on an end-over-end rotation. The flow-through was collected. The column was washed with 10 mL of washing buffer and 2 mL of cleavage buffer (1x PBS, 140 mM Na_2HPO_4, 1.8 mM KHPO. 138 mM NaCl, and 2.7 mM KCl pH 7.2). 1 mL of PBS and thrombin proteases was added to a closed column and rotated overnight at room temperature. The eluate was drained and washed with 2 mL of cleavage buffer. Coomassie stain (G-250, Bio-Rad) gel was run to check for the efficacy of the purification.

The fragments were diluted in exchange protein buffer (20 mM Tris-HCl (pH 7.4), 100 mM KOAc, 2 mM MgOAc, 1 mM PMSF, 10% glycerol) and concentrated using 10K 20mL concentrator following a standard protocol (Thermofisher).

2.8 Affinity purification

Yeast strains were grown overnight in YPD and diluted into 100 mL cultures to an OD_{600} 0.1. Cells were harvested at mid-log and whole cell extracts of glucose repleted and glucose depleted cultures were collected as previously described. The cell pellets were mixed with 2x the pellet volume of lysis buffer (30 mM HEPES pH 7.4, 100 mM KOAc, 2 mM MgOAc, 1 mM DTT protease inhibitor), and lysed using bead beating for 1 minute 6 times with equal volume of 0.5 mm glass beads. Whole cell extracts were collected by centrifugation and protein was quantified using a Bradford assay.

Glutathione Sepharose was washed in a washing buffer (1x PBS, 0.1% NP-40, 0.5 M NaCl, 1 mM DTT, 1 mM EDTA, 1 mM EGTA, and 1 mM PMSF). GST purification was performed prior to cleavage of GST. 20 µL of GST fragment, 25 µL of crude extract, and 300 µL of lysis buffer were combined in an Eppendorf tube for 2h at 4°C on an end-over-end rotation. The samples then were spun down at maximum speed for 20 seconds, supernatant was removed, and 25 µL of sample buffer was added. Western blot procedure was performed.

Following membrane activation, the membranes were incubated overnight at 4°C with 1:1000 anti-HA primary antibody (Sigma-Aldrich) in 5% milk PBS-T. Next day, blots were washed with PBS-T three times, incubated with 1:1000 goat-anti-mouse secondary antibody (Bio-Rad) for 2 hours, then washed with PBS-T three times again. Blots were developed with Clarity Western ECL substrate (Bio-Rad) and protein bands were visualized with the Bio-Rad Chemidoc™ XRS system. Blots were then washed with PBS-T three times again, and

incubated with 1:5000 anti-GST primary antibody (Sigma-Aldrich) overnight in 5% milk PBS-T. Next day, blots were washed with PBS-T three times, incubated with 1:5000 goat-anti-rabbit secondary antibody (Bio-Rad) for 2 hours, then washed with PBS-T three times again. Lastly, blots were developed with Clarity Western ECL substrate (Bio-Rad) and protein bands were visualized with the Bio-Rad Chemidoc™ XRS system. Relative protein abundance was quantified using ImageLab Software and each band was normalized to the total protein signal of the lane then calculated relative to the WT signal of the protein. This was done with 3 biological replicates.

2.9 Electrophoretic mobility shift assay

The interaction between Pab1 and $PolyA_{20}$ was assessed by electrophoretic gel mobility shift assay (EMSA). The RNAs used in this study were generated from hydrolyzed Cy5-$PolyA_{20}$-Cy5 and $PolyA_{20}$ (Sigma). Proteins were diluted in a protein buffer (20 mM Tris-HCl pH 7.4, 100 mM KOAc, 2 mM MgOAc, 10% glycerol) to a final concentration of 0.2 µg/µL. Binding reactions (20 µL) were incubated in 4 µL of 5x binding buffer (50 mM Tris-HCl (pH 7.5), 50 mM NaCl, 200 mM KCl, 5 mM $MgCl_2$, 5 mM EDTA, 0.5 mM DTT, 250 mM BSA), protein buffer, 4 µL of RNA, and 0.4 nM, 4 nM, 40 nM, 400 nM, 800 nM, 2000 nM, 4000 nM or 5000 nM of either Pab1 RRM1-RRM2, Pab1-K131R RRM1-RRM2, or Pab1-K131Q RRM1-RRM2 with its respective concentration at 30°C for 30 minutes. 1.5mm thick 10% non-denaturing polyacrylamide gel (37.5:1, w/w) was submerged in 0.4x TBE (1x stock: 0.13 M Tris (pH 7.6), 45 mM boric acid, 2.5 mM EDTA) and was pre-run for 30 minutes at 20 V. While running at 20 V, 10 µL of the samples were loaded and ran for 2.5h at 55 V. All electrophoresis was run at 4°C submerged in a bucket of ice. The gel was removed from the casting system and scanned by the Typhoon Variable Mode Imager (GE Healthcare). Relative

RNA binding was quantified using ImageQuant Software 8.2 (ImageQuant TL 8.2 image analysis software) and each band was normalized to the relative known RNA band. This was done with 2 biological replicates.

3.0 Results

3.1 Pab1-K131 mutation impacts glucose deprived stress granule formation

Using a plasmid-based expression system our lab previously screened known lysine acetylation sites on Pab1 and determined that the acetylation mimic *PAB1-K131Q-GFP* displayed a reduction in glucose deprived stress granules (Figure 3B). To confirm these results were not an artifact of the plasmid system, I used integrated mutants via CRISPR/Cas9 created by Sylvain. CRISPR/Cas9 was used to create *PAB1-K131R-GFP* (non-acetylated mimic), and *PAB1-K131Q-GFP* (acetylated mimic) at their endogenous genomic location. I confirmed that while *PAB1-K131R-GFP* cells form glucose deprived stress granules similar to WT *PAB1-GFP*, *PAB1-K131Q-GFP* cells had a significant decrease in the formation of stress granules after 10 minutes of glucose deprivation (Figure 4A, and 4B).

Previous research has shown that NuA4 mutants do not abolish glucose deprived stress granule formation, but significantly delay their formation (Rollins et al., 2017). Hence, the reduction in stress granules after 10 minutes of glucose deprivation may reflect a delay in formation, but not a true reduction. To test for this possibility, I performed a time course experiment where stress granule formation was assessed after 10, 20, 30, 60 and 90 minutes of glucose deprivation. As expected, *PAB1-GFP* and *PAB1-K131R-GFP* cells formed glucose deprived stress granules and then slowly resolve the stress granules over a 90-minute time course. However, glucose deprived stress granule formation remained low in *PAB1-K131Q-GFP* cells (Figure 4C), indicating the reduction of SG formation in the K131 acetylation mimic is not reflective of a delay. My results suggest that *PAB1-GFP* incorporation into glucose deprived stress granules is regulated by the acetylation state of K131.

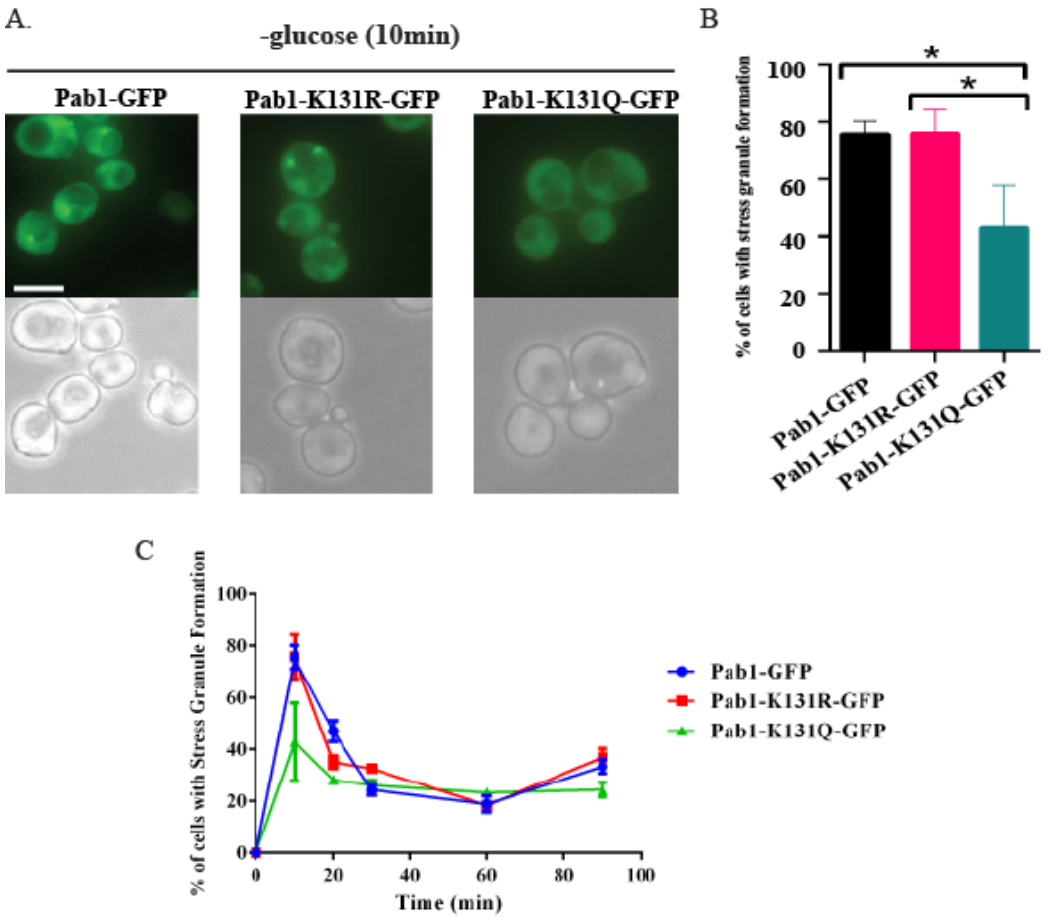

Figure 4*: Glucose deprived stress granule formation is reduced in PAB1-K131Q-GFP mutant strain*. Wild type cells expressing endogenously tagged *PAB1-GFP* (YKB3114), *PAB1-K131R-GFP* (YKB4395), or *PAB1-K131Q-GFP* (YKB4396) were cultured in YPD media at 30°C to mid-log phase (0 minute), were subjected to glucose deprivation for 10, 20, 30, 60, and 90 minutes, and immediately assessed for stress granules. A) Representative brightfield and fluorescent images of cells after 10 minutes of glucose deprivation. Scale bar represents 10µm. B) Quantification of the percentage of cells with stress granule formation after 10 minutes of glucose deprivation. Results are the average of three biological replicates, a minimum of 100 cells per replicate were scored, error bars indicate SEM. *$p<0.05$ determined using a two-way ANOVA test. C) Time course of the percentage of cells with stress granules at 10, 20, 30, 60, and 90 minutes. Results are the average of three biological replicates, a minimum of 100 cells per replicate were scored, and error bars indicate SEM.

3.2 Pab1-K131 mutations do not impact protein levels

One possible reason that could explain a decrease in glucose deprived stress granules in *PAB1-K131Q-GFP* cells is due to changes in protein expression levels. To assess this possibility, I performed quantitative western blot analysis to assess protein levels of Pab1-GFP, Pab1-K131R-GFP, Pab1-K131Q-GFP under glucose repleted (YPD) or glucose depleted (YP) conditions. Though protein levels of Pab1-K131R-GFP were reduced compared to Pab1-GFP, this was not significant. Regardless of the conditions, Pab1-K131Q-GFP protein levels were not significantly changed compared to Pab1-GFP (Figure 5A, and 5B). This suggests that the decrease in glucose deprived stress granule formation in *PAB1-K131Q-GFP* cells is not due to changes in protein.

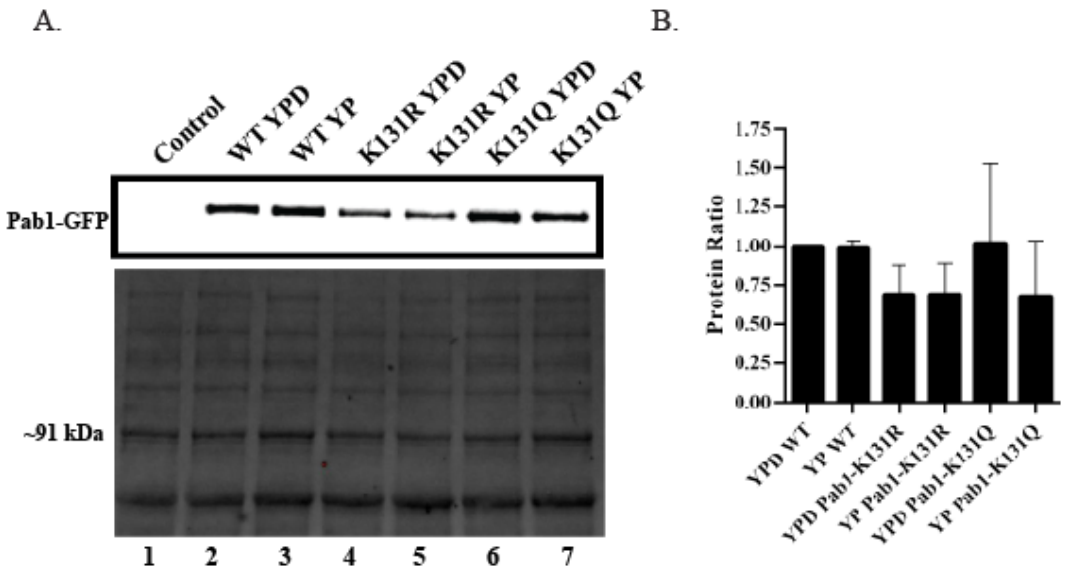

Figure 5*: K131 mutants regulate glucose deprived stress granules independently of Pab1 protein levels.* Wild type (control YKB1079) or WT cells expressing endogenously tagged *PAB1-GFP* (WT YKB3114), *PAB1-K131R-GFP* (YKB4395) or *PAB1-K131Q-GFP* (YKB4396) were grown to mid-log phase at 30°C in YPD media and subjected to glucose deprivation (YP) for 10 minutes. Protein extraction was performed from 100mL cultures and 30 µg/mL whole cell extract was resolved on a 1x TGX Stain-free Fastcast Acrylamide gel prior to western blot analysis using antibody against GFP. A) Representative anti-GFP western blot (top panel) and total protein blot (bottom panel). B) Quantification of western blots for three independent biological replicates where the *PAB1-GFP* band intensity was normalized to total protein. Error bars indicate SEM. Differences between the samples were proven to be insignificant through two-way ANOVA tests.

3.3 PAB1-K131Q impacts stress granule formation upon ethanol, raffinose, and vanillin

Previous research showed that a decrease in stress granule formation in NuA4 mutants was specific to glucose deprivation, but that NuA4 did not impact the formation of stress granules by other stressors such as ethanol or heat shock (Rollins et al., 2017). Therefore, I sought to determine if *PAB1-K131Q* only impacted the formation of glucose deprived stress granules or if it impacts the formation of stress granules under other stressors. Sylvain first assessed *PAB1-GFP* stress granule formation after 30-minute heat shock and found there were no significant differences in the percentage of cells that form heat shock stress granules between *PAB1-GFP*, *PAB1-K131R-GFP*, and *PAB1-K131Q-GFP* cells (Figure 6A and 6B). I extended this analysis to assess the impact of *PAB1-K131* mutations on other environmental stresses that induce stress granule formation including ethanol (Martani et al., 2015), glycerol (Mattenberger et al., 2017), raffinose (Shah et al., 2013), and vanillin (Iwaki et al., 2013). *PAB1-K131Q-GFP* cells showed a significant reduction in stress granule formation in 20nM ethanol, 2% raffinose, and 30nM vanillin but did not impact 3% glycerol induced SG formation (Figure 6C and 6D). Though *PAB1-K131Q-GFP* cells had a reduced rate of SG formation under these stressors, dot assays indicated this mutation does not result in detectable impacts on growth on agar plates containing ethanol, raffinose or vanillin (Figure 6E). This suggests that acetylation mimicking *PAB1-GFP* decreases stress granule formation only for a subset of cellular stresses, including glucose deprivation, ethanol, raffinose, and vanillin.

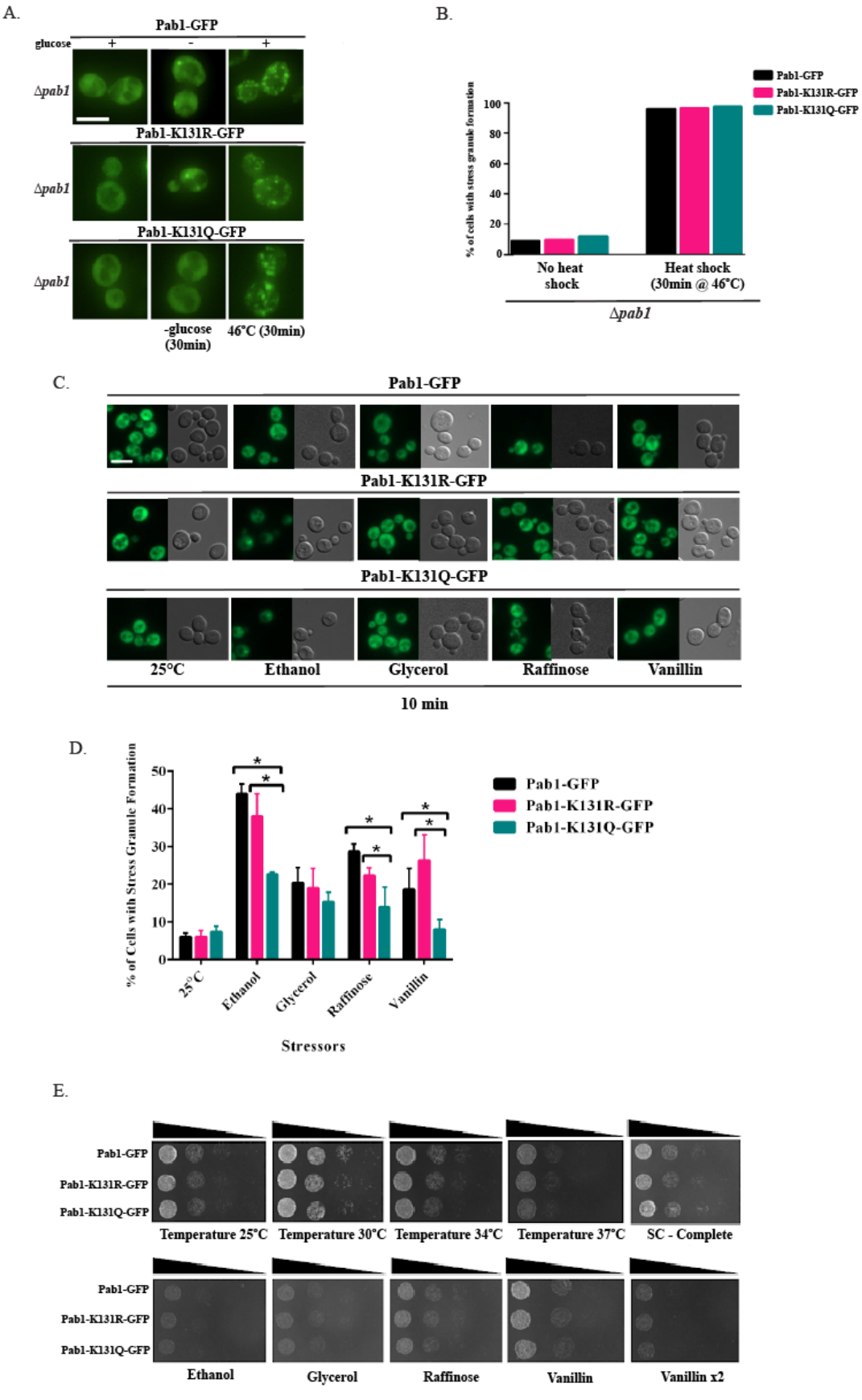
A.
Pab1-GFP
glucose
+
-
+
Δpab1
Pab1-K131R-GFP
Δpab1
Pab1-K131Q-GFP
Δpab1
-glucose (30min)
46°C (30min)
B.
Pab1-GFP
Pab1-K131R-GFP
Pab1-K131Q-GFP
% of cells with stress granule formation
100
80
60
40
20
0
No heat shock
Heat shock (30min @ 46°C)
Δpab1
C.
Pab1-GFP
Pab1-K131R-GFP
Pab1-K131Q-GFP
25°C
Ethanol
Glycerol
Raffinose
Vanillin
10 min
D.
% of Cells with Stress Granule Formation
50
40
30
20
10
0
*
*
*
*
*
*
Pab1-GFP
Pab1-K131R-GFP
Pab1-K131Q-GFP
25°C
Ethanol
Glycerol
Raffinose
Vanillin
Stressors
E.
Pab1-GFP
Pab1-K131R-GFP
Pab1-K131Q-GFP
Temperature 25°C
Temperature 30°C
Temperature 34°C
Temperature 37°C
SC - Complete
Pab1-GFP
Pab1-K131R-GFP
Pab1-K131Q-GFP
Ethanol
Glycerol
Raffinose
Vanillin
Vanillin x2

Figure 6*: PAB1-K131Q-GFP impacts stress granule formation upon ethanol, raffinose, and vanillin treatment in Saccharomyces cerevisiae.* A) *PAB1-GFP* (YKB3114), *PAB1-K131R-GFP* (YKB4395), and *PAB1-K131Q-GFP* (YKB4396) were cultured in YPD media at 30°C and exponential-phase cells were subjected to 30 minutes of heat shock at 46ºC in pre-warmed media. Representative BF and fluorescent images after 30 minutes of heat shock. B) Quantitative analysis on SG formation in *PAB1-GFP*, *PAB1-K131R-GFP*, and *PAB1-K131Q-GFP*. C) *PAB1-GFP* (YKB3114), *PAB1-K131R-GFP* (YKB4395), and *PAB1-K131Q-GFP* (YKB4396) were cultured in YPD media at 30°C and exponential-phase cells were subjected to 30 minutes of 25°C stress, 20mM ethanol stress, 3% glycerol stress, 2% raffinose stress, and 30nM vanillin stress in either YPD or YP media. Representative brightfield and fluorescent images after 30-minutes of treatment. D) Quantitative analysis after 30 min of stress granule formation in 25°C, 20mM ethanol, 3% glycerol, 2% raffinose, and 30nM vanillin. E) 5-serial diluted dot assay of mutant mimics of K131 amongst various stressors: 25°C, 30°C, 34°C, 37°C, SC-complete, 20mM ethanol, 3% glycerol, 2% raffinose, 30nM vanillin, vanillin x2. Results average of three biological replicates, minimum of 100 cells/replicate, error bars indicate SEM. *$p<0.05$ determined using a two-way ANOVA test. Scale bar represents 10μm.

3.4 Genetic screening identifies KAT/KDAC regulating Pab1 acetylation sites

My results suggest that the acetylation mimic *PAB1-K131Q-GFP* decreases glucose deprived stress granule formation. I proposed a model where KAT(s) acetylating Pab1-K131 inhibits glucose-deprived stress granule formation while KDAC(s) deacetylating Pab1-K131 is required for stress granule formation (Figure 7A). If this model was true, I predict there would be a KAT mutant(s) with elevated stress granule formation, due to decreased Pab1-K131 acetylation that would be suppressed by *PAB1-K131Q-GFP* acetylation mimic (Figure 7B). Similarly, the mutant of the KDAC responsible for deacetylation of Pab1-K131 would have decreased stress granule formation, due to increased Pab1-K131 acetylation, that would be suppressed by *PAB1-K131R-GFP,* unacetylated mimic. To identify the potential KAT(s) and KDAC(s) regulating the acetylation state of Pab1-K131, Rollins et al. (2017) systematically screened deletion mutants of all non-essential KAT and KDAC proteins. The screen suggested that mutants of Gcn5, Rpd3, and Hos3 showed a two-fold increase in stress granule formation under non-stress conditions. Moreover, Hst1 and Sir2 mutants also showed an increase in stress granule formation under non-stress conditions (Buchan et al., 2013). For these reasons, a systematic genetic screen was conducted on plasmid KAT mutants (*gcn5Δ*, s*as2Δsas3Δ*, *eaf1Δ*, *eaf7Δ*, *gcn5Δhpa2Δhpa3Δ*) and KDAC mutants (*rpd3Δ, sir2Δhst1Δhst2Δ*, *hos3Δ*). Each mutant was transformed with a plasmid expressing *PAB1-GFP*, *PAB1-K131R-GFP*, or *PAB1-K131Q-GFP* and the rates of stress granule formation upon glucose repletion and glucose deprivation was measured (Figure 7C and 7D, respectively). Only the KDAC mutant *rpd3Δ* displayed the anticipated phenotypes, decreased glucose deprived stress granule formation that was fully suppressed by *PAB1-K131R-GFP* and was epistatic with *PAB1-K131Q-GFP* (Figure 7D, Figure S1). Although the other mutants do not fit the expected

outcome, the results suggest that there are several KAT/KDAC mutants involved in the formation of glucose deprived stress granules.

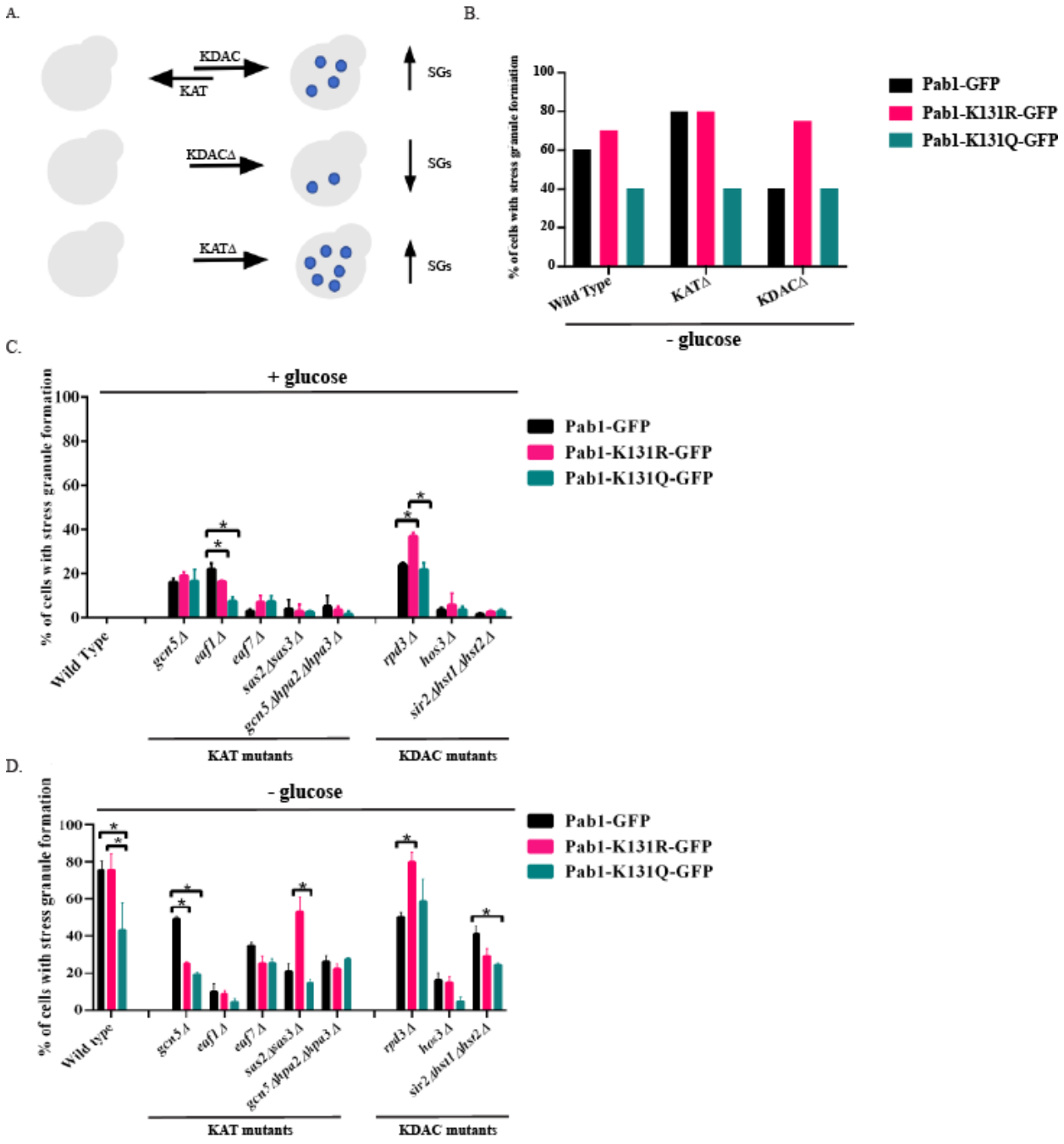

***Figure** 7: Systematic genetic screening of single, double, and triple KAT/KDAC mutants.* A) A predicted graphical representation of KAT/KDAC mutants results in the level of stress granules in the cell. KDAC would be required to deacetylate this site to allow for stress granule formation to occur, opposite holds for KAT. B) A hypothetical result of KAT/KDAC mutants under wild type, K-R mimic, or K-Q mimic under glucose deprivation. C) Quantification analysis on Wild Type (*PAB1-GFP*

(YKB3114); *PAB1-K131R-GFP* (YKB4395); *PAB1-K131Q-GFP* (YKB4396), *gcn5Δ PAB1-GFP* (YKB4177), *gcn5Δ PAB1-K131R-GFP* (YKB4178), *gcn5Δ PAB1-K131Q-GFP* (YKB4179), *rpd3Δ PAB1-GFP* (YKB4180), *rpd3Δ PAB1-K131R-GFP* (YKB4181), *rpd3Δ PAB1-K131Q-GFP* (YKB4182), *sas2Δsas3Δ PAB1-GFP* (YKB4161), *sas2Δsas3Δ PAB1-K131R-GFP* (YKB4162), *sas2Δsas3Δ PAB1-K131Q-GFP* (YKB4163), *sir2Δhst1Δhst2Δ PAB1-GFP* (YKB4166), *sir2Δhst1Δhst2Δ PAB1-K131R-GFP* (YKB4167), *sir2Δhst1Δhst2Δ PAB1-K131Q-GFP* (YKB4168), *eaf1Δ PAB1-GFP* (YKB4175), *eaf1Δ PAB1-K131R-GFP (*YKB4964), *eaf1Δ PAB1-K131Q-GFP* (YKB4965), *eaf7Δ PAB1-GFP* (YKB4969), *eaf7Δ PAB1-K131R-GFP* (YKB4970), *eaf7Δ PAB1-K131Q-GFP* (YKB4971), *gcn5Δhpa2Δhpa3Δ PAB1-GFP* (YKB4172), *gcn5Δhpa2Δhpa3Δ PAB1-K131R-GFP* (YKB4173), *gcn5Δhpa2Δhpa3Δ PAB1-K131Q-GFP* (YKB4174), *hos3Δ PAB1-GFP* (YKB4966), *hos3Δ PAB1-K131R-GFP* (YKB4967), *hos3Δ PAB1-K131Q-GFP* (YKB4968) were cultured in SCD-URA media at 30°C. D) Quantification analysis on Wild Type (*PAB1-GFP* (YKB3114); *PAB1-K131R-GFP* (YKB4395); *PAB1-K131Q-GFP* (YKB4396), *gcn5Δ PAB1-GFP* (YKB4177), *gcn5Δ PAB1-K131R-GFP* (YKB4178), *gcn5Δ PAB1-K131Q-GFP* (YKB4179), *rpd3Δ PAB1-GFP* (YKB4180), *rpd3Δ PAB1-K131R-GFP* (YKB4181), *rpd3Δ PAB1-K131Q-GFP* (YKB4182), *sas2Δsas3Δ PAB1-GFP* (YKB4161), *sas2Δsas3Δ PAB1-K131R-GFP* (YKB4162), *sas2Δsas3Δ PAB1-K131Q-GFP* (YKB4163), *sir2Δhst1Δhst2Δ PAB1-GFP* (YKB4166), *sir2Δhst1Δhst2Δ PAB1-K131R-GFP* (YKB4167), *sir2Δhst1Δhst2Δ PAB1-K131Q-GFP* (YKB4168), *eaf1Δ PAB1-GFP* (YKB4175), *eaf1Δ PAB1-K131R-GFP (*YKB4964), *eaf1Δ PAB1-K131Q-GFP* (YKB4965), *eaf7Δ PAB1-GFP* (YKB4969), *eaf7Δ PAB1-K131R-GFP* (YKB4970), *eaf7Δ PAB1-K131Q-GFP* (YKB4971), *gcn5Δhpa2Δhpa3Δ PAB1-GFP* (YKB4172), *gcn5Δhpa2Δhpa3Δ PAB1-K131R-GFP* (YKB4173), *gcn5Δhpa2Δhpa3Δ PAB1-K131Q-GFP* (YKB4174), *hos3Δ PAB1-GFP* (YKB4966), *hos3Δ PAB1-K131R-GFP* (YKB4967), *hos3Δ PAB1-K131Q-GFP* (YKB4968) were cultured in SCD-URA media at 30°C and exponential-phase cells were subjected to 10-minutes of glucose deprivation. Error bars represent SEM, *$p<0.05$ determined by two-way ANOVA test.

3.5 KDAC Rpd3 mutant impacts glucose deprived stress granule formation

Although *gcn5Δ* and *eaf1Δ* did not display the anticipated phenotypes, Rollins et al.(2017) showed that *eaf1Δ* and *gcn5Δ* had significant impact on glucose deprived stress granule formation. Since *eaf1Δ* and *gcn5Δ* had significant increase in stress granule formation under glucose deprivation compared to glucose repleted conditions, *eaf1Δ* and *gcn5Δ* were also analyzed along with *rpd3Δ*. Results were confirmed using endogenously integrated strains expressing *PAB1-GFP*, *PAB1-K131R-GFP* and *PAB1-K131Q-GFP* in *rpd3Δ*, *eaf1Δ* and *gcn5Δ* strain backgrounds. Strains were cultured to log phase (time 0) and stress granules were measured after 10 minutes of glucose deprivation. As previously seen with plasmids, in both *eaf1Δ* and *gcn5Δ* glucose deprived stress granule formation was reduced, after 10 minutes of glucose deprivation, with both K131 mutants compared to wildtype *PAB1-GFP* (Figure S2A and S2E, respectively) and this was not reflective of a delay in stress granule formation (Figure S2B and S2F, respectively). Since *eaf1Δ* and *gcn5Δ PAB1-K131Q-GFP* cells are displaying the significant reduction just like *PAB1-K131R-GFP*, suggests that these KATs are likely not responsible for acetylation at K131.

The integrated mutants replicated plasmid findings in *rpd3Δ* cells. *PAB1-K131R-GFP* reduces glucose deprived stress granules, but the *PAB1-K131Q-GFP* was not significantly different from *PAB1-GFP* (Figure 8A). Moreover, this was not reflective of a delay in stress granule formation (Figure 8B).

Though *PAB1-K131Q-GFP* and *PAB1-K131R-GFP* did not impact protein levels in wild type cells (Figure 5), another possible reason that could explain the stress granule formation seen in *eaf1Δ, gcn5Δ, rpd3Δ,* are changes in protein levels. A quantitative western blot analysis was conducted between Pab1-GFP, Pab1-K131R-GFP, Pab1-K131Q-GFP with respective KAT/KDAC mutants under glucose repleted (YPD) or 10 minute glucose depleted

(YP) conditions. Although there were no significant differences between protein levels of Pab1-GFP, Pab1-K131R-GFP and Pab1-K131Q-GFP in *eaf1Δ* and *gcn5Δ* cells upon glucose depletion (Figure S2C-D and S2G-H, respectively), Pab1-GFP levels were significantly reduced in *rpd3Δ* independent of the K131 mutation (Figure 8C-D). This suggests that decreases in Pab1-GFP protein levels in *rpd3Δ* upon glucose deprivation may contribute to the decrease of glucose deprived SG formation in the *rpd3Δ* background, however protein levels do not contribute to the ability of *PAB1-K131R-GFP* to suppress defects in glucose deprived SG formation in *rpd3Δ* cells.

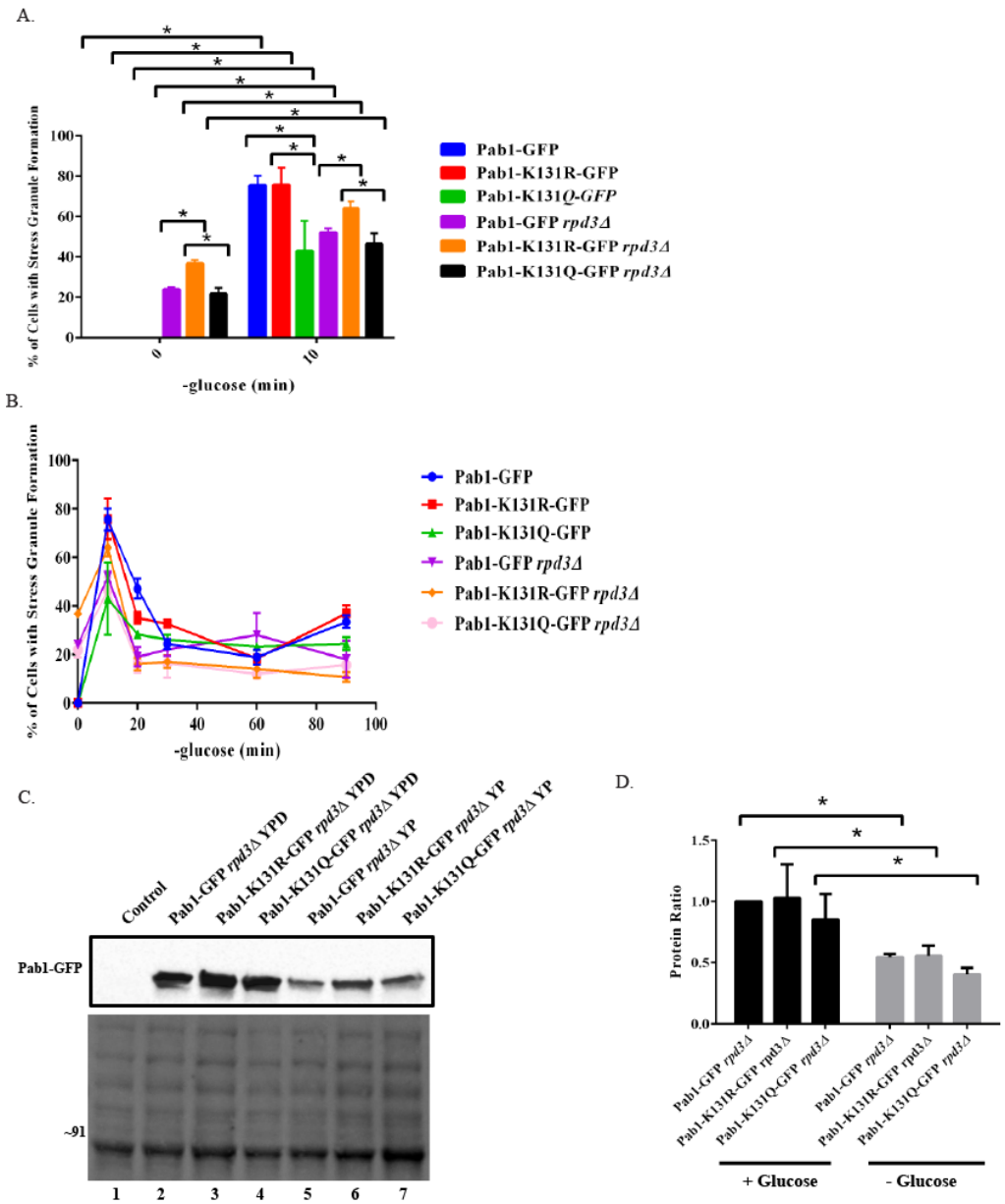

Figure 8: *rpd3Δ affects stress granule formation.* A) Quantitative analyses on the stress granule formation of 0-, 10 min of glucose deprivation in integrated *rpd3Δ PAB1-GFP* (YKB5142), *rpd3Δ PAB1-K131R-GFP* (YKB5143), *rpd3Δ PAB1-K131Q-GFP* (YKB5144) strains. B) Quantitative analyses on the stress granule formation of 0-, 10-, 20-, 30-, 60-, and 90- min of glucose deprivation in *rpd3Δ PAB1-GFP* (YKB5142), *rpd3Δ PAB1-K131R-GFP* (YKB5143), *rpd3Δ PAB1-K131Q-GFP* (YKB5144). C) Western blot analysis of wildtype *rpd3Δ* Pab1-GFP (YKB5142), *rpd3Δ* Pab1-K131R-GFP (YKB5143), *rpd3Δ* Pab1-K131Q-GFP (YKB5144) under glucose deprived/replete conditions. Quantitative western blot visualized on a nitrocellulose membrane. Lane 1 is a negative control. Lanes 2, 3, and 4 are strains in glucose replete media. Lanes 5, 6, and 7 are strains in glucose deprived media. Representative anti-GFP western blot (top panel) and total protein blot (bottom panel). D) Quantification of western blots for three independent biological replicates where the Pab1-GFP *rpd3Δ* band intensity was normalized to total protein. Results are the average of three biological replicates, a minimum of 100 cells per replicate were scored, error bars indicate SEM. *p<0.05 determined using a two-way ANOVA test.

3.6 Purification of Pab1 RRM1-RRM2 fragments

Two possible molecular mechanisms can occur with Pab1 mimics: affect the binding of eIF4G1 and/or affect the binding of the Poly(A) mRNA (Figure 9A). To decipher the molecular mechanism of eIF4G1 binding, an affinity purification took place (see Methods 2.8). To decipher the molecular mechanism of binding of poly(A) mRNA, electromobility shift assay took place (see Methods 2.9). In order to achieve a potential model, GST constructs, made by GenScript, were purified by following the GST purification protocol (see Methods 2.7). Further, 10 µL of samples from each step of the GST purification was taken to measure the efficacy of the purification (Figure 9B-E). Lastly, the fragments were concentrated and diluted to equal loading. These purified fragments are visualized under a Coomassie stain free gel (Figure 9F).

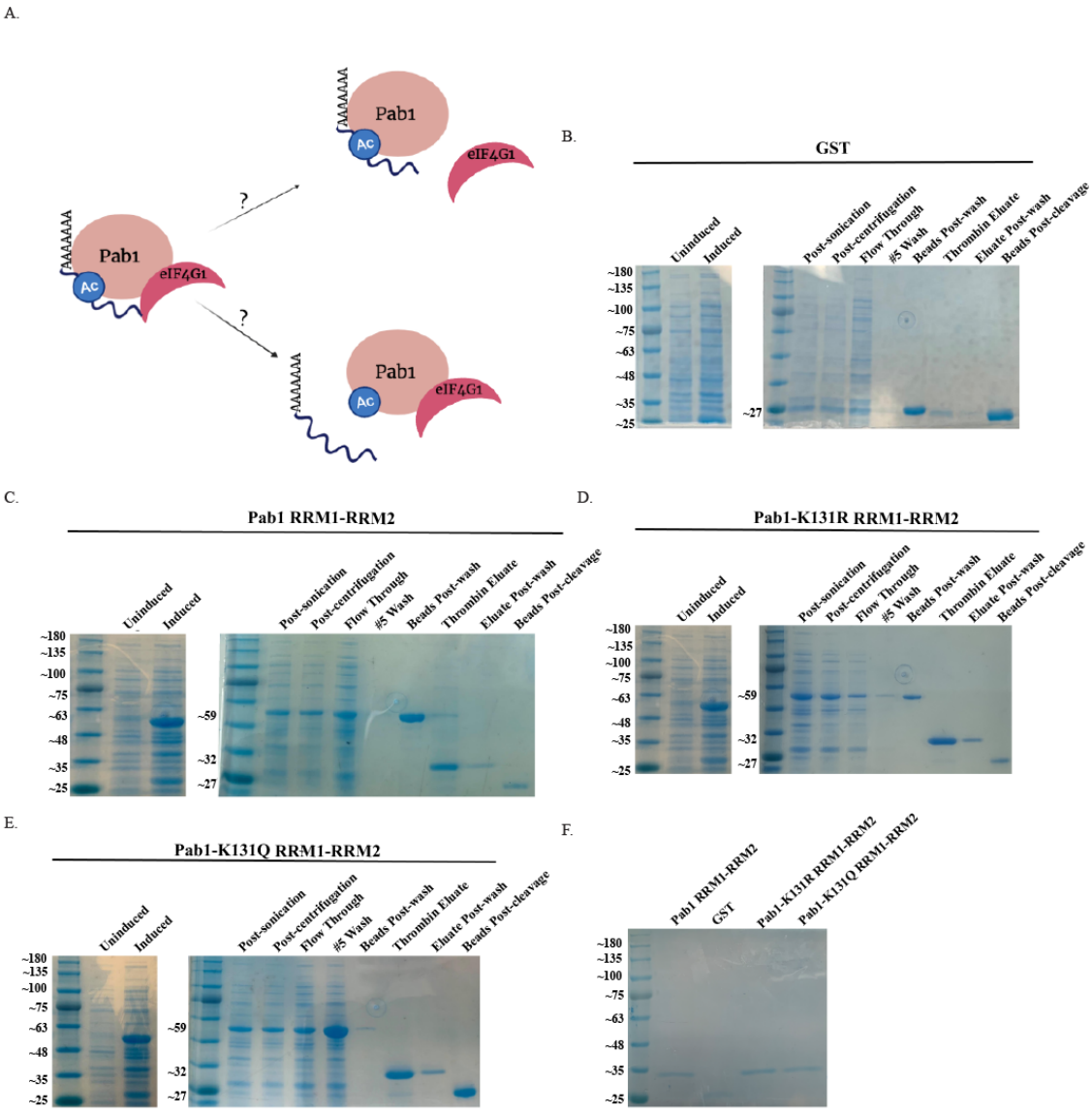

Figure 9*: Molecular mechanism of Pab1-K131 acetylation.* A) A schematic graphical representation of the potential causes of acetylation mimics of Pab1. Two potential causes that can be affected are the binding of eIF4G and/or the binding the Poly(A) mRNA. B) Each step from purifying empty GST vector was run on a Coomassie stain gel. C) Each step from purifying Pab1 RRM1-RRM2 fragment was run on a Coomassie stain gel. D) Each step from purifying Pab1-K131R RRM1-RRM2 fragment was run on a Coomassie stain gel. E) Each step from purifying Pab1-K131Q RRM1-RRM2 fragment was run on a Coomassie stain gel. F) GST (PKB 352), Pab1 RRM1-RRM2 *(*PKB 349), Pab1-K131R RRM1-RRM2 (PKB 350), and Pab1-K131Q RRM1-RRM2 (PKB 351) were concentrated, diluted to the same concentration, and ran on Coomassie stain gel.

3.7 Binding of eIF4G1-HA to Pab1 RRM1-RRM2 domain is not impacted by Pab1-K131 mutations

Previous work demonstrates that the RRM2 domain of Pab1 binds directly to eIF4G1, a binding component for mRNA translation (Kessler & Sachs 1998, Safaee et al., 2012). Moreover, eIF4G1 co-localizes in stress granules along with Pab1 (Brengues & Parker 2007, Hoyle et al., 2007). Hence I sought to determine if the Pab1-K131Q or Pab1-K131R mutants impacted interaction with eIF4G1.

Initially, co-immunoprecipitation was performed with glucose repleted conditions using whole cell extracts from Pab1-GFP, eIF4G1-HA, Pab1-K131R-GFP, Pab1-K131Q-GFP, Pab1-GFP eIF4G1-HA, Pab1-K131R-GFP eIF4G1-HA, and Pab1-K131Q-GFP eIF4G1-HA. Despite multiple attempts of optimization, I could not reduce background binding of eIF4G1-HA to either GFP sepharose or GFP magnetic beads (Figure S3).

As an alternative approach I opted to perform batch affinity purification using purified Glutathione S-transferase (GST) fragments of Pab1 RRM1-RRM2 domain (aa1 = 210) and whole cell extracts from WT and eIF4G1-HA expressing cells. *GST-PAB1 RRM1-RRM2*, *GST-PAB1-K131R RRM1-RRM2*, and *GST-PAB1-K131Q RRM1-RRM2* expression constructs were synthesized by GeneScript, expressed in *E.coli* and purified following a GST purification protocol (Figure 9B-F, see Methods 2.7). Each construct was confirmed by independent sequencing and importantly each construct produced similar levels of GST-fusion proteins (Figure 9F). For the batch affinity experiment, *GST-PAB1 RRM1-RRM2*, *GST-PAB1-K131R RRM1-RRM2*, and *GST-PAB1-K131Q RRM1-RRM2* were purified by a standard GST purification protocol but not cleaved by thrombin. Whole cell extracts from WT and eIF4G1-HA expressing cells were prepared from cultures grown in glucose replete media and subjected to 10 minutes of glucose depletion before harvesting as previously described (see Methods

2.8). Whole cell extracts were incubated with glutathione Sepharose bound with GST, GST-Pab1 RRM1-RRM2, GST-Pab1-K131R RRM1-RRM2, and GST-Pab1-K131Q RRM1-RRM2, for 2h at 4°C, prior to washes and analysis by western blot. Following incubation, samples were spun, and beads were collected to proceed with western blot procedure. There were no significant differences observed in binding of eIF4G1-HA regardless of mutant and glucose deprivation (Figure 10A-D). This suggests that the acetylation state of Pab1-K131 does not impact eIF4G1 interaction at least *in vitro*.

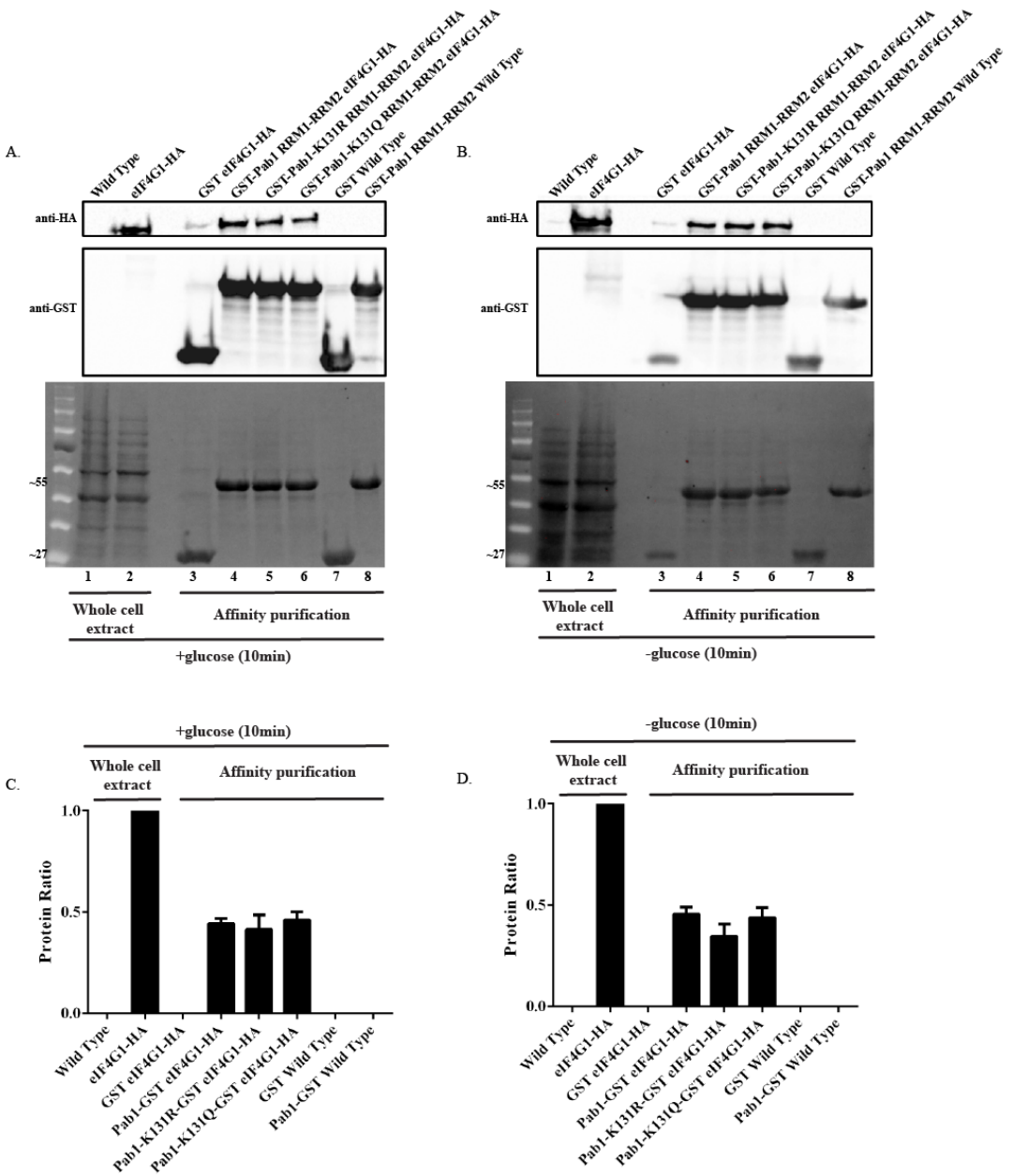

Figure 10*: K131 mutants do not impact eIF4G binding upon glucose deprivation.* A) Affinity purification analysis performed by incubating GST-Pab1 RRM1-RRM2 (PKB349), GST-Pab1-K131R RRM1-RRM2 (PKB350), and GST-Pab1-K131Q RRM1-RRM2 (PKB351) with eIF4G1-HA. Representative anti-HA western blot (top panel), anti-GST western blot (middle panel), and total protein blot (bottom panel). B) Affinity purification analysis performed by incubating GST-Pab1 RRM1-RRM2 (PKB349), GST-Pab1-K131R RRM1-RRM2 (PKB350), and GST-Pab1-K131Q RRM1-RRM2 (PKB351) with eIF4G1-HA after 10 minutes of glucose deprivation. Representative anti-HA western blot (top panel), anti-GST western blot (middle panel), and total protein blot (bottom panel). C) Quantification of western blots for three independent biological replicates, glucose repleted HA band intensity normalized to total protein. D) Quantification of western blots for three independent biological replicates, glucose depleted HA band intensity normalized to total protein. Error bars indicate SEM. Differences between the samples were proven to be insignificant through two-way ANOVA tests.

3.8 Preliminary results suggest Pab1-K131Q RRM1-RRM2 reduces the binding to poly(A) mRNA

Another possible molecular mechanism that may explain the changes in glucose deprived stress granule formation in *PAB1-K131Q-GFP* mutant is changes in Poly(A) RNA binding. Indeed, Pab1-K131 has been implicated in RNA binding (Deardorff and Sachs, 1997; Deo et al., 1999, Yao et al., 2007, Kuhn and Pieler, 1996). Hence, I performed electrophoretic mobility shift assays to determine if Pab1-K131 acetylation impact interaction with Poly(A) RNA. As previous Poly(A) Pab1 binding studies have utilized purified RRM1-RRM2 fusions (Yao et al., 2007), I thrombin cleaved the GST-Pab1 RRM1-RMM2 to produce Pab1 RRM1-RRM2 fragments (Figure 9B-E). Cy5-Poly(A)$_{20}$-Cy5 was incubated with Pab1 RRM1-RRM2, Pab1-K131R RRM1-RRM2, or Pab1-K131Q RRM1-RRM2 with either concentration of 0.4 nM, 4 nM, 40 nM, 400 nM, 800nM, 2000 nM, 4000nM, or 5000 nM of protein in a binding reaction at 30°C for 30 minutes prior to running a Native-PAGE gel. As previously shown, incubation of Cy5-Poly(A)$_{20}$-Cy5 with Pab1 RRM1-RRM2 results in a shift of the Cy5-Poly(A)$_{20}$-Cy5 band which can be competed away upon co-incubation with increasing amounts of untagged Poly(A)$_{20.}$ So far, this experiment has been completed two times with two biological replicates (Figure 11A-E and 11F-J, respectively). My preliminary results suggest that Pab1-K131R RRM1-RMM2 binds Cy5-Poly(A)$_{20}$-Cy5 similar to that of the WT Pab1 RRM1-RMM2 protein fragment. In contrast, Pab1-K131Q RRM1-RRM2 binding to Cy5-Poly(A)$_{20}$-Cy5 is dramatically reduced. This suggest that acetylation mimic at Pab1-K131 reduces its ability of Pab1 RRM1-RRM2 fragment to bind onto Poly(A) mRNA (Figure 11).

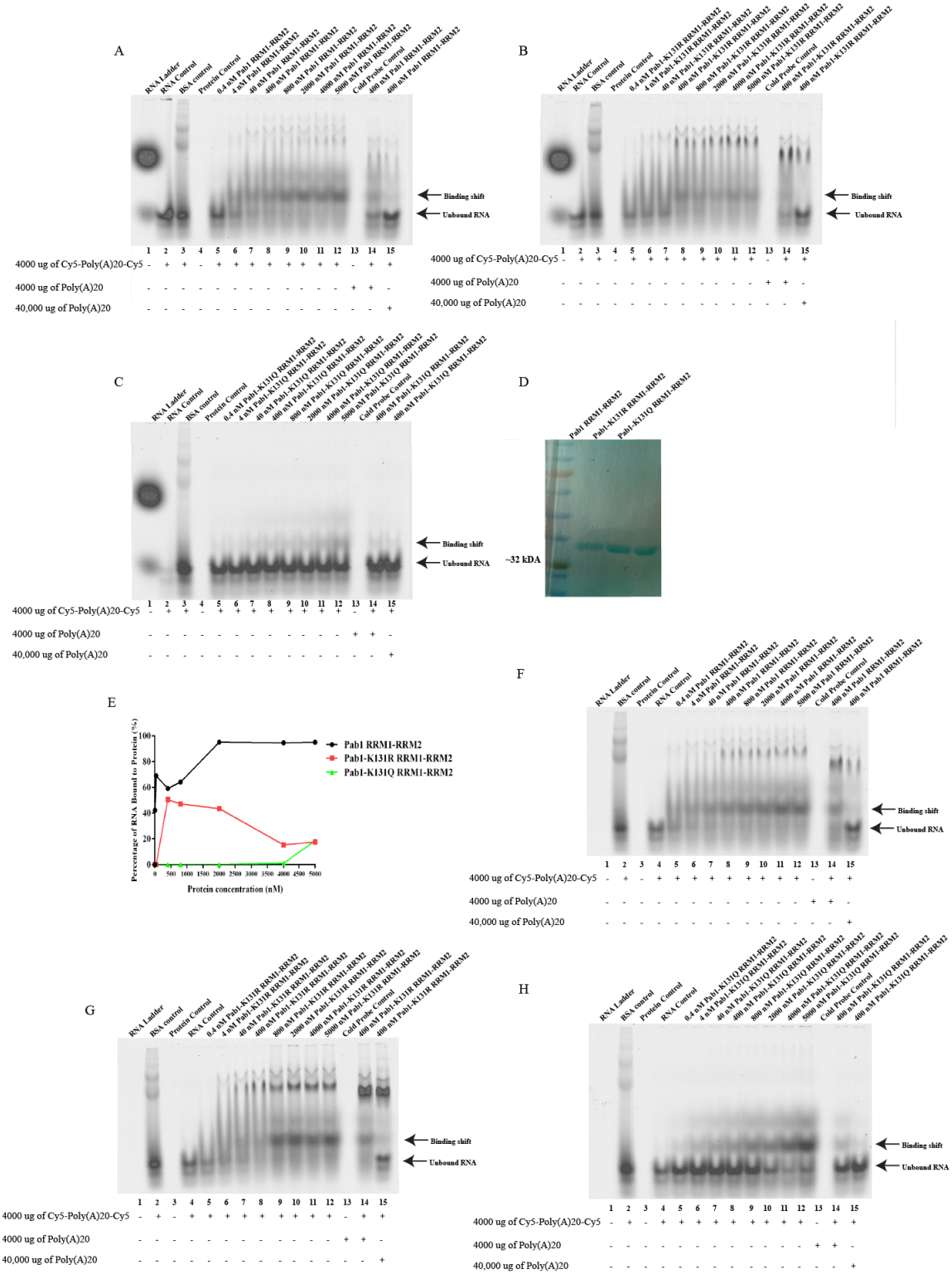
A
RNA Ladder
RNA Control
BSA control
Protein Control
0.4 nM Pab1 RRM1-RRM2
4 nM Pab1 RRM1-RRM2
40 nM Pab1 RRM1-RRM2
400 nM Pab1 RRM1-RRM2
800 nM Pab1 RRM1-RRM2
2000 nM Pab1 RRM1-RRM2
4000 nM Pab1 RRM1-RRM2
5000 nM Pab1 RRM1-RRM2
Cold Probe Control
400 nM Pab1 RRM1-RRM2
400 nM Pab1 RRM1-RRM2
Binding shift
Unbound RNA
1 2 3 4 5 6 7 8 9 10 11 12 13 14 15
4000 ug of Cy5-Poly(A)20-Cy5 - + + - + + + + + + + + - + +
4000 ug of Poly(A)20 - - - - - - - - - - - - + + -
40,000 ug of Poly(A)20 - - - - - - - - - - - - - - +
B
RNA Ladder
RNA Control
BSA control
Protein Control
0.4 nM Pab1-K131R RRM1-RRM2
4 nM Pab1-K131R RRM1-RRM2
40 nM Pab1-K131R RRM1-RRM2
400 nM Pab1-K131R RRM1-RRM2
800 nM Pab1-K131R RRM1-RRM2
2000 nM Pab1-K131R RRM1-RRM2
4000 nM Pab1-K131R RRM1-RRM2
5000 nM Pab1-K131R RRM1-RRM2
Cold Probe Control
400 nM Pab1-K131R RRM1-RRM2
400 nM Pab1-K131R RRM1-RRM2
Binding shift
Unbound RNA
1 2 3 4 5 6 7 8 9 10 11 12 13 14 15
4000 ug of Cy5-Poly(A)20-Cy5 - + + - + + + + + + + + - + +
4000 ug of Poly(A)20 - - - - - - - - - - - - + + -
40,000 ug of Poly(A)20 - - - - - - - - - - - - - - +
C
RNA Ladder
RNA Control
BSA control
Protein Control
0.4 nM Pab1-K131Q RRM1-RRM2
4 nM Pab1-K131Q RRM1-RRM2
40 nM Pab1-K131Q RRM1-RRM2
400 nM Pab1-K131Q RRM1-RRM2
800 nM Pab1-K131Q RRM1-RRM2
2000 nM Pab1-K131Q RRM1-RRM2
4000 nM Pab1-K131Q RRM1-RRM2
5000 nM Pab1-K131Q RRM1-RRM2
Cold Probe Control
400 nM Pab1-K131Q RRM1-RRM2
400 nM Pab1-K131Q RRM1-RRM2
Binding shift
Unbound RNA
1 2 3 4 5 6 7 8 9 10 11 12 13 14 15
4000 ug of Cy5-Poly(A)20-Cy5 - + + - + + + + + + + + - + +
4000 ug of Poly(A)20 - - - - - - - - - - - - + + -
40,000 ug of Poly(A)20 - - - - - - - - - - - - - - +
D
Pab1 RRM1-RRM2
Pab1-K131R RRM1-RRM2
Pab1-K131Q RRM1-RRM2
~32 kDA
E
Percentage of RNA Bound to Protein (%)
Protein concentration (nM)
Pab1 RRM1-RRM2
Pab1-K131R RRM1-RRM2
Pab1-K131Q RRM1-RRM2
F
RNA Ladder
BSA control
Protein Control
RNA Control
0.4 nM Pab1 RRM1-RRM2
4 nM Pab1 RRM1-RRM2
40 nM Pab1 RRM1-RRM2
400 nM Pab1 RRM1-RRM2
800 nM Pab1 RRM1-RRM2
2000 nM Pab1 RRM1-RRM2
4000 nM Pab1 RRM1-RRM2
5000 nM Pab1 RRM1-RRM2
Cold Probe Control
400 nM Pab1 RRM1-RRM2
400 nM Pab1 RRM1-RRM2
Binding shift
Unbound RNA
1 2 3 4 5 6 7 8 9 10 11 12 13 14 15
4000 ug of Cy5-Poly(A)20-Cy5 - + - + + + + + + + + + - + +
4000 ug of Poly(A)20 - - - - - - - - - - - - + + -
40,000 ug of Poly(A)20 - - - - - - - - - - - - - - +
G
RNA Ladder
BSA control
Protein Control
RNA Control
0.4 nM Pab1-K131R RRM1-RRM2
4 nM Pab1-K131R RRM1-RRM2
40 nM Pab1-K131R RRM1-RRM2
400 nM Pab1-K131R RRM1-RRM2
800 nM Pab1-K131R RRM1-RRM2
2000 nM Pab1-K131R RRM1-RRM2
4000 nM Pab1-K131R RRM1-RRM2
5000 nM Pab1-K131R RRM1-RRM2
Cold Probe Control
400 nM Pab1-K131R RRM1-RRM2
400 nM Pab1-K131R RRM1-RRM2
Binding shift
Unbound RNA
1 2 3 4 5 6 7 8 9 10 11 12 13 14 15
4000 ug of Cy5-Poly(A)20-Cy5 - + - + + + + + + + + + - + +
4000 ug of Poly(A)20 - - - - - - - - - - - - + + -
40,000 ug of Poly(A)20 - - - - - - - - - - - - - - +
H
RNA Ladder
BSA control
Protein Control
RNA Control
0.4 nM Pab1-K131Q RRM1-RRM2
4 nM Pab1-K131Q RRM1-RRM2
40 nM Pab1-K131Q RRM1-RRM2
400 nM Pab1-K131Q RRM1-RRM2
800 nM Pab1-K131Q RRM1-RRM2
2000 nM Pab1-K131Q RRM1-RRM2
4000 nM Pab1-K131Q RRM1-RRM2
5000 nM Pab1-K131Q RRM1-RRM2
Cold Probe Control
400 nM Pab1-K131Q RRM1-RRM2
400 nM Pab1-K131Q RRM1-RRM2
Binding shift
Unbound RNA
1 2 3 4 5 6 7 8 9 10 11 12 13 14 15
4000 ug of Cy5-Poly(A)20-Cy5 - + - + + + + + + + + + - + +
4000 ug of Poly(A)20 - - - - - - - - - - - - + + -
40,000 ug of Poly(A)20 - - - - - - - - - - - - - - +

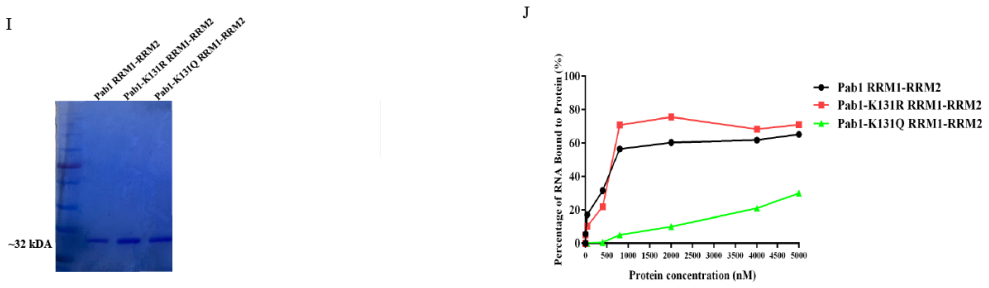

Figure 11*: Preliminary data indicate Pab1-K131Q RRM1-RRM2 reduces binding to poly(A) mRNA.* Electromobility shift assay were performed by incubating purified Pab1 RRM1-RRM2 (PKB349), Pab1-K131R RRM1-RRM2 (PKB350) or Pab1-K131Q RRM1-RRM2 (PKB351) at concentrations of 0.4-, 4-, 40-, 400-, 800-, 2000-, 4000-, and 5000nM with Cy5-Poly(A)$_{20}$-Cy5 mRNA in a binding reaction for 30 minutes at 30°C. For each fusion two unique purification were performed and here I present representative EMSA images from the two biological replicates for Pab1 RRM1-RRM2 (Panel A & F), Pab1-K131R RRM1-RRM2 (Panel B & G) and Pab1-K131Q RRM1-RRM2 (Panel C & H). For each ESMA Lane 1 is the RNA ladder, lane 2 is the Cy5-Poly(A)$_{20}$-Cy5 control (second biological replicate is in lane 4), lane 3 is the BSA control (second biological replicate is lane 2), lane 4 is the protein control (second biological replicate is lane 3), lane 5-12 is the titration of protein with Cy5-Poly(A)$_{20}$-Cy5 , lane 13 is cold probe control, lane 14 contains 1:1 ratio between Cy5-Poly(A)$_{20}$-Cy5 and cold probe, and lane 15 contains 1:10 ratio between Cy5-Poly(A)$_{20}$-Cy5 and cold probe. D and I) Coomassie stain SDS-PAGE gel of 12µg of Pab1 RRM1-RRM2, Pab1-K131R RRM1-RRM2, and Pab1-K131Q RRM1-RRM2. E and J) Relative RNA binding was quantified and each band was normalized to the relative known RNA band. Percentage of RNA binding to different concentrations of Pab1 RRM1-RRM2 frgments were computed.

4.0 Discussion

As Pab1 is an essential protein for SG formation and is a target of acetylation, it is important to understand the effect of Pab1 acetylation on stress granules dynamics. Here I show that the acetylation mimic *PAB1-K131Q-GFP* decreases stress granule formation upon glucose deprivation, ethanol, raffinose, and vanillin. Rpd3, an enzyme involved in lysine deacetylation, has a significant impact in regulating protein levels upon glucose deprivation, independent of mutation. Remarkably, my work indicates that acetylation mimic or unacetylated K131 mutants do not impact Pab1 cellular protein levels and interaction with eIF4G1, rather my work suggests acetylation at K131 may impact interaction with poly(A) RNA.

4.1 Acetylation mimic of PAB1-K131Q-GFP reduces stress granule formation of a subset of environmental stresses.

Intrigingly, my work indicates that the *PAB1-K131Q-GFP* mutant display reduced SG formation not just upon glucose deprivation (Figure 3 and 4) but also reduced SG formation on exposure to under ethanol, raffinose, and vanillin (Figure 6D). However, the acetylation mimic does not globally decrease SG formation as it has no discernable impact of SG formation upon heat shock and glycerol (Figure 6). It is certainly not unique idea that distinct acetylation code or acetylation dependent pathways regulate SG formation under distinct conditions. Indeed though mutants of NuA4 impact glucose deprived stress granule formation, this KAT does not appear to contribute heat stress SG formation (Rollins et al., 2017).

Though I have not presented evidence that acetylation state or sites on SG proteins change upon various stresses, global acetylome studies have shown massive acetylome remodelling upon many environmental changes, including starvation (Henriksen et al., 2012). How could

an acetylation code contribute to stress-dependent SG formation? Brambilla and colleagues (2017) showed that stress granule formation under heat shock and glucose deprivation is different. Glucose deprived stress granules relied on RRM1 and RRM2 domains of Pab1 (Brambilla et al., 2017). However, stress granules formed under heat shock also relied on the RRM3 domain of Pab1 (Brambilla et al., 2017). As lysine acetylation has an established role in regulating protein-protein interactions (Protter and Parker, 2016, Wheeler et al., 2016, Van Treeck et al., 2018), one possibility is that lysine acetylation sites and/or proteins that are acetylated not only change upon stresses, but regulate SG protein interactions. Indeed as discussed in the introduction, the composition SG proteins and RNA dramatically change from stress to stress. For example, Pbp1 and Pub1 are required for glucose deprived and ethanol-dependent stress granule formation but are not required for the formation of stress granules upon heat shock (Buchan, Muhlrad et al. 2008, Kato et al., 2011). Another example is eIF3 is found in stress granules upon heat shock but not in glucose deprived stress granules (Buchan, Muhlrad et al. 2008).

Could the *PAB1-K131Q-GFP* acetylation mimic be influencing stress dependent aggregation of proteins like Pbp1 and Pub1? Or the aggregation of other stress dependent factors that drive SG formation? Future studies should look at the effect of the acetylation state of Pab1-K131 protein interactions such as Pbp1 and Pub1. Further to truly discern if there truly is a SG "acetylation code" will require quantitative mass spectrometry approaches under various conditions.

4.2 Identification of KAT/KDACs impact stress granule formation upon acetylation mimic.

Given the central role that Pab1 plays in SG formation (Swisher and Parker, 2010) and my finding that *PAB1-K131Q*-GFP mutants decrease the formation of a subset of

environmentally induced SG, it is important to identify the KAT and KDAC enzymes involved in regulating the acetylation state of Pab1 specifically at K131. My genetic screen suggests that the KDAC Rpd3 maybe involved in regulation of Pab1-K131 acetylation under glucose deprivation. *rpd3Δ* cells displayed decreased stress granule formation upon glucose deprivation that was fully suppressed by *PAB1-K131R-GFP* and was epistatic with *PAB1-K131Q-GFP* (Figure 7D and 8A). Further, Rpd3 may be involved in regulation of protein levels of Pab1, independent of mutation (Figure 8C). Though *PAB1-K131Q-GFP* and *PAB1-K131R-GFP* did not impact protein levels in wild type cells (Figure 5), upon glucose depletion *PAB1-GFP* levels were significantly reduced in *rpd3Δ,* independent of mutation (Figure 8C and 8D). Given Rpd3 established role in transcription (Kadosh and Struhl, 1998, Nakajima et al., 2016, Biswas et al., 2008), a likely scenario is Rpd3 is regulating transcription of Pab1 under this stress. Regardless of the mechanism, the decrease in Pab1-GFP protein levels in *rpd3Δ* cannot explain fully the reduction for glucose deprived SG in this mutant, as the Pab1-K131R-GFP suppresses despite having a similar reduction in protein levels as Pab1-GFP and Pab1-K131Q-GFP.

My work suggests Rpd3 may be the KDAC responsible for deacetylation of Pab1-K131 and for robust formation of glucose deprived SG. It suggests a model where Pab1-K131 may be acetylated under non-stress conditions, contributing to the inhibition of SG formation under non-stress conditions. However, upon glucose deprivation Pab1-K131 needs to be deacetylated by Rpd3 for full SG formation to occur. As noted above, *Pab1-K131Q-GFP* can still from glucose deprived SGs, albeit at a lower rate, which suggests this is just one signaling pathway contributing to glucose deprived SG formation. Further work will be required to test this theory, including stress granule formation under other stressors in *rpd3Δ* cells. While we know that Pab1-K131 acetylation state may also contribute to SG formation under ethanol, raffinose,

and vanillin, we do not know if Rpd3 is also implicated in regulating SG formation for these stresses.

What is the KAT required for Pab1-K131 acetylation? I anticipated that the deletion mutant of the KAT(s) responsible for Pab1-K131 acetylation would have increased SGs that would be suppressed by *PAB1-K131Q* (acetylation mimic) (Figure 7B). However, none of the KAT mutants screened displayed this phenotype, including *eaf1Δ* and *gcn5Δ* which have both been implicated in the formation of SG under glucose deprivation. While it may be counter-intuitive that a KAT(s) required for glucose deprived SG formation may also have a role in inhibition or disassembly of glucose deprived SG, could these KATs have both an activating and inactivating role? My work suggests this is unlikely as *PAB1-K131Q* did not rescue any of the SG formation defects. To find the KAT(s) responsible may require the systematic assessment of not just all KATs in yeast, but potentially double and triple mutants. Future studies should look at *rpd3Δ* of double mutants with KATs *eaf1Δ* and *gcn5Δ.*

4.3 Molecular mechanisms of Pab1-K131 acetylation

RNA recognition motif (RRM) is a common protein domain with roles in post-transcriptional processes such as pre-mRNA processing, mRNA nuclear export, translational regulation, and mRNA decay (Maris et al., 2005, Erkmann and Kutay, 2004, Deschenes-Furry et al., 2006). Pab1 has 4 RRMs that are highly conserved among cytoplasmic Pab1 family of proteins. The RRM domains associate directly with the RNA molecule, and mediate protein-protein interactions. For example, Pab1 RRM2 domain mediate the association with eIF4G1 initiation complex that is required for the closed-loop structure between the mRNA cap and poly(A) tail for translation (Sachs et al., 1997, Tarun and Sachs, 1997, Wells et al., 1998, Amrani et al., 2006, Safaee et al., 2012). Pab1 RRM1-RRM2 are more important for the

binding of the poly(A) tail while RRM3-RRM4 domains are more important for the binding of the poly(U) tail. The RRM2 domain has the highest affinity and specificity for poly(A) RNA (Deardorff and Sachs, 1997). Further studies showed that RRM2 of Pab1 in association with eIF4G1 is a prerequisite for poly(A) tail-dependent translation and that their interaction, along with other regions of Pab1, are needed for stimulation (Kessler and Sachs, 1998).

As previously mentioned, eIF4G1 is an initiation complex of mRNA translation that is required for binding onto Pab1 on the RRM2 domain (Gallie, 2014). Furthermore, upon glucose deprivation, eIF4G1 co-localized in stress granules with Pab1 (Buchan et al., 2008; Yang et al., 2014). Through affinity purification analysis, I determined that GST-Pab1 RRM1-RRM2, GST-Pab1-K131R RRM1-RRM2, GST-Pab1-K131Q RRM1-RRM2 fragments equally purified eIF4G1-HA (Figure 10). This is not unexpected as previous studies indicated eIF4G1 binds to residues 184-186 on Pab1 (Young, 2016).

Previous mutational scan studies have shown that the Pab1-K131 is sensitive to almost all amino acid substitutions and that this site directly bound to RNA (Melamed et al., 2013). One possible reason for the reduction of glucose deprived stress granules is that Pab1-K131 acetylation might have disrupted the interaction with RNA failing to aggregate the proteins into stress granules. Furthermore, since RNA binding domain is located on RRM2 of Pab1 (Deardorff and Sachs, 1997; Deo et al., 1999; Yao et al., 2007, Kuhn and Pieler, 1996) it is also important to look at the impact of RNA binding in the acetylation mimic of Pab1-K131. Based on my hypothesis, I predicted that non-acetylated mimic (R) has a stronger binding affinity compared to acetylated mimic (Q) because since RNA phosphate backbone is associated with a strong negative electrostatic field, interactions with positively charged residues are more likely to occur (Law et al., 2006). Indeed, my preliminary electromobility shift assays showed that Pab1-K131 acetylation mimic (Q) has a reduced ability to bind onto

poly(A) mRNA .

Originally, I anticipated the non-acetylated mimic Pab1-K131 to behave in the same pattern as the WT. However, Pab1-K131R RRM1-RRM2 binds to Poly(A)$_{20}$ mRNA more efficiently than the WT. This can be due to several reasons: (i) due to the size of the side chain of arginine, it might be interacting with other residues thus increasing the efficiency of poly(A) mRNA binding, (ii) changes in protein conformation, although this possibility is least likely due to a stable secondary structure, (iii) increased NH_2 of arginine disturbing hydrogen bonds that is needed to stabilize poly(A) binding.

Based on molecular structure predictions SIFT (SIFT online) showed that any mutation on K131 is unfavourable. Moreover, Missense3D predictions (Missense3D portal online) and Dynamut predictions (Dynamut: Prediction Submission; Figure S5) showed that non-acetylated mimic (R) breaks the original salt bridge bond between K131 to D208 and creates salt bridges between R131 to E251. It also creates multiple hydrogen bounds around its side chain: R131-E206, R131-D208, R131-E251 around NH_1, and R131-E206, R131-D208 around NH_2. Whereas acetylated mimic (Q) breaks the original salt bridge bond without replacing with a new salt bridge, and no hydrogen bonds are formed. This could explain that non-acetylated mimic (R) has a higher affinity to the poly(A) mRNA compared to acetylated mimic (Q), although similar results are not seen under WT.

Due to decreased stress granule formation under acetylation mimic of Pab1-K131, the fate of the RNA is unknown: it can be either shuttled to processing bodies or back into translation. Future studies should decipher the fate of mRNA due to acetylation mimic of Pab1-K131.

5.0 Conclusion

This study is crucial to understand the importance of the assembly/disassembly of the formation of stress granules, the molecules involved in these processes and organelle regulation dynamics. Stress granules have been implicated in various diseases, from ALS to cancer. Understanding the importance of the assembly of stress granules will be useful when exploring potential treatment options for such diseases. By mimicking the acetylation site of Pab1-K131, I showed a significant decrease in the stress granules formed under glucose deprivation. The KDAC enzyme Rpd3 may be a part of this role by affecting the Pab1 cellular protein levels. Moreover, acetylation mimic of Pab1-K131 reduces its ability to bind onto RNA, showing that acetylation of this lysine residue is pivotal in the regulation of stress granule dynamics.

6.0 References

AKA, J. A., KIM, G. W. & YANG, X. J. 2011. K-acetylation and its enzymes: overview and new developments. *Handb Exp Pharmacol,* 206**,** 1-12.

ALLARD, S., UTLEY, R. T., SAVARD, J., CLARKE, A., GRANT, P., BRANDL, C. J., PILLUS, L., WORKMAN, J. L. & COTE, J. 1999. NuA4, an essential transcription adaptor/histone H4 acetyltransferase complex containing Esa1p and the ATM-related cofactor Tra1p. *EMBO J,* 18**,** 5108-19.

AMRANI, N., SACHS, M. S. & JACOBSON, A. 2006. Early nonsense: mRNA decay solves a translational problem. Nat Rev Mol Cell Biol, 7, 415-25.

ANDERSON, P. & KEDERSHA, N. 2006. RNA granules. *The Journal of cell biology,* 172**,** 803-8.

ANDERSON, P. & KEDERSHA, N. 2008. Stress granules: the Tao of RNA triage. *Trends Biochem Sci,* 33**,** 141-50.

ANDERSON, P. & KEDERSHA, N. 2009. RNA granules: post-transcriptional and epigenetic modulators of gene expression. *Nat Rev Mol Cell Biol,* 10**,** 430-6.

ANGUS-HILL, M. L., DUTNALL, R. N., TAFROV, S. T., STERNGLANZ, R. & RAMAKRISHNAN, V. 1999. Crystal structure of the histone acetyltransferase Hpa2: A tetrameric member of the Gcn5-related N-acetyltransferase superfamily. *J Mol Biol,* 294**,** 1311-25.

ARIMOTO, K., FUKUDA, H., IMAJOH-OHMI, S., SAITO, H. & TAKEKAWA, M. 2008. Formation of stress granules inhibits apoptosis by suppressing stress-responsive MAPK pathways. *Nat Cell Biol,* 10**,** 1324-32.

AUGER, A., GALARNEAU, L., ALTAF, M., NOURANI, A., DOYON, Y., UTLEY, R. T., CRONIER, D., ALLARD, S. & COTE, J. 2008. Eaf1 is the platform for NuA4 molecular assembly that evolutionarily links chromatin acetylation to ATP-dependent exchange of histone H2A variants. *Mol Cell Biol,* 28**,** 2257-70.

BABIARZ, J. E., HALLEY, J. E. & RINE, J. 2006. Telomeric heterochromatin boundaries require NuA4-dependent acetylation of histone variant H2A.Z in Saccharomyces cerevisiae. *Genes Dev,* 20**,** 700-10.

BERNSTEIN, B. E., TONG, J. K. & SCHREIBER, S. L. 2000. Genomewide studies of histone deacetylase function in yeast. Proc Natl Acad Sci U S A, 97, 13708-13.

BISWAS, D., TAKAHATA, S. & STILLMAN, D. J. 2008. Different genetic functions for the Rpd3(L) and Rpd3(S) complexes suggest competition between NuA4 and Rpd3(S). *Mol Cell Biol,* 28**,** 4445-58.

BOUDREAULT, A. A., CRONIER, D., SELLECK, W., LACOSTE, N., UTLEY, R. T., ALLARD, S., SAVARD, J., LANE, W. S., TAN, S. & COTE, J. 2003. Yeast enhancer of polycomb defines global Esa1-dependent acetylation of chromatin. *Genes Dev,* 17**,** 1415-28.

BRADFORD, M. M. 1976. A rapid and sensitive method for the quantitation of microgram quantities of protein utilizing the principle of protein-dye binding. *Anal Biochem,* 72**,** 248-54.

BRAMBILLA, M., MARTANI, F. & BRANDUARDI, P. 2017. The recruitment of the Saccharomyces cerevisiae poly(A)-binding protein into stress granules: new insights into the contribution of the different protein domains. *FEMS Yeast Res,* 17. DOI: 10.1093/femsyr/fox059

BRENGUES, M., PARKER, R. (2007). Accumulation of polyadenylated mRNA, Pab1p, eIF4E, and eIF4G with P-bodies in Saccharomyces cerevisiae. *Mol Cell Biol*, 18, 2592-2602.

BROOK, M., MCCRACKEN, L., REDDINGTON, J. P., LU, Z. L., MORRICE, N. A. & GRAY, N. K. 2012. The multifunctional poly(A)-binding protein (PABP) 1 is subject to extensive dynamic post-translational modification, which molecular modelling suggests plays an important role in co-ordinating its activities. *Biochem J,* 441**,** 803-12.

BRANGWYNNE, C. P. 2013. Phase transitions and size scaling of membrane-less organelles. *The Journal of cell biology,* 203**,** 875-81.

BRUNE, C., MUNCHEL, S. E., FISCHER, N., PODTELEJNIKOV, A. V. & WEIS, K. 2005. Yeast poly(A)-binding protein Pab1 shuttles between the nucleus and the cytoplasm and functions in mRNA export. *RNA,* 11**,** 517-31.

BUCHAN, J. R., KOLAITIS, R. M., TAYLOR, J. P. & PARKER, R. 2013. Eukaryotic stress granules are cleared by autophagy and Cdc48/VCP function. *Cell,* 153**,** 1461-74.

BUCHAN, J. R., MUHLRAD, D. & PARKER, R. 2008. P bodies promote stress granule assembly in Saccharomyces cerevisiae. *The Journal of cell biology,* 183**,** 441-55.

BUCHAN, J. R., NISSAN, T. & PARKER, R. 2010. Analyzing P-bodies and stress granules in Saccharomyces cerevisiae. *Methods Enzymol,* 470**,** 619-40.

BUCHAN, J. R. & PARKER, R. 2009. Eukaryotic stress granules: the ins and outs of translation. *Mol Cell,* 36**,** 932-41.

CASTELLANI, R. J., GUPTA, Y., SHENG, B., SIEDLAK, S. L., HARRIS, P. L., COLLER, J. M., PERRY, G., LEE, H. G., TABATON, M., SMITH, M. A., WANG, X. & ZHU, X. 2011. A novel origin for granulovacuolar degeneration in aging and Alzheimer's disease: parallels to stress granules. *Lab Invest,* 91**,** 1777-86.

CIPOLAT MIS, M. S., BRAJKOVIC, S., FRATTINI, E., DI FONZO, A. & CORTI, S. 2016. Autophagy in motor neuron disease: Key pathogenetic mechanisms and therapeutic targets. *Mol Cell Neurosci,* 72**,** 84-90.

CLARKE, A. S., LOWELL, J. E., JACOBSON, S. J. & PILLUS, L. 1999. Esa1p is an essential histone acetyltransferase required for cell cycle progression. Mol Cell Biol, 19, 2515-26.

DEARDORFF, J. A. & SACHS, A. B. 1997. Differential effects of aromatic and charged residue substitutions in the RNA binding domains of the yeast poly(A)-binding protein. *J Mol Biol,* 269**,** 67-81.

DE LEEUW, F., ZHANG, T., WAUQUIER, C., HUEZ, G., KRUYS, V. & GUEYDAN, C. 2007. The cold-inducible RNA-binding protein migrates from the nucleus to cytoplasmic stress granules by a methylation-dependent mechanism and acts as a translational repressor. *Exp Cell Res,* 313**,** 4130-44.

DECKER, C. J. & PARKER, R. 2012. P-bodies and stress granules: possible roles in the control of translation and mRNA degradation. *Cold Spring Harb Perspect Biol,* 4**,** a012286.

DESCHENES-FURRY, J., PERRONE-BIZZOZERO, N. & JASMIN, B. J. 2006. The RNA-binding protein HuD: a regulator of neuronal differentiation, maintenance and plasticity. *Bioessays,* 28**,** 822-33.

DEO, R. C., BONANNO, J. B., SONENBERG, N. & BURLEY, S. K. 1999. Recognition of polyadenylate RNA by the poly(A)-binding protein. *Cell,* 98**,** 835-45.

DOYON, Y., SELLECK, W., LANE, W. S., TAN, S. & COTE, J. 2004. Structural and functional conservation of the NuA4 histone acetyltransferase complex from yeast to humans. *Mol Cell Biol,* 24**,** 1884-96.

DRAZIC, A., MYKLEBUST, L. M., REE, R. & ARNESEN, T. 2016. The world of protein acetylation. *Biochim Biophys Acta,* 1864**,** 1372-401.

Dynamut: Prediction Submission. Biosig.unimelb.edu.au, http://biosig.unimelb.edu.au/dynamut/prediction.

EBERHARTER, A., JOHN, S., GRANT, P. A., UTLEY, R. T. & WORKMAN, J. L. 1998. Identification and analysis of yeast nucleosomal histone acetyltransferase complexes. *Methods,* 15**,** 315-21.

EHRENHOFER-MURRAY, A. E., RIVIER, D. H. & RINE, J. 1997. The role of Sas2, an acetyltransferase homologue of Saccharomyces cerevisiae, in silencing and ORC function. *Genetics,* 145**,** 923-34.

ELBAUM-GARFINKLE, S., KIM, Y., SZCZEPANIAK, K., CHEN, C. C., ECKMANN, C. R., MYONG, S. & BRANGWYNNE, C. P. 2015. The disordered P granule protein LAF-1 drives phase separation into droplets with tunable viscosity and dynamics. *Proc Natl Acad Sci U S A,* 112**,** 7189-94.

ERKMANN, J. A. & KUTAY, U. 2004. Nuclear export of mRNA: from the site of transcription to the cytoplasm. *Exp Cell Res,* 296**,** 12-20.

FERIC, M., VAIDYA, N., HARMON, T. S., MITREA, D. M., ZHU, L., RICHARDSON, T. M., KRIWACKI, R. W., PAPPU, R. V. & BRANGWYNNE, C. P. 2016. Coexisting Liquid Phases Underlie Nucleolar Subcompartments. *Cell,* 165**,** 1686-1697.

FOURNIER, M. J., COUDERT, L., MELLAOUI, S., ADJIBADE, P., GAREAU, C., COTE, M. F., SONENBERG, N., GAUDREAULT, R. C. & MAZROUI, R. 2013. Inactivation of the mTORC1-eukaryotic translation initiation factor 4E pathway alters stress granule formation. *Mol Cell Biol,* 33**,** 2285-301.

GALDIERI, L., ZHANG, T., ROGERSON, D., LLESHI, R. & VANCURA, A. 2014. Protein acetylation and acetyl coenzyme a metabolism in budding yeast. *Eukaryot Cell,* 13**,** 1472-83.

GALLIE, D. R. 2014. The role of the poly(A) binding protein in the assembly of the Cap-binding complex during translation initiation in plants. *Translation (Austin),* 2**,** e959378. DOI: 10.4161/2169074X.2014.959378

GINSBERG, S. D., GALVIN, J. E., CHIU, T. S., LEE, V. M., MASLIAH, E. & TROJANOWSKI, J. Q. 1998. RNA sequestration to pathological lesions of neurodegenerative diseases. Acta Neuropathol, 96, 487-94.

GLOZAK, M. A., SENGUPTA, N., ZHANG, X. & SETO, E. 2005. Acetylation and deacetylation of non-histone proteins. *Gene,* 363**,** 15-23.

GOULET, I., BOISVENUE, S., MOKAS, S., MAZROUI, R. & COTE, J. 2008. TDRD3, a novel Tudor domain-containing protein, localizes to cytoplasmic stress granules. *Hum Mol Genet,* 17**,** 3055-74.

GRANT, P. A., DUGGAN, L., COTE, J., ROBERTS, S. M., BROWNELL, J. E., CANDAU, R., OHBA, R., OWEN-HUGHES, T., ALLIS, C. D., WINSTON, F., BERGER, S. L. & WORKMAN, J. L. 1997. Yeast Gcn5 functions in two multisubunit complexes to acetylate nucleosomal histones: characterization of an Ada complex and the SAGA (Spt/Ada) complex. *Genes Dev,* 11**,** 1640-50.

GREGORETTI, I. V., LEE, Y. M. & GOODSON, H. V. 2004. Molecular evolution of the histone deacetylase family: functional implications of phylogenetic analysis. *J Mol Biol,* 338**,** 17-31.

HENRIKSEN, P., WAGNER, S. A., WEINERT, B. T., SHARMA, S., BACINSKAJA, G., REHMAN, M., JUFFER, A. H., WALTHER, T. C., LISBY, M. & CHOUDHARY, C. 2012. Proteome-wide analysis of lysine acetylation suggests its broad regulatory scope in Saccharomyces cerevisiae. *Mol Cell Proteomics,* 11**,** 1510-22.

HILLIKER, A., GAO, Z., JANKOWSKY, E. & PARKER, R. 2011. The DEAD-box protein Ded1 modulates translation by the formation and resolution of an eIF4F-mRNA complex. *Mol Cell,* 43**,** 962-72.

HOUSELEY, J., RUBBI, L., GRUNSTEIN, M., TOLLERVEY, D. & VOGELAUER, M. 2008. A ncRNA modulates histone modification and mRNA induction in the yeast GAL gene cluster. Mol Cell, 32, 685-95.

HOYLE, N. P., CASTELLI, L. M., CAMPBELL, S. G., HOLMES, L. E. & ASHE, M. P. 2007. Stress-dependent relocalization of translationally primed mRNPs to cytoplasmic granules that are kinetically and spatially distinct from P-bodies. *The Journal of cell biology,* 179**,** 65-74.

ImageQuant TL 8.2 Image Analysis Software. Cytiva, https://www.cytivalifesciences.com/en/us/shop/molecular-biology/nucleic-acid-electrophoresis--blotting--and-detection/molecular-imaging-for-nucleic-acids/imagequant-tl-8-2-image-analysis-software-p-09518.

ITO, D. & SUZUKI, N. 2011. Conjoint pathologic cascades mediated by ALS/FTLD-U linked RNA-binding proteins TDP-43 and FUS. Neurology, 77, 1636-43.

IWAKI, A., OHNUKI, S., SUGA, Y., IZAWA, S. & OHYA, Y. 2013. Vanillin inhibits translation and induces messenger ribonucleoprotein (mRNP) granule formation in saccharomyces cerevisiae: application and validation of high-content, image-based profiling. *PLoS One,* 8**,** e61748. DOI: 10.1371/journal/pone.0061748

JAIN, S., WHEELER, J. R., WALTERS, R. W., AGRAWAL, A., BARSIC, A. & PARKER, R. 2016. ATPase-Modulated Stress Granules Contain a Diverse Proteome and Substructure. *Cell,* 164**,** 487-98.

KADOSH, D. & STRUHL, K. 1998. Histone deacetylase activity of Rpd3 is important for transcriptional repression in vivo. *Genes Dev,* 12**,** 797-805.

KAMIENIARZ, K. & SCHNEIDER, R. 2009. Tools to tackle protein acetylation. *Chem Biol,* 16**,** 1027-9.

KATO, K., YAMAMOTO, Y. & IZAWA, S. 2011. Severe ethanol stress induces assembly of stress granules in Saccharomyces cerevisiae. *Yeast,* 28**,** 339-47.

KEDERSHA, N., CHEN, S., GILKS, N., LI, W., MILLER, I. J., STAHL, J. & ANDERSON, P. 2002. Evidence that ternary complex (eIF2-GTP-tRNA(i)(Met))-deficient preinitiation complexes are core constituents of mammalian stress granules. *Mol Biol Cell,* 13**,** 195-210.

KEDERSHA, N., CHO, M. R., LI, W., YACONO, P. W., CHEN, S., GILKS, N., GOLAN, D. E. & ANDERSON, P. 2000. Dynamic shuttling of TIA-1 accompanies the recruitment of mRNA to mammalian stress granules. *The Journal of cell biology,* 151**,** 1257-68.

KEDERSHA, N. L., GUPTA, M., LI, W., MILLER, I. & ANDERSON, P. 1999. RNA-binding proteins TIA-1 and TIAR link the phosphorylation of eIF-2 alpha to the assembly of mammalian stress granules. *The Journal of cell biology,* 147**,** 1431-42.

KEOGH, M. C., MENNELLA, T. A., SAWA, C., BERTHELET, S., KROGAN, N. J., WOLEK, A., PODOLNY, V., CARPENTER, L. R., GREENBLATT, J. F., BAETZ, K. & BURATOWSKI, S. 2006. The Saccharomyces cerevisiae histone H2A variant Htz1 is acetylated by NuA4. *Genes Dev,* 20**,** 660-5.

KESSLER, S. H., & SACHS, A. B. (1998). RNA recognition motif 2 of yeast Pab1p is required for its functional interaction with eukaryotic translation initiation factor 4G. *Mol Cell Biol*, 18, 51-57.

KHONG, A., JAIN, S., MATHENY, T., WHEELER, J. R. & PARKER, R. 2018. Isolation of mammalian stress granule cores for RNA-Seq analysis. *Methods,* 137**,** 49-54.

KLEFF, S., ANDRULIS, E. D., ANDERSON, C. W. & STERNGLANZ, R. 1995. Identification of a gene encoding a yeast histone H4 acetyltransferase. *J Biol Chem,* 270**,** 24674-7.

KNUTSEN, J. H., RODLAND, G. E., BOE, C. A., HALAND, T. W., SUNNERHAGEN, P., GRALLERT, B. & BOYE, E. 2015. Stress-induced inhibition of translation independently of eIF2alpha phosphorylation. *J Cell Sci,* 128**,** 4420-7.

KUECHLER, E. R., BUDZYNSKA, P. M., BERNARDINI, J. P., GSPONER, J. & MAYOR, T. 2020. Distinct Features of Stress Granule Proteins Predict Localization in Membraneless Organelles. *J Mol Biol,* 432**,** 2349-2368.

KUHN, U. & PIELER, T. 1996. Xenopus poly(A) binding protein: functional domains in RNA binding and protein-protein interaction. J Mol Biol, 256, 20-30.

KUHN, U. & WAHLE, E. 2004. Structure and function of poly(A) binding proteins. *Biochim Biophys Acta,* 1678**,** 67-84.

KWON, S., ZHANG, Y. & MATTHIAS, P. 2007. The deacetylase HDAC6 is a novel critical component of stress granules involved in the stress response. *Genes Dev,* 21**,** 3381-94.

LAFON, A., CHANG, C. S., SCOTT, E. M., JACOBSON, S. J. & PILLUS, L. 2007. MYST opportunities for growth control: yeast genes illuminate human cancer gene functions. Oncogene, 26, 5373-84.

LAW, M. J., LINDE, M. E., CHAMBERS, E. J., OUBRIDGE, C., KATSAMBA, P. S., NILSSON, L., HAWORTH, I. S. & LAIRD-OFFRINGA, I. A. 2006. The role of positively charged amino acids and electrostatic interactions in the complex of U1A protein and U1 hairpin II RNA. Nucleic Acids Res, 34, 275-85.

LAMBERT, J. P., MITCHELL, L., RUDNER, A., BAETZ, K. & FIGEYS, D. 2009. A novel proteomics approach for the discovery of chromatin-associated protein networks. *Mol Cell Proteomics,* 8**,** 870-82.

LEE, K. K. & WORKMAN, J. L. 2007. Histone acetyltransferase complexes: one size doesn't fit all. *Nat Rev Mol Cell Biol,* 8**,** 284-95.

LI, Y. R., KING, O. D., SHORTER, J. & GITLER, A. D. 2013. Stress granules as crucibles of ALS pathogenesis. *J Cell Biol,* 201**,** 361-72.

LIN, Y., PROTTER, D. S., ROSEN, M. K. & PARKER, R. 2015. Formation and Maturation of Phase-Separated Liquid Droplets by RNA-Binding Proteins. *Mol Cell,* 60**,** 208-19.

LIN, Y. Y., LU, J. Y., ZHANG, J., WALTER, W., DANG, W., WAN, J., TAO, S. C., QIAN, J., ZHAO, Y., BOEKE, J. D., BERGER, S. L. & ZHU, H. 2009. Protein acetylation microarray reveals that NuA4 controls key metabolic target regulating gluconeogenesis. *Cell,* 136**,** 1073-84.

LONGTINE, M. S., MCKENZIE, A., 3RD, DEMARINI, D. J., SHAH, N. G., WACH, A., BRACHAT, A., PHILIPPSEN, P. & PRINGLE, J. R. 1998. Additional modules for versatile and economical PCR-based gene deletion and modification in Saccharomyces cerevisiae. *Yeast,* 14**,** 953-61.

LOSCHI, M., LEISHMAN, C. C., BERARDONE, N. & BOCCACCIO, G. L. 2009. Dynein and kinesin regulate stress-granule and P-body dynamics. *J Cell Sci,* 122**,** 3973-82.

LUO, Y., NA, Z. & SLAVOFF, S. A. 2018. P-Bodies: Composition, Properties, and Functions. *Biochemistry,* 57**,** 2424-2431.

MANGUS, D. A., SMITH, M. M., MCSWEENEY, J. M. & JACOBSON, A. 2004. Identification of factors regulating poly(A) tail synthesis and maturation. *Mol Cell Biol,* 24**,** 4196-206.

MARIS, C., DOMINGUEZ, C. & ALLAIN, F. H. 2005. The RNA recognition motif, a plastic RNA-binding platform to regulate post-transcriptional gene expression. *FEBS J,* 272**,** 2118-31.

MARTANI, F., MARANO, F., BERTACCHI, S., PORRO, D. & BRANDUARDI, P. 2015. The Saccharomyces cerevisiae poly(A) binding protein Pab1 as a target for eliciting stress tolerant phenotypes. *Sci Rep,* 5**,** 18318.

MATTENBERGER, F., SABATER-MUNOZ, B., HALLSWORTH, J. E. & FARES, M. A. 2017. Glycerol stress in Saccharomyces cerevisiae: Cellular responses and evolved adaptations. *Environ Microbiol,* 19**,** 990-1007.

MCDANIEL, S. L. & STRAHL, B. D. 2013. Stress-free with Rpd3: a unique chromatin complex mediates the response to oxidative stress. Mol Cell Biol, 33, 3726-7.

MELAMED, D., YOUNG, D. L., GAMBLE, C. E., MILLER, C. R. & FIELDS, S. 2013. Deep mutational scanning of an RRM domain of the Saccharomyces cerevisiae poly(A)-binding protein. *RNA,* 19**,** 1537-51.

MILLAR, C. B., XU, F., ZHANG, K. & GRUNSTEIN, M. 2006. Acetylation of H2AZ Lys 14 is associated with genome-wide gene activity in yeast. *Genes Dev,* 20**,** 711-22.

Missense3D Portal. Missense3D, http://missense3d.bc.ic.ac.uk/.

MITCHELL, L., HUARD, S., COTRUT, M., POURHANIFEH-LEMERI, R., STEUNOU, A. L., HAMZA, A., LAMBERT, J. P., ZHOU, H., NING, Z., BASU, A., COTE, J., FIGEYS, D. A. & BAETZ, K. 2013. mChIP-KAT-MS, a method to map protein interactions and acetylation sites for lysine acetyltransferases. *Proc Natl Acad Sci U S A,* 110**,** E1641-50.

MITCHELL, L., LAMBERT, J. P., GERDES, M., AL-MADHOUN, A. S., SKERJANC, I. S., FIGEYS, D. & BAETZ, K. 2008. Functional dissection of the NuA4 histone acetyltransferase reveals its role as a genetic hub and that Eaf1 is essential for complex integrity. *Mol Cell Biol,* 28**,** 2244-56.

MOKAS, S., MILLS, J. R., GARREAU, C., FOURNIER, M. J., ROBERT, F., ARYA, P., KAUFMAN, R. J., PELLETIER, J. & MAZROUI, R. 2009. Uncoupling stress granule assembly and translation initiation inhibition. *Molecular biology of the cell,* 20**,** 2673-83.

MOLLET, S., COUGOT, N., WILCZYNSKA, A., DAUTRY, F., KRESS, M., BERTRAND, E. & WEIL, D. 2008. Translationally repressed mRNA transiently cycles through stress granules during stress. *Molecular biology of the cell,* 19**,** 4469-79.

MULLIN, C., DUNING, K., BARNEKOW, A., RICHTER, D., KREMERSKOTHEN, J. & MOHR, E. 2004. Interaction of rat poly(A)-binding protein with poly(A)- and non-poly(A) sequences is preferentially mediated by RNA recognition motifs 3+4. *FEBS Lett,* 576**,** 437-41.

NAKAJIMA, E., SHIMAJI, K., UMEGAWACHI, T., TOMIDA, S., YOSHIDA, H., YOSHIMOTO, N., IZAWA, S., KIMURA, H. & YAMAGUCHI, M. 2016. The Histone Deacetylase Gene Rpd3 Is Required for Starvation Stress Resistance. *PLoS One,* 11**,** e0167554.

NAMKOONG, S., HO, A., WOO, Y. M., KWAK, H. & LEE, J. H. 2018. Systematic Characterization of Stress-Induced RNA Granulation. *Mol Cell,* 70**,** 175-187 e8.

NONHOFF, U., RALSER, M., WELZEL, F., PICCINI, I., BALZEREIT, D., YASPO, M. L., LEHRACH, H. & KROBITSCH, S. 2007. Ataxin-2 interacts with the DEAD/H-box RNA helicase DDX6 and interferes with P-bodies and stress granules. Molecular biology of the cell, 18, 1385-96.

NOTT, T. J., PETSALAKI, E., FARBER, P., JERVIS, D., FUSSNER, E., PLOCHOWIETZ, A., CRAGGS, T. D., BAZETT-JONES, D. P., PAWSON, T., FORMAN-KAY, J. D. &

BALDWIN, A. J. 2015. Phase transition of a disordered nuage protein generates environmentally responsive membraneless organelles. *Mol Cell,* 57**,** 936-947.

NOVER, L., SCHARF, K. D. & NEUMANN, D. 1983. Formation of cytoplasmic heat shock granules in tomato cell cultures and leaves. *Mol Cell Biol,* 3**,** 1648-55.

OHN, T., KEDERSHA, N., HICKMAN, T., TISDALE, S. & ANDERSON, P. 2008. A functional RNAi screen links O-GlcNAc modification of ribosomal proteins to stress granule and processing body assembly. *Nat Cell Biol,* 10**,** 1224-31.

OHSHIMA, D., ARIMOTO-MATSUZAKI, K., TOMIDA, T., TAKEKAWA, M. & ICHIKAWA, K. 2015. Spatio-temporal Dynamics and Mechanisms of Stress Granule Assembly. *PLoS Comput Biol,* 11**,** e1004326. DOI: 10.1371/journal.pcbi.1004326

OLIVER, S. S. & DENU, J. M. 2011. Disrupting the reader of histone language. *Angew Chem Int Ed Engl,* 50**,** 5801-3.

PESERICO, A. & SIMONE, C. 2011. Physical and functional HAT/HDAC interplay regulates protein acetylation balance. *J Biomed Biotechnol,* 2011**,** 371832.

PINSKAYA, M. & MORILLON, A. 2009. Histone H3 lysine 4 di-methylation: a novel mark for transcriptional fidelity? Epigenetics, 4, 302-6.

POLEVODA, B. & SHERMAN, F. 2002. The diversity of acetylated proteins. Genome Biol, 3, reviews0006.

PROTTER, D. S. W. & PARKER, R. 2016. Principles and Properties of Stress Granules. *Trends Cell Biol,* 26**,** 668-679.

RAMASWAMI, M., TAYLOR, J. P. & PARKER, R. 2013. Altered ribostasis: RNA-protein granules in degenerative disorders. *Cell,* 154**,** 727-36.

ROLLINS, M., HUARD, S., MORETTIN, A., TAKUSKI, J., PHAM, T. T., FULLERTON, M. D., COTE, J. & BAETZ, K. 2017. Lysine acetyltransferase NuA4 and acetyl-CoA regulate glucose-deprived stress granule formation in Saccharomyces cerevisiae. *PLoS Genet,* 13**,** e1006626. DOI: 10.1371/journal.pgen.1006626

ROSSETTO, D., CRAMET, M., WANG, A. Y., STEUNOU, A. L., LACOSTE, N., SCHULZE, J. M., COTE, V., MONNET-SAKSOUK, J., PIQUET, S., NOURANI, A., KOBOR, M. S. & COTE, J. 2014. Eaf5/7/3 form a functionally independent NuA4 submodule linked to RNA polymerase II-coupled nucleosome recycling. *EMBO J,* 33**,** 1397-415.

ROTH, S. Y., DENU, J. M. & ALLIS, C. D. 2001. Histone acetyltransferases. *Annu Rev Biochem,* 70**,** 81-120.

RUIZ-ROIG, C., VIEITEZ, C., POSAS, F. & DE NADAL, E. 2010. The Rpd3L HDAC complex is essential for the heat stress response in yeast. Mol Microbiol, 76, 1049-

SACHS, A. B., DAVIS, R. W. & KORNBERG, R. D. 1987. A single domain of yeast poly(A)-binding protein is necessary and sufficient for RNA binding and cell viability. *Mol Cell Biol,* 7**,** 3268-76.

SACHS, A. B., SARNOW, P. & HENTZE, M. W. 1997. Starting at the beginning, middle, and end: translation initiation in eukaryotes. *Cell,* 89**,** 831-8.

SADOUL, K., WANG, J., DIAGOURAGA, B. & KHOCHBIN, S. 2011. The tale of protein lysine acetylation in the cytoplasm. *J Biomed Biotechnol,* 2011**,** 970382. DOI: 10.1155/2011/970382

SAFAEE, N., KOZLOV, G., NORONHAM, A, M., XIE, J., WILDS, C, J., GEHRING, K. (2012). Interdomain allostery promotes assembly of the poly(A) mRNA complex with PABP and eIF4G. Mol Cell Biol, 48, 375-86

SCHOLES, D. T., BANERJEE, M., BOWEN, B. & CURCIO, M. J. 2001. Multiple regulators of Ty1 transposition in Saccharomyces cerevisiae have conserved roles in genome maintenance. *Genetics,* 159**,** 1449-65.

SHAH, K. H., ZHANG, B., RAMACHANDRAN, V. & HERMAN, P. K. 2013. Processing body and stress granule assembly occur by independent and differentially regulated pathways in Saccharomyces cerevisiae. Genetics, 193, 109-23.

SHETH, U. & PARKER, R. 2003. Decapping and decay of messenger RNA occur in cytoplasmic processing bodies. Science, 300, 805-8.

SHORE, D. 2000. The Sir2 protein family: A novel deacetylase for gene silencing and more. Proc Natl Acad Sci U S A, 97, 14030-2.

SIFT. StackPath, https://sift.bii.a-star.edu.sg/.

SMITH, E. R., EISEN, A., GU, W., SATTAH, M., PANNUTI, A., ZHOU, J., COOK, R. G., LUCCHESI, J. C. & ALLIS, C. D. 1998. ESA1 is a histone acetyltransferase that is essential for growth in yeast. *Proc Natl Acad Sci U S A,* 95**,** 3561-5.

SMITH, J. S., AVALOS, J., CELIC, I., MUHAMMAD, S., WOLBERGER, C. & BOEKE, J. D. 2002. SIR2 family of NAD(+)-dependent protein deacetylases. *Methods Enzymol,* 353**,** 282-300.

SOLOMON, S., XU, Y., WANG, B., DAVID, M. D., SCHUBERT, P., KENNEDY, D. & SCHRADER, J. W. 2007. Distinct structural features of caprin-1 mediate its interaction with G3BP-1 and its induction of phosphorylation of eukaryotic translation initiation factor 2alpha, entry to cytoplasmic stress granules, and selective interaction with a subset of mRNAs. *Mol Cell Biol,* 27**,** 2324-42.

SONENBERG, N. & HINNEBUSCH, A. G. 2009. Regulation of translation initiation in eukaryotes: mechanisms and biological targets. *Cell,* 136**,** 731-45.

SQUATRITO, M., GORRINI, C. & AMATI, B. 2006. Tip60 in DNA damage response and growth control: many tricks in one HAT. *Trends Cell Biol,* 16**,** 433-42.

STEGER, D. J., EBERHARTER, A., JOHN, S., GRANT, P. A. & WORKMAN, J. L. 1998. Purified histone acetyltransferase complexes stimulate HIV-1 transcription from preassembled nucleosomal arrays. *Proc Natl Acad Sci U S A,* 95**,** 12924-9.

STEUNOU, A. L., CRAMET, M., ROSSETTO, D., ARISTIZABAL, M. J., LACOSTE, N., DROUIN, S., COTE, V., PAQUET, E., UTLEY, R. T., KROGAN, N., ROBERT, F., KOBOR, M. S. & COTE, J. 2016. Combined Action of Histone Reader Modules Regulates NuA4 Local Acetyltransferase Function but Not Its Recruitment on the Genome. *Mol Cell Biol,* 36**,** 2768-2781.

STOECKLIN, G. & KEDERSHA, N. 2013. Relationship of GW/P-bodies with stress granules. *Adv Exp Med Biol,* 768**,** 197-211.

SWISHER, K. D. & PARKER, R. 2010. Localization to, and effects of Pbp1, Pbp4, Lsm12, Dhh1, and Pab1 on stress granules in Saccharomyces cerevisiae. *PLoS One,* 5**,** e10006. DO1: 10.1371/journal.pone.0010006

TAKAHARA, T. & MAEDA, T. 2012. Transient sequestration of TORC1 into stress granules during heat stress. Mol Cell, 47, 242-52.

TAKECHI, S. & NAKAYAMA, T. 1999. Sas3 is a histone acetyltransferase and requires a zinc finger motif. *Biochem Biophys Res Commun,* 266**,** 405-10.

TARUN, S. Z., JR., WELLS, S. E., DEARDORFF, J. A. & SACHS, A. B. 1997. Translation initiation factor eIF4G mediates in vitro poly(A) tail-dependent translation. Proc Natl Acad Sci U S A, 94, 9046-51.

THEDIECK, K., HOLZWARTH, B., PRENTZELL, M. T., BOEHLKE, C., KLASENER, K., RUF, S., SONNTAG, A. G., MAERZ, L., GRELLSCHEID, S. N., KREMMER, E., NITSCHKE, R., KUEHN, E. W., JONKER, J. W., GROEN, A. K., RETH, M., HALL, M. N. & BAUMEISTER, R. 2013. Inhibition of mTORC1 by astrin and stress granules prevents apoptosis in cancer cells. *Cell,* 154**,** 859-74.

TOTH, A., CIOSK, R., UHLMANN, F., GALOVA, M., SCHLEIFFER, A. & NASMYTH, K. 1999. Yeast cohesin complex requires a conserved protein, Eco1p(Ctf7), to establish cohesion between sister chromatids during DNA replication. *Genes Dev,* 13**,** 320-33.

TOURRIERE, H., CHEBLI, K., ZEKRI, L., COURSELAUD, B., BLANCHARD, J. M., BERTRAND, E. & TAZI, J. 2003. The RasGAP-associated endoribonuclease G3BP assembles stress granules. *J Cell Biol,* 160**,** 823-31.

TOURRIERE, H., GALLOUZI, I. E., CHEBLI, K., CAPONY, J. P., MOUAIKEL, J., VAN DER GEER, P. & TAZI, J. 2001. RasGAP-associated endoribonuclease G3Bp: selective RNA degradation and phosphorylation-dependent localization. *Mol Cell Biol,* 21**,** 7747-60.

T Test Calculator. GraphPad, http://www.graphpad.com/quickcalcs/ttest1/?Format=SD%29.
VAN DEN ENDE, W. 2013. Multifunctional fructans and raffinose family oligosaccharides. *Front Plant Sci,* 4**,** 247.

VAN TREECK, B., PROTTER, D. S. W., MATHENY, T., KHONG, A., LINK, C. D. & PARKER, R. 2018. RNA self-assembly contributes to stress granule formation and defining the stress granule transcriptome. *Proc Natl Acad Sci U S A,* 115**,** 2734-2739.

WANG, J., CHOI, J. M., HOLEHOUSE, A. S., LEE, H. O., ZHANG, X., JAHNEL, M., MAHARANA, S., LEMAITRE, R., POZNIAKOVSKY, A., DRECHSEL, D., POSER, I., PAPPU, R. V., ALBERTI, S. & HYMAN, A. A. 2018. A Molecular Grammar Governing the Driving Forces for Phase Separation of Prion-like RNA Binding Proteins. *Cell,* 174**,** 688-699 e16.

WEBSTER, M. W., CHEN, Y. H., STOWELL, J. A. W., ALHUSAINI, N., SWEET, T., GRAVELEY, B. R., COLLER, J. & PASSMORE, L. A. 2018. mRNA Deadenylation Is Coupled to Translation Rates by the Differential Activities of Ccr4-Not Nucleases. *Mol Cell,* 70**,** 1089-1100 e8.

WEK, R. C., JIANG, H. Y. & ANTHONY, T. G. 2006. Coping with stress: eIF2 kinases and translational control. *Biochem Soc Trans,* 34**,** 7-11.

WELLS, S. E., HILLNER, P. E., VALE, R. D. & SACHS, A. B. 1998. Circularization of mRNA by eukaryotic translation initiation factors. Mol Cell, 2, 135-40.

WHEELER, J. R., MATHENY, T., JAIN, S., ABRISCH, R. & PARKER, R. 2016. Distinct stages in stress granule assembly and disassembly. *Elife,* 5. DOI: 10.7554/eLife.18413

WIEDNER, H. J. & GIUDICE, J. 2021. It's not just a phase: function and characteristics of RNA-binding proteins in phase separation. Nat Struct Mol Biol, 28, 465-473.

WITTSCHIEBEN, B. O., OTERO, G., DE BIZEMONT, T., FELLOWS, J., ERDJUMENT-BROMAGE, H., OHBA, R., LI, Y., ALLIS, C. D., TEMPST, P. & SVEJSTRUP, J. Q. 1999. A novel histone acetyltransferase is an integral subunit of elongating RNA polymerase II holoenzyme. *Mol Cell,* 4**,** 123-8.

WRIGHT, P. E. & DYSON, H. J. 2015. Intrinsically disordered proteins in cellular signalling and regulation. *Nat Rev Mol Cell Biol,* 16**,** 18-29.

XIONG, Y. & GUAN, K. L. 2012. Mechanistic insights into the regulation of metabolic enzymes by acetylation. *J Cell Biol,* 198**,** 155-64.

YANG, X., SHEN, Y., GARRE, E., HAO, X., KRUMLINDE, D., CVIJOVIC, M., ARENS, C., NYSTROM, T., LIU, B. & SUNNERHAGEN, P. 2014. Stress granule-defective mutants deregulate stress responsive transcripts. *PLoS Genet,* 10**,** e1004763. DOI: 10.1371/journal/pgen.1004763

YANG, X. J. & SETO, E. 2008. Lysine acetylation: codified crosstalk with other posttranslational modifications. *Mol Cell,* 31**,** 449-61.

YAO, G., CHIANG, Y. C., ZHANG, C., LEE, D. J., LAUE, T. M. & DENIS, C. L. 2007. PAB1 self-association precludes its binding to poly(A), thereby accelerating CCR4 deadenylation in vivo. *Mol Cell Biol,* 27**,** 6243-53.

YI, C., MA, M., RAN, L., ZHENG, J., TONG, J., ZHU, J., MA, C., SUN, Y., ZHANG, S., FENG, W., ZHU, L., LE, Y., GONG, X., YAN, X., HONG, B., JIANG, F. J., XIE, Z., MIAO, D., DENG, H. & YU, L. 2012. Function and molecular mechanism of acetylation in autophagy regulation. *Science,* 336**,** 474-7.

YOUN, J. Y., DYAKOV, B. J. A., ZHANG, J., KNIGHT, J. D. R., VERNON, R. M., FORMAN-KAY, J. D. & GINGRAS, A. C. 2019. Properties of Stress Granule and P-Body Proteomes. *Mol Cell,* 76**,** 286-294.

YOUNG, D. L. (2016). High throughput determination of sequence-function relationships in protein and RNA. Retrieved from University of Washington

ZHANG, C., LEE, D. J., CHIANG, Y. C., RICHARDSON, R., PARK, S., WANG, X., LAUE, T. M. & DENIS, C. L. 2013. The RRM1 domain of the poly(A)-binding protein from Saccharomyces cerevisiae is critical to control of mRNA deadenylation. *Mol Genet Genomics,* 288**,** 401-12.

7.0 Contributions/Collaborations

GenScript transformed desired Pab1 constructs into pGEX-4T-1 vectors for EMSA assays. Blais Lab (University of Ottawa) helped perform EMSA.

8.0 Appendices

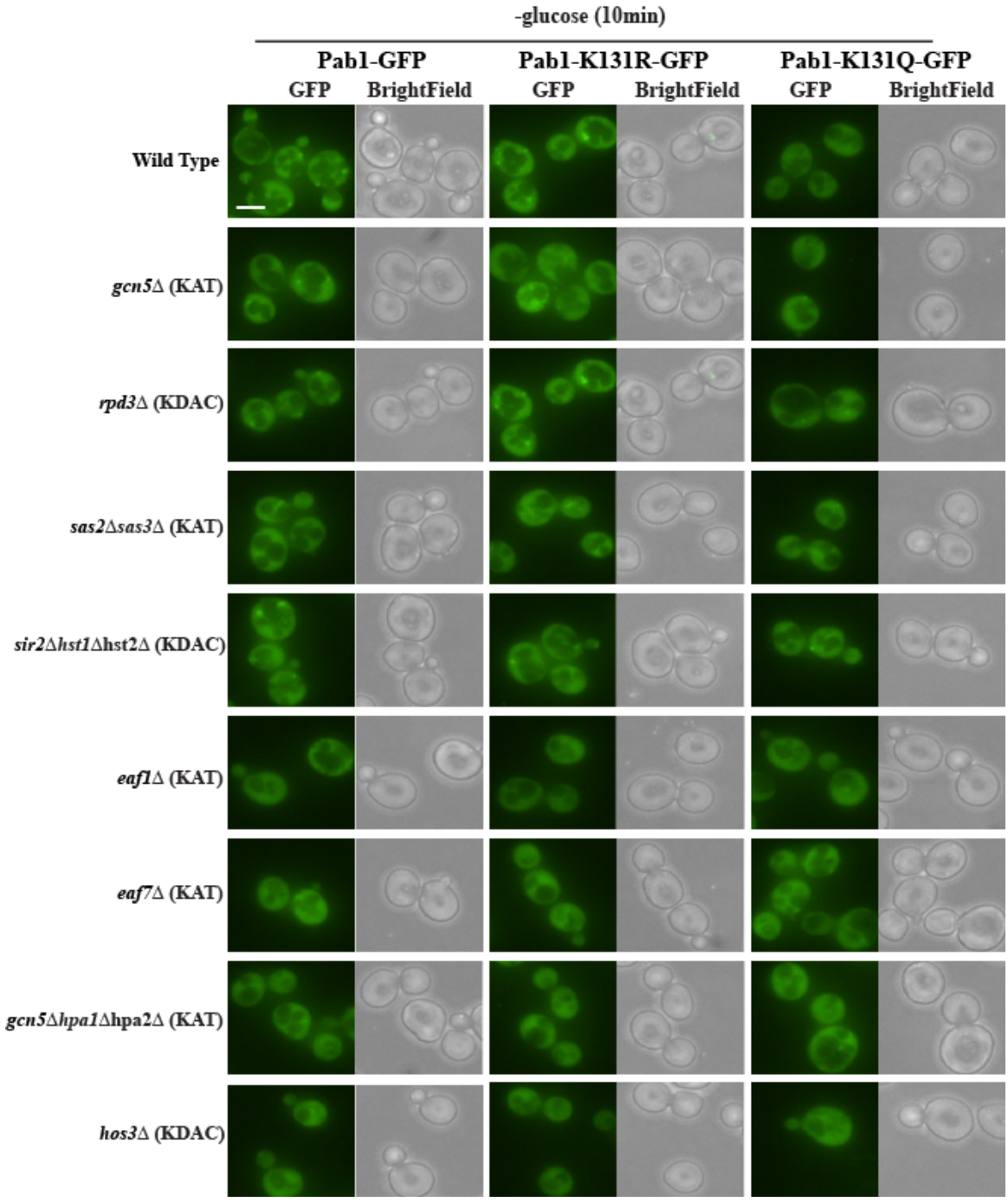

Supplemental Figure 1*: Microscopy pictures of KAT/KDAC mutants upon glucose depleted condition.* Cultures of Wild Type (*PAB1-GFP* (YKB3114); *PAB1-K131R-GFP* (YKB4395); *PAB1-K131Q-GFP* (YKB4396), *gcn5Δ PAB1-GFP* (YKB4177)*, gcn5Δ PAB1-K131R-GFP* (YKB4178), *gcn5Δ PAB1-K131Q-GFP* (YKB4179), *rpd3Δ PAB1-GFP* (YKB4180), *rpd3Δ PAB1-K131R-GFP* (YKB4181), *rpd3Δ PAB1-K131Q-GFP* (YKB4182), *sas2Δsas3Δ PAB1-GFP* (YKB4161), *sas2Δsas3Δ PAB1-K131R-GFP* (YKB4162), *sas2Δsas3Δ PAB1-K131Q-GFP* (YKB4163), *sir2Δhst1Δhst2Δ PAB1-GFP*

(YKB4166), *sir2Δhst1Δhst2Δ PAB1-K131R-GFP* (YKB4167), *sir2Δhst1Δhst2Δ PAB1-K131Q-GFP* (YKB4168), *eaf1Δ PAB1-GFP* (YKB4175), *eaf1Δ PAB1-K131R-GFP (*YKB4964), *eaf1Δ PAB1-K131Q-GFP* (YKB4965), *eaf7Δ PAB1-GFP* (YKB4969), *eaf7Δ PAB1-K131R-GFP* (YKB4970), *eaf7Δ PAB1-K131Q-GFP* (YKB4971), *gcn5Δhpa2Δhpa3Δ PAB1-GFP* (YKB4172), *gcn5Δhpa2Δhpa3Δ PAB1-K131R-GFP* (YKB4173), *gcn5Δhpa2Δhpa3Δ PAB1-K131Q-GFP* (YKB4174), *hos3Δ PAB1-GFP* (YKB4966), *hos3Δ PAB1-K131R-GFP* (YKB4967), *hos3Δ PAB1-K131Q-GFP* (YKB4968) were treated in SC-URA media for 10 minutes. Representative brightfield and fluorescent images after 30-minutes of treatment. Scale bar represents 10μm.

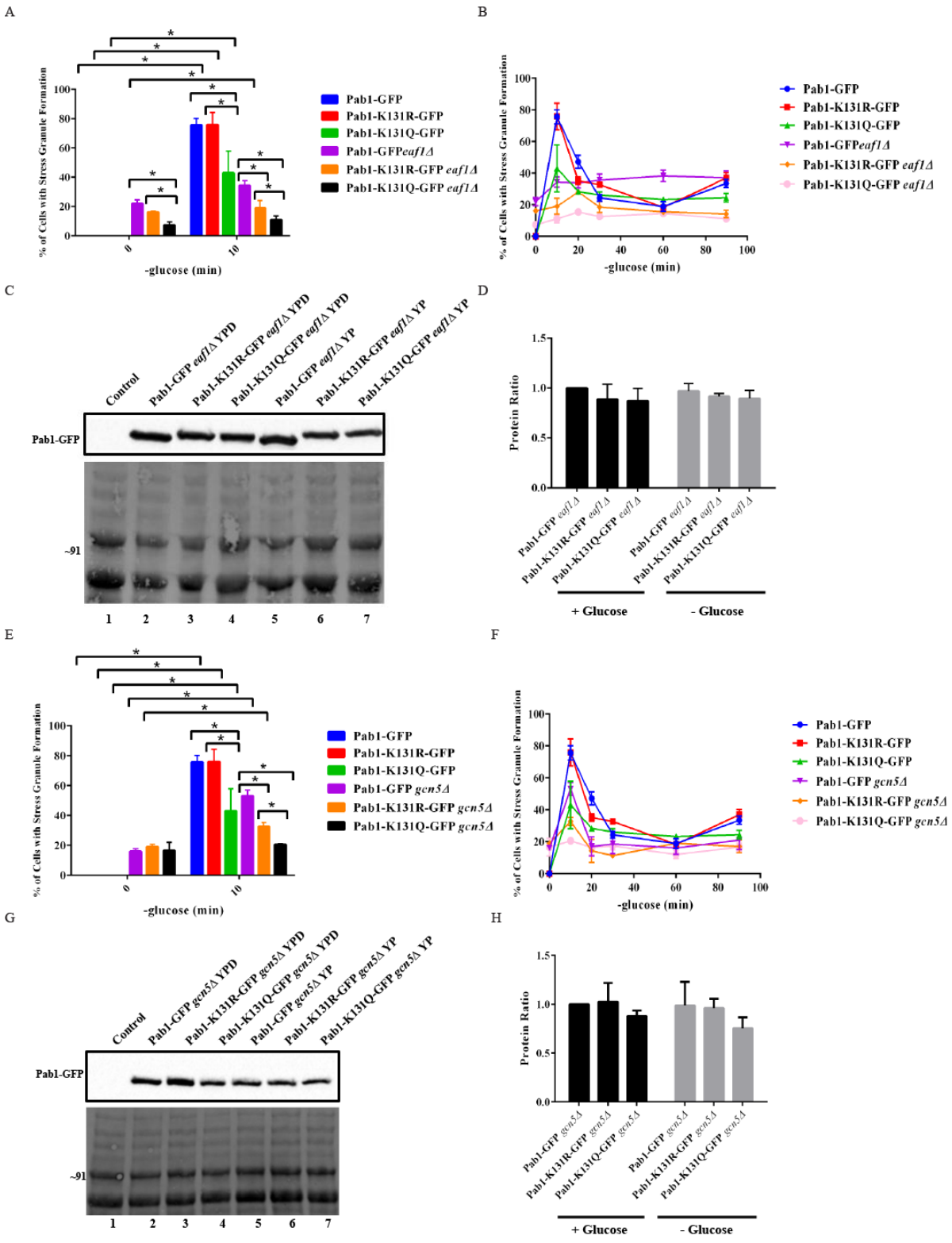

Supplemental Figure 2: *eaf1Δ and gcn5Δ does not affect stress granule formation upon K131 acetylation.* A) Quantitative analyses on the stress granule formation of 0-, 10 min of glucose deprivation in *eaf1Δ PAB1-GFP* (YKB5136), *eaf1Δ PAB1-K131R-GFP (*YKB5137), and *eaf1Δ PAB1-*

K131Q-GFP (YKB5138) B) Quantitative analyses on the stress granule formation of 0-, 10-, 20-, 30-, 60-, and 90- min of glucose deprivation in *eaf1Δ PAB1-GFP* (YKB5136), *eaf1Δ PAB1-K131R-GFP (*YKB5137), and *eaf1Δ PAB1-K131Q-GFP* (YKB5138) C) Western blot analysis of wildtype *eaf1Δ* Pab1-GFP (YKB5136), *eaf1Δ* Pab1-K131R-GFP *(*YKB5137), and *eaf1Δ* Pab1-K131Q-GFP (YKB5138) under glucose deprived/replete conditions. Quantitative western blot for *eaf1Δ* proteins visualized on a nitrocellulose membrane. Lane 1 is a negative control. Lane 2, 3, and 4 are strains in glucose replete media. Lane 5, 6, and 7 are strains in glucose deprived media. Representative anti-GFP western blot (top panel) and total protein blot (bottom panel). D) Quantification of western blots for three independent biological replicates where the Pab1-GFP *eaf1Δ* band intensity was normalized to total protein. E) Quantitative analyses on the stress granule formation of 0-, 10 min of glucose deprivation in *gcn5Δ PAB1-GFP* (YKB5139)*, gcn5Δ PAB1-K131R-GFP* (YKB5140), and *gcn5Δ PAB1-K131Q-GFP* (YKB5141). F) Quantitative analyses on the stress granule formation of 0-, 10-, 20-, 30-, 60-, and 90- min of glucose deprivation in *gcn5Δ PAB1-GFP* (YKB5139)*, gcn5Δ PAB1-K131R-GFP* (YKB5140), and *gcn5Δ PAB1-K131Q-GFP* (YKB5141). G) Western blot analysis of wildtype *gcn5Δ* Pab1-GFP (YKB5139)*, gcn5Δ* Pab1-K131R-GFP (YKB5140), and *gcn5Δ* Pab1-K131Q-GFP (YKB5141) under glucose deprived/replete conditions. Quantitative western blot for *gcn5Δ* proteins visualized on a nitrocellulose membrane. Lane 1 is a negative control. Lane 2, 3, and 4 are strains in glucose replete media. Lane 5, 6, and 7 are strains in glucose deprived media. Representative anti-GFP western blot (top panel) and total protein blot (bottom panel). H) Quantification of western blots for three independent biological replicates where the Pab1-GFP *gcn5Δ* band intensity was normalized to total protein. Results are the average of three biological replicates, a minimum of 100 cells per replicate were scored, error bars indicate SEM. *$p<0.05$ determined using a two-way ANOVA test.

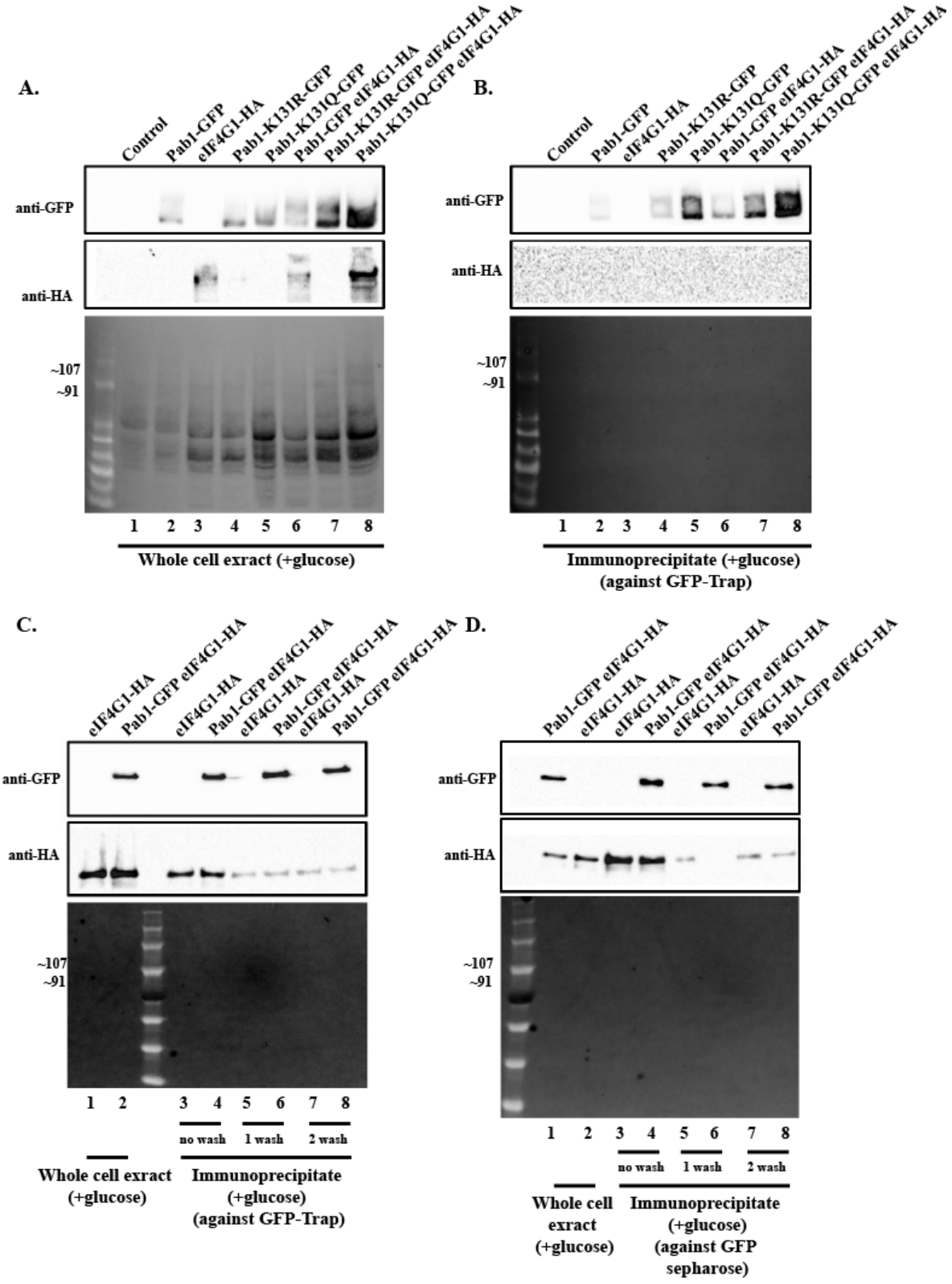

Supplemental Figure 3: *Co-immunoprecipitation's difficulty showing the binding of eIF4G1 to Pab1-K131 mutants.* A) Western blot analysis of whole cell extracts of wildtype Pab1-GFP (YKB3114), eIF4G1-HA (YKB4703), Pab1-K131R-GFP (YKB4395), and Pab1-K131Q-GFP (YKB4396), Pab1-

GFP eIF4G1-HA (YKB4705), Pab1-K131R-GFP eIF4G1-HA (YKB4707), and Pab1-K131Q-GFP eIF4G1-HA (YKB4709) under glucose replete conditions. Quantitative western blot for whole cell extract of proteins visualized on a nitrocellulose membrane. Representative anti-GFP western blot (top panel), anti-HA blot (middle panel), and total protein blot (bottom panel). B) Western blot analysis of immunoprecipitated wildtype Pab1-GFP (YKB3114), eIF4G1-HA (YKB4703), Pab1-K131R-GFP (YKB4395), and Pab1-K131Q-GFP (YKB4396), Pab1-GFP eIF4G1-HA (YKB4705), Pab1-K131R-GFP eIF4G1-HA (YKB4707), and Pab1-K131Q-GFP eIF4G1-HA (YKB4709) under glucose repleted conditions. Quantitative western blot for immunoprecipitated proteins visualized on a nitrocellulose membrane. Representative anti-GFP western blot (top panel), anti-HA blot (middle panel), and total protein blot (bottom panel). Discarded due to no band detection of HA tagged proteins on immunoprecipated blot. C) Western blot analysis of eIF4G1-HA (YKB4703) and Pab1-GFP eIF4G1-HA (YKB4705) under glucose replete conditions, by optimizing for the proteins by changing buffers, volumes, incubation periods. Lane 1 and 2 are whole cell extracts of protein. Lane 3 and 4 proteins were not washed. Lane 5 and 6 proteins were washed once with washing buffer. Lane 7 and 8 were washed twice with washing buffer. Immunoprecipitated proteins were against magnetic GFP beads. Quantitative western blot for proteins visualized on a nitrocellulose membrane. Representative anti-GFP western blot (top panel), anti-HA blot (middle panel), and total protein blot (bottom panel). Discarded due to multiple background noise. D) Western blot analysis of eIF4G1-HA (YKB4703) and Pab1-GFP eIF4G1-HA (YKB4705) under glucose replete conditions, by optimizing for proteins using GFP Sepharose instead of GFP magnetic beads. Lane 1 and 2 are whole cell extracts of protein. Lane 3 and 4 proteins were not washed. Lane 5 and 6 proteins were washed once with washing buffer. Lane 7 and 8 were washed twice with washing buffer. Immunoprecipitated proteins were against GFP Sepharose. Quantitative western blot for proteins visualized on a nitrocellulose membrane. Representative anti-GFP western blot (top panel), anti-HA blot (middle panel), and total protein blot (bottom panel). Discarded due to sticky proteins.

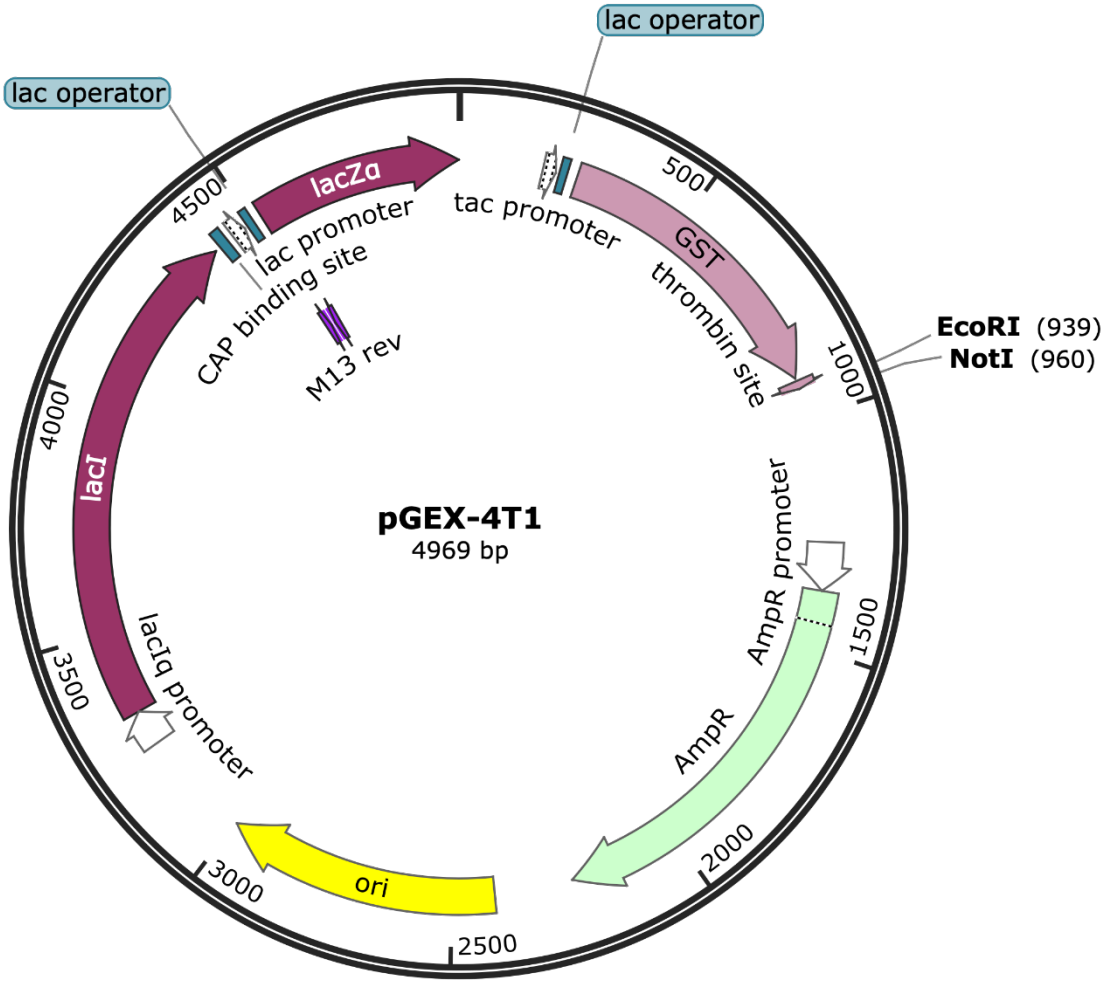

Supplemental Figure 4: *pGEX-4T-1 vector.* Map of pGEX-4T-1 vector used to insert constructs needed for affinity purification and electromobility shift assays.

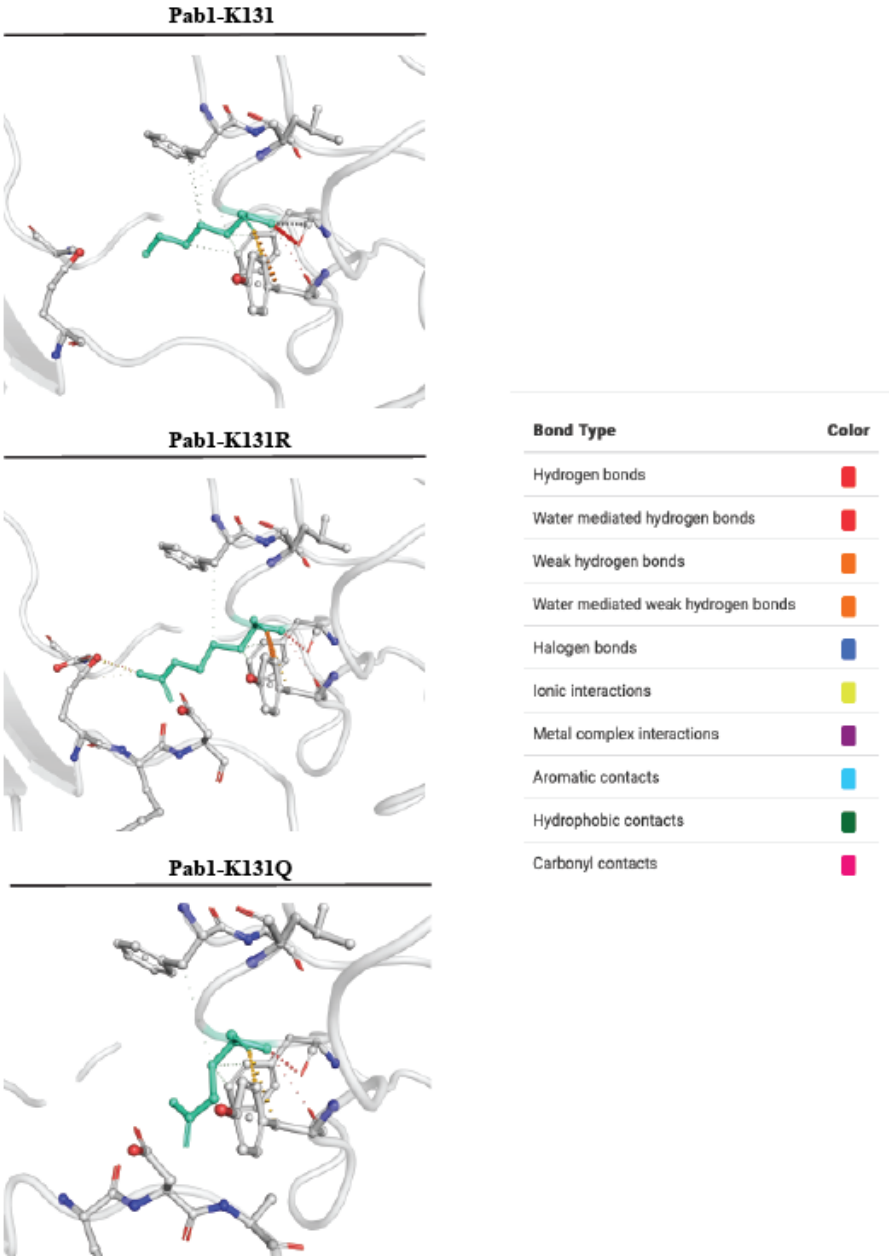

Supplemental Figure 5: *Pab1 and mutants predicted protein structures.* Predicted protein structures from Dynamut (Dynamut: Prediction Submission) of Pab1-K131 (top panel), Pab1-K131R (middle panel), and Pab1-K131Q (bottom panel). Different bonds and interactions are colour coded aligned to the legend on the right.

Table 1: Strains used in this study

Strain	Genotype	Source
YKB1079	MATa his3Δ1leu2Δ0met15Δ0ura3Δ0	Kaern Lab
YKB3114	MATa his3Δ1leu2Δ0met15Δ0ura3Δ0 Pab1-GFP::HIS	This study
YKB4033	MATa his3Δ1leu2Δ0met15Δ0ura3Δ0 Pab1-GFP::URA (WT) *pab1Δ*KAN	This study
YKB4035	MATa his3Δ1leu2Δ0met15Δ0ura3Δ0 Pab1-K131R-GFP::URA *pab1Δ*KAN	This study
YKB4036	MATa his3Δ1leu2Δ0met15Δ0ura3Δ0 Pab1-K131Q-GFP::URA *pab1Δ*KAN	This study
YKB4037	MATa his3Δ1leu2Δ0met15Δ0ura3Δ0 Pab1-K7R-GFP::URA *pab1Δ*KAN	This study
YKB4038	MATa his3Δ1leu2Δ0met15Δ0ura3Δ0 Pab1-K7Q-GFP::URA *pab1Δ*KAN	This study
YKB4039	MATa his3Δ1leu2Δ0met15Δ0ura3Δ0 Pab1-K288R-GFP::URA *pab1Δ*KAN	This study
YKB4040	MATa his3Δ1leu2Δ0met15Δ0ura3Δ0 Pab1-K288R-GFP::URA *pab1Δ*KAN	This study
YKB4041	MATa his3Δ1leu2Δ0met15Δ0ura3Δ0 Pab1-K504R-GFP::URA *pab1Δ*KAN	This study
YKB4042	MATa his3Δ1leu2Δ0met15Δ0ura3Δ0 Pab1-K504Q-GFP::URA *pab1Δ*KAN	This study
YKB4395	MATa his3Δ1leu2Δ0met15Δ0ura3Δ0 Pab1-K131R-GFP::HIS	This study
YKB4396	MATa his3Δ1leu2Δ0met15Δ0ura3Δ0 Pab1-K131Q-GFP::HIS	This study
YKB4969	MATa his3Δ1leu2Δ0met15Δ0ura3Δ0lys2Δ0 Pab1-GFP::HIS *eaf7ΔNAT*	This study
YKB4970	MATa his3Δ1leu2Δ0met15Δ0ura3Δ0lys2Δ0 Pab1-K131R-GFP::HIS *eaf7ΔNAT*	This study
YKB4971	MATa his3Δ1leu2Δ0met15Δ0ura3Δ0lys2Δ0	This study

	Pab1-K131Q-GFP::HIS *eaf7ΔNAT*	
YKB4175	MATa his3Δ1leu2Δ0met15Δ0ura3Δ0 Pab1-GFP::HIS *eaf1ΔNAT*	This study
YKB4965	MATa his3Δ1leu2Δ0met15Δ0ura3Δ0lys2Δ0 Pab1-K131R-GFP::HIS *eaf1ΔNAT*	This study
YKB4964	MATa his3Δ1leu2Δ0met15Δ0ura3Δ0lys2Δ0 Pab1-K131Q-GFP::HIS *eaf1ΔNAT*	This study
YKB4177	MATa his3Δ1leu2Δ0met15Δ0ura3Δ0 Pab1-GFP::HIS *gcn5ΔNAT*	This study
YKB4178	MATa his3Δ1leu2Δ0met15Δ0ura3Δ0 Pab1-K131R-GFP::HIS *gcn5ΔNAT*	This study
YKB4179	MATa his3Δ1leu2Δ0met15Δ0ura3Δ0 Pab1-K131Q-GFP::HIS *gcn5ΔNAT*	This study
YKB4180	MATa his3Δ1leu2Δ0met15Δ0ura3Δ0 Pab1-GFP::HIS *rpd3ΔKAN*	This study
YKB4181	MATa his3Δ1leu2Δ0met15Δ0ura3Δ0 Pab1-K131R-GFP::HIS *rpd3ΔKAN*	This study
YKB4182	MATa his3Δ1leu2Δ0met15Δ0ura3Δ0 Pab1-K131Q-GFP::HIS *rpd3ΔKAN*	This study
YKB4966	MATa his3Δ1leu2Δ0met15Δ0ura3Δ0lys2Δ0 Pab1-GFP::HIS *hos3ΔKAN*	This study
YKB4967	MATa his3Δ1leu2Δ0met15Δ0ura3Δ0lys2Δ0 Pab1-K131R-GFP::HIS *hos3ΔKAN*	This study
YKB4968	MATa his3Δ1leu2Δ0met15Δ0ura3Δ0 Pab1-K131Q-GFP::HIS *hos3ΔKAN*	This study
YKB4161	MATa his3Δ1leu2Δ0met15Δ0ura3Δ0lys2Δ0 Pab1-GFP::HIS *sas2KANΔsas3ΔNAT*	This study
YKB4162	MATa his3Δ1leu2Δ0met15Δ0ura3Δ0 Pab1-K131R-GFP::HIS *sas2ΔKANsas3ΔNAT*	This study
YKB4163	MATa his3Δ1leu2Δ0met15Δ0ura3Δ0 Pab1-K131Q-GFP::HIS *sas2ΔKANsas3ΔNAT*	This study
YKB4172	MATa his3Δ1leu2Δ0met15Δ0ura3Δ0 Pab1-GFP::HIS *gcn5ΔKANhpa2ΔNAThpa3ΔHIS*	This study

YKB4173	MATa his3Δ1leu2Δ0met15Δ0ura3Δ0 Pab1-K131R-GFP::HIS *gcn5ΔKANhpa2ΔNAThpa3ΔHIS*	This study
YKB4174	MATa his3Δ1leu2Δ0met15Δ0ura3Δ0 Pab1-K131Q-GFP::HIS *gcn5ΔKANhpa2ΔNAThpa3ΔHIS*	This study
YKB4166	MATa his3Δ1leu2Δ0met15Δ0ura3Δ0 Pab1-GFP::HIS *sir2ΔKANhst1ΔNAThst2ΔHIS*	This study
YKB4167	MATa his3Δ1leu2Δ0met15Δ0ura3Δ0 Pab1-K131R-GFP::HIS *sir2ΔKANhst1ΔNAThst2ΔHIS*	This study
YKB4168	MATa his3Δ1leu2Δ0met15Δ0ura3Δ0 Pab1-K131Q-GFP::HIS *sir2ΔKANhst1ΔNAThst2ΔHIS*	This study
YKB4703	MATa his3Δ1leu2Δ0met15Δ0ura3Δ0 TIF4631-HA::KAN	This study
YKB5136	MATa his3Δ1leu2Δ0met15Δ0ura3Δ0 Pab1-GFP::HIS *eaf1ΔKAN* (integration)	This study
YKB5137	MATa his3Δ1leu2Δ0met15Δ0ura3Δ0 Pab1-K131R-GFP::HIS *eaf1ΔKAN* (integration)	This study
YKB5138	MATa his3Δ1leu2Δ0met15Δ0ura3Δ0 Pab1-K131Q-GFP::HIS *eaf1ΔKAN* (integration)	This study
YKB5139	MATa his3Δ1leu2Δ0met15Δ0ura3Δ0 Pab1-GFP::HIS *gcn5ΔKAN* (integration)	This study
YKB5140	MATa his3Δ1leu2Δ0met15Δ0ura3Δ0 Pab1-K131R-GFP::HIS *gcn5ΔKAN* (integration)	This study
YKB5141	MATa his3Δ1leu2Δ0met15Δ0ura3Δ0 Pab1-K131Q-GFP::HIS *gcn5ΔKAN* (integration)	This study
YKB5142	MATa his3Δ1leu2Δ0met15Δ0ura3Δ0 Pab1-GFP::HIS *rpd3ΔKAN* (integration)	This study
YKB5143	MATa his3Δ1leu2Δ0met15Δ0ura3Δ0 Pab1-K131R-GFP::HIS *rpd3ΔKAN* (integration)	This study
YKB5144	MATa his3Δ1leu2Δ0met15Δ0ura3Δ0 Pab1-K131Q-GFP::HIS *rpd3ΔKAN* (integration)	This study

Table 2: Plasmids used in this study

Plasmid	Component	Source
PKB6	pFA6-#1 OR BPH841 KANMX6-KO	Longtine Yeast [1998, 14(10):953-61]
PKB5	NATMX6-KO	This study
PKB8	pFA6a-#3 or BPH843 HISMX6-KO	Longtine Yeast [1998, 14(10):953-61]
PKB192	pRP1362	Parker Lab
PKB 11	pFA6a-#7 BPH847 HA Tag	Longtine Yeast [1998, 14(10):953-61]
PKB352	Empty GST vector	Borrowed from Downey Lab
PKB349	pGEX-4T-1	GenScript
PKB350	pGEX-4T-1	GenScript
PKB351	pGEX-4T-1	GenScript

Table 3: Oligonucleotides used in this study

Primer	Sequence	Description	Source
OKB1709	5'TATGTTCAGTGCATTAATGGGAGA AAGTGATGACGAAGAG CGGATCCCCGGGTTAATTAA'3	Forward HA Tag to TIF4631	This Study
OKB1710	5'TCCAAGTGACATTTTCGATAC TTAACATGATCTATTCATGAATTCGA GCTCGTTTAAAC'3	Reverse HA Tag to TIF4631	This Study
OKB2133	5'CAAGAGCTAATATGTTCGACG CATTAATGAATAACGATGGGGACAG TGATCGGATCCCCGGGTTAATTAA'3	Forward HA TAG to TIF4332	This Study
OKB2134	5'ATGAATTAAAAAGGAAAAAGACT AGCTTATCGTTTCTAAAAG AAAATCTTGAATTCGAGCTCGTTTAA AC'3	Reverse HA Tag to TIF4632	This Study
OKB1458	5'CTCCAGTTCCAAGGAAAGAGGTTT CTGTTTTACTTAATAGCGGATCCCCG GGTTAATTAA'3	Forward primer to knockout Pab1	This Study
OKB1460	5'TTCCGCGAAAACTAACATTCTGCC GTTAATAATGAGACCTGAATTCGAG CTC GTTTAAAC'3	Reverse Primer to knockout Pab1	This Study
OKB1456	5'ATGGCTGATATTACTGATAGGACA GCT GAA CAA TTG GAA'3	Forward primer for K7R in Pab1-GFP	This Study
OKB1458	5'TTCCAATTGTTCAGCTGTCCTATCA GTAATATCAGCCAT'3	Reverse primer for K7R in Pab1-GFP	This Study
OKB1455	5'ATGGCTGATATTACTGATCAGACA GCT GAACAATTGGAA'3	Forward primer for K7Q in Pab1-GFP	This Study
OKB1457	5'TTCCAATTGTTCAGCTGTCTGATCA GT AATATCAGCCAT'3	Reverse primer for K7Q in Pab1-GFP	This Study
OKB1594	5'TCTGGTAACATCTTTATCAGG AACTTGCACCCTGATATT'3	Forward primer for Pab1-K131R	This Study
OKB1596	5'AATATCAGGGTGGAAGTTCCT GATAAAGATGTTACCAGA'3	Reverse primer for Pab1-K131R	This Study
OKB1593	5'TCTGGTAACATCTTTATCCAG	Forward primer for	This Study

	AACTTGCACCCTGATATT’3	Pab1-K131Q	
OKB1595	5’AATATCAGGGTGGAAGTTCTGGATAAAGATGTTACCAGA’3	Reverse primer for Pab1-K131Q	This Study
OKB1598	5’TCTGAACTAAATGGAGAAAGGTTATACGTTGGTCGTGCC’3	Forward primer for K228R in Pab1-GFP	This Study
OKB1600	5’GGCACGACCAACGTATAACCTTTCTCCATTTAGTTCAGA’3	Reverse primer for K288Q in Pab1-GFP	This Study
OKB1597	5’TCTGAACTAAATGGAGAACAGTTATACGTTGGTCGTGCC’3	Forward primer for K288Q in Pab1-GFP	This Study
OKB1599	5’GGCACGACCAACGTATAACTGTTCTCCATTTAGTTCAGA’3	Reverse primer for K288Q in Pab1-GFP	This Study
OKB1706	5’AACCAATTTTATCAACAAAGGCAAAGACAAGCTTTGGGT’3	Forward primer for K504R	This Study
OKB1708	5’ACCCAAAGCTTGTCTTTGCCTTTGTTGATAAAATTGGTT’3	Reverse primer for K504R in Pab1-GFP	This Study
OKB1705	5’AACCAATTTTATCAACAACAGCAAAGACAAGCTTTGGGT’3	Forward primer for K504Q in Pab1-GFP	This Study
OKB1707	5’ACCCAAAGCTTGTCTTTGCTGTTGTTGATAAAATTGGTT’3	Reverse primer for K504Q in Pab1-GFP	This Study
OKB2112	5’GCAGTGAAAGATAAATGATCAAGCCTTGTTGTCAATATCAGTTTTAGAGCTAGAAATAGC’3	Forward primer for Pab1-GFP integration (PAM seq #33)	This Study
OKB2109	5’TGATATTGACAACAAGGCTT’3	Reverse primer for Pab1-GFP integration (PAM seq #33)	This Study
OKB262	5’CATACAAAACATTCGTGGCTACAACTCGATATCCGTGCAGCGGATCCCC	Forward primer for *rpd3Δ*KAN	This Study

	GGGTTAATTAA’3		
OKB263	5’TCACATTATTTATATTCGTATATAC TTCCAACTCTTTTTTGAATTCGAGCT CGTTTAAAC’3	Reverse primer for *rpd3Δ*KAN	This Study
OKB1901	5’CAAAAGTCTTCAGTTAACTCAGGT TCGTATTCTACATTAGCGGATCCCCG GGTTAATTAA’3	Forward primer for *gcn5Δ*KAN	This Study
OKB1902	5’TCTTCGAAAGGAATAGTAGCGGAA AAGCTTCTTCTACGCAGAATTCGAG CTCGTTTAAAC’3	Reverse primer for *gcn5Δ*KAN	This Study
OKB982	5’ATTGGAGGCTCCTATTTTCTAGTT GCTTTTTGTTTTCACTCGCAAAAA AAACATGGAGGCCCAGAATACCC’3	Forward primer for *sas2Δ*KAN	This Study
OKB983	5’TATTCTATCCTGAAATACATATGC CATTAAGTTACATCCTGAATAGAT TCCAGTATAGCGACCAGCATTCAC’3	Reverse primer for *sas2Δ*KAN	This Study
OKB1976	5’CTCTCTCTTCTTCCTTCTTCATTAAT TAGTCTCCGTATAA TTTGCAGATACGGATCCCCGGGTTA ATTAA’3	Forward primer for *sas3Δ*NAT	This Study
OKB1977	5’TTAATAATGTTACATGTATATGCTT ATATCCAATATATACCCATCGCCGC GAATTCGAGCTCGTTTAAAC’3	Reverse primer for *sas3Δ*NAT	This Study
OKB2206	5’TCGGTAGACACATTCAAACCATTT TTCCCTCATCGGCACATTAAAGCTGG CGGATCCCCGGGTTAATTAA’3	Forward primer for *sir2Δ*KAN	This Study
OKB2207	5’TGTAAATTGATATTAATTTGGCACT TTTAAATTATTAAATTGCCTTCTACG AATTCGAGCTCGTTTAAAC’3	Reverse primer for *sir2Δ*KAN	This Study
OKB2864	5’ACGAACACTTCTCTTCTTTTTTGTT GTTTTTGTGAGAAAAAAAAATCTAA ACATGGAGGCCCAGAATACCC’3	Forward primer for *hst1Δ*NAT	This Study
OKB2965	5’CTCCCCCTTCTGTGTTTTCTTCTTTT TTTTTTTTTTTTTTTTTTTGGAATCAG TATAGCGACCAGCATTCAC’3	Reverse primer for *hst1Δ*NAT	This Study
OKB1957	5’GCCCGTCACTGAGCTACCAACCAG	Forward primer for	This Study

	ACGTACCGCGATCTCTCCGTGTTTCG CGGATCCCCGGGTTAATTAA'3	*hst2Δ*HIS	
OKB1958	5'AGATGAATAAGGAAAAAAAAAGG GGGACGGAAAACATTGCAACCAACA CAGAATTCGAGCTCTTTAAAC'3	Reverse primer for *hst2Δ*HIS	This Study
OKB220	5'AAAGATTATTTAGAGACATCATAA TCAAAAGTACAGTTTCCGCCTCAAA GACATGGAGGCCCAGAATACCC'3	Forward primer for *eaf1Δ*NAT	This Study
OKB221	5'AGCCTGGTTAAAAAAAAAAAAAG ATCAGTATCGTAAAGTCGTAAAGTT AGGCAGTATAGCGACCAGCATTCAC' 3	Reverse primer for *eaf1Δ*NAT	This Study
OKB1422	5'GGAGTTTATTAGAAGTTGCTAGCT GCTAGTGAAGAAAAGGCGGATCCCC GGGTTAATTAA'3	Forward primer for *eaf7Δ*KAN	This Study
OKB153	5'GGATGAGCGTTTATTATCGCGATC TATATATGAGCAGTGAGAATTCGAG CTCGTTTAAAC'3	Reverse primer for *eaf7Δ*KAN	This Study
OKB973	5'GCTCTTAGTATTTTATATGCCAAG AAAGCAAACAGCCCTTTCTGTGTA GCACATGGAGGCCCAGAATACCC'3	Forward primer for *hpa2Δ*NAT	This Study
OKB974	5'TTTAATTTTTTTTTTTCTATACATCC ATACTACTGAGGTAATTAGTGTTTC AGTATAGCGACCAGCATTCAC'3	Reverse primer for *hpa2Δ*NAT	This Study
OKB2862	5'AGATATTTAAAAGCGGAAAACGG GCATATAAAATAGATGAGTGCAGAC TA CGGATCCCCGGGTTAATTAA'3	Forward primer for *hpa3Δ*HIS	This Study
OKB2863	5'TAGAAGCTAGAGTTATCTCTATAC ACAGTAGTCTACATTACACAGCGGT T GAATTCGAGCTCGTTTAAAC'3	Reverse primer for *hpa3Δ*HIS	This Study
OKB2858	5'TAACGAAAAAAAGGGCTCTGGAA GTAAACAGAGAAATTCGACGATATA ATCGGATCCCCGGGTTAATTAA'3	Forward primer for *hos3Δ*KAN	This Study
OKB2859	5'TATGCGTCACTTCTTTAGTGGGTTC AAGACAACATTATATATGCATTGGT	Reverse primer for *hos3Δ*KAN	This Study

	A GAATTCGAGCTCGTTTAAAC'3		
OKB2970	5'GTGAGCCGCCCAAAAGTCTTCAGT TAACTCAGGTTCGTATTCTACATTAG ACATGGAGGCCCAGAATACCC'3	Forward primer for *gcn5Δ*NAT	This Study
OKB2971	5'ATTTATTTCTTCTTCGAAAGGAATA GTAGCGGAAAAGCTTCTTCTACGCA CAGTATAGCGACCAGCATTCAC'3	Reverse primer for *gcn5Δ*NAT	This Study
OKB2860	5'GTGAGCCGCCCAAAAGTCTTCAGT TAACTCAGGTTCGTATTCTACATTAG C GGATCCCCGGGTTAATTAA'3	Forward primer for *gcn5ΔKAN*	This Study
OK 2861	5'ATTTATTTCTTCTTCGAAAGGAATA GTAGCGGAAAAGCTTCTTCTACGCA GAATTCGAGCTCGTTTAAAC'3	Reverse primer for *gcn5ΔKAN*	This Study
OKB262	5'CATACAAAACATTCGTGGCTACAA CTCGATATCCGTGCAGCGGATCCCC GGGTTAATTAA'3	Forward primer for *rpd3ΔKAN*	This Study
OKB263	5'TCACATTATTTATATTCGTATATAC TTCCAACTCTTTTTTGAATTCGAGCT CGTTTAAAC'3	Reverse primer for *rpd3ΔKAN*	This Study
OKB3055	5'GAATTCATGGCAGATATAACTGAC AAAACAGCTGAACAACTTGAGAACC TGAACATTCAGGATGATCAGAAACA GGCTGCCACGGGTAGCGAATCTCAG AGCGTCGAAAACAGCTCTGCCAGCC TGTACGTTGGTGACCTGGAGCCGTCT GTTTCCGAGGCGCACCTGTACGACA TCTTCAGCCCAATTGGTTCGGTGTCC TCCATCCGTGTTTGTCGTGACGCTAT CACCAAGACCAGCTTGGGCTATGCG TATGTAAATTTTAATGATCACGAAG CTGGTCGCAAGGCGATCGAGCAGTT AAACTACACTCCGATCAAGGGCCGC CTGTGCCGTATTATGTGGTCGCAACG TGACCCGAGCCTGAGAAAAAAGGGC TCAGGTAATATTTTCATCAAAAATCT GCACCCGGATATTGACAACAAGGCG CTCTACGACACCTTTAGTGTGTTTGG TGACATCCTGTCCAGCAAGATTGCA ACGGATGAAAACGGCAAGAGCAAA GGCTTCGGTTTCGTGCACTTTGAAGA	Wild type of Pab1 RRM1-RRM2	Created by GenScript

	AGAGGGCGCAGCGAAAGAGGCGAT CGATGCACTGAACGGCATGTTGCTG AACGGTCAAGAAATTTATGTTGCGC CGCATCTGAGCCGTAAGGAGCGCGA CAGCCAATTGGAGGAAACCAAAGCG CATTATACCAATTTGTACGTGAAAA ACTGAGCGGCCGC'3		
OKB3056	5'GAATTCATGGCAGATATAACTGAC AAAACAGCTGAACAATTGGAGAACC TCAACATCCAGGATGATCAGAAACA GGCAGCTACGGGTTCCGAGAGCCAA AGCGTGGAAAACAGCTCTGCAAGCT TGTACGTGGGTGACCTGGAACCATC CGTTAGCGAAGCGCACCTGTACGAC ATCTTCTCCCCGATCGGCAGCGTCAG CTCGATTCGTGTTTGTCGCGATGCGA TTACCAAGACCAGCCTGGGTTATGC GTATGTGAACTTTAACGATCATGAG GCGGGTAGAAAGGCGATCGAGCAGC TTAACTATACTCCGATTAAAGGTCGC CTGTGCCGCATTATGTGGTCACAGC GTGACCCGTCCTTACGTAAGAAAGG TAGCGGTAATATTTTCATCCGTAATC TGCATCCGGACATCGATAACAAGGC GCTGTACGACACCTTTTCTGTTTTTG GCGACATTCTGTCCAGCAAGATCGC CACCGATGAAAACGGCAAAAGCAA GGGTTTCGGCTTCGTGCACTTTGAAG AGGAAGGCGCTGCTAAAGAGGCGAT TGACGCCTTGAATGGTATGCTGCTG AATGGCCAAGAGATCTACGTTGCAC CGCATTTGTCTCGTAAAGAACGTGA CAGCCAACTGGAGGAAACCAAGGCG CACTATACGAATTTGTACGTCAAAA ACTGAGCGGCCGC'3	Pab1-K131R RRM1-RRM2	Created by GenScript
OKB3057	5'GAATTCATGGCAGATATAACTGAC AAAACAGCTGAACAATTGGAGAACT TGAACATTCAGGATGACCAGAAACA GGCTGCGACTGGTTCGGAGAGCCAA AGCGTGGAAAACAGCAGTGCGAGCC TCTACGTGGGTGACTTGGAGCCGAG CGTTTCCGAAGCCCACCTGTACGAC ATCTTTTCTCCGATTGGTTCTGTAAG CTCCATTCGTGTTTGTCGCGACGCGA	Pab1-K131Q RRM1-RRM2	Created by GenScript

	TTACCAAAACCAGCCTGGGTTATGC ATATGTGAATTTCAACGATCATGAA GCGGGTCGCAAGGCTATCGAACAGT TGAACTATACCCCGATTAAAGGAAG ACTTTGCCGTATTATGTGGTCGCAAC GCGACCCAAGCCTGCGTAAGAAAGG CTCTGGTAACATTTTCATCCAGAATC TGCATCCGGATATCGATAATAAAGC TCTGTACGATACCTTTTCCGTTTTTG GCGACATCCTGAGCTCCAAGATCGC CACGGATGAAAACGGCAAAAGCAA GGGCTTCGGCTTCGTGCACTTTGAAG AGGAGGGTGCAGCGAAGGAGGCCA TCGACGCGCTGAATGGCATGCTGCT GAATGGTCAGGAGATCTATGTTGCA CCGCATCTGAGCCGTAAGGAACGTG ACTCCCAATTAGAGGAAACCAAGGC GCACTACACGAACCTGTACGTCAAA AACTGAGCGGCCGC’3		

9.0 Curriculum Vitae

Sangavi Sivananthan

EDUCATION

2019 - 2021	**MSc. Biochemistry specializing in Human and Molecular Genetics** University of Ottawa Research: Determining the effects of Pab1 acetylation at K131 on stress granule dynamics in Saccharomyces cerevisiae Supervisor: Dr. Kristin Baetz
2016 - 2019	**B.Sc. (Hons.) Human Biology and Psychology** University of Toronto Scarborough Honors Thesis: The effect of background complexity on infants' visual perception Supervisor: Mark Schmuckler
2012 - 2016	**Ontario Secondary School Diploma** Lester B. Pearson Collegiate Institute Specialist High Skill Major – Health and Wellness

AWARDS & SCHOLARSHIPS

2019	University of Ottawa financial support in terms of scholarship ($35,000)
2018	University of Toronto Scarborough Dean's List, Life Sciences and Psychology
2017	University of Toronto Scarborough Dean's List, Life Sciences and Psychology
2016	University of Toronto President's Entrance Scholarship ($2,000) University of Toronto Scarborough
2016	University of Toronto President's Entrance Scholarship ($1,500) – Declined University of Toronto St. George
2016	Pearson's Scholar – 94% Lester B. Pearson CI

AWARDS & SCHOLARSHIPS - Continued

2016	Kinesiology Award Lester B. Pearson CI
2015	Faculty of Medicine - Youth Summer Program Entrance Scholarship ($1,500) University of Toronto St. George
2015	Faculty of Medicine – Youth Summer Program: First Prize Winner University of Toronto St. George
2014	Sunnybrook Hospital Co-op Scholarship ($500) Sunnybrook Hospital
2014	Academic of Excellence in the Dual Credit Program of Trans-Cultural Health Centennial College
2013	Owens-Corning Fiberglass: Runner - Up Prize Lester B. Pearson Collegiate Institut
2012	Level 2 completion in Keyboard Yamaha Music School
2011	Level 1 completion in Keyboard Yamaha Music School

RESEARCH EXPERIENCE

2019 - Present **Master Student**
Faculty of Medicine - Biochemistry
University of Ottawa

Responsibilities: I am working under the supervision of Dr. Baetz and taking the lead role in my own project. I am interested in the formation of stress granules under stressful conditions, as it is seen in both neurodegenerative diseases and various cancers. I work with many tools to achieve my project such as, western blot analysis, fluorescent microscopy, co-immunoprecipitation, dot and binding assays.

RESEARCH EXPERIENCE - Continued

2018 - 2019 **Thesis Student**
Department of Psychology – Infant Laboratory
University of Toronto Scarborough

Responsibilities: I am working under the supervision of Dr. Schmuckler and taking the lead role in a position that would require me to put in at least 20 hours a week. I worked on infants' visual perception research project, specifically researching the effects of background complexity. My role was to recruit participants, experiment, and analyze data. Special tools that I used were Infant Eye Tracker and Blender Animation.

2018 - 2019 **Research Assistant**
Department of Psychology – Music Laboratory
University of Toronto Scarborough

Responsibilities: I assisted Dr. Cirelli with an infants' music cognition research project and that took a critical position that would require me to put in at least 15 hours a week. My specific roles were recruiting participants and assisting in running experiments. Special tool that I used to assist with was Infant Eye Tracker

2017 - 2018 **Research Assistant**
Department of Psychology – Infant Laboratory
University of Toronto Scarborough

Responsibilities: I assisted Dr. Schmuckler with infants' motor, postural, and music cognition research projects. I took on a critical role that would require me to put in at least 15 hours a week. My specific roles are recruiting participants, assisting in running experiments, coding the video-taped sessions, and assisting with the analysis of data. Special tools that I used are GaitRite Mat, Infant's Eye Tracker, and Postural Balance.

Sangavi Sivananthan

VOLUNTEER EXPERIENCE

2017 **Nurse Aid Volunteer**
Mount Sinai Hospital

Responsibilities: Dedicated volunteer committing at least 10 hours a week in the Surgical Oncology Unit. My responsibilities were assisting Nurses and affiliated professionals with patients, and taking urine and blood samples to the laboratory rooms. Knowledge not only obtained by hands-on, but also reading doctors' notes and examining laboratory results.

2017 **Invigilator – Math Kangaroo Contest**
University of Toronto Scarborough

Responsibilities: Assisted in the organization and preparation in a math contest for elementary aged children. Moreover, I also examined the room during the test, and assisted in marking the tests.

2015 - 2017 **Volunteer**
Scarborough General Hospital

Responsibilities: Managed expenses and customers independently with a great deal of responsibility. Excellent skills in entering and organizing data.

2015 **Team Leader - Toronto 2015 Pan Am/Parapan Am Games**
Markham Pan Am Centre

Responsibilities: I had to monitor areas, deliver services, and identify potential issues. Took a lead position that required me to lead, plan, and coordinate a team, including shift debriefs. Excellent problem solving, and accountability skills obtained.

2015 **Co-op Student**
Sunnybrook Hospital

Responsibilities: Dedicated co-op student to learn in the Surgical Oncology Unit as a nurse aide trainee. Shadowed various occupations whom worked on that floor.

Sangavi Sivananthan

WORK EXPERIENCE

2018 - 2019 **Customer Service Manager**
Walmart – Scarborough Town Centre

Responsibilities: Show strong work ethics to various tasks involved in, but not limited to, Cashier, Courtesy Desk, and Self-Check out. Dedicated manager committing at least 20 hours per week. Excellent organization and scheduling skills. Gained tremendous problem-solving skills from dealing with customer complaints and needs.

2017 **Teacher**
TUSGU - Bellamy and Ellesmere location

Responsibilities: Dedicated teacher committing at least 8 hours per week teaching students in grades 1-8 in English and Math. Affective communication, writing, and reading skills obtained.

WORKSHOPS/CERTIFICATES

2018 **Service Host Training**
Walmart – Scarborough Town Centre
Training in emergencies, rules and regulations, equipment usage

2016 **More Feet on the Ground**
University of Toronto Scarborough
Training in how to recognize, respond, and refer students experienced mental health issues

2015 **First Aid / CPR Training**
Workplace Medical Corporation
Standard First Aid and CPR level: HCP
AED Awareness

2015 **Advanced Leaders Challenge**
Lester B. Pearson CI
Training in workplace rights and responsibilities, common workplace hazards, addressing workplace safety, and safety management

2015 **Younger Worker Awareness Program**
Lester B. Pearson CI
Training in health and safety awareness

Sangavi Sivananthan

PRESENTATIONS

Sivananthan, S., Huard, S., Baetz, K. (2020). *Determining the effects of Pab1 acetylation at K131 on stress granule dynamics in Saccharomyces cerevisiae*. Online poster presentation at the 2020 TAGC conference.

Sivananthan, S., & Schmuckler, M. (2019). *The effect of background complexity on 8-, 10-, and 12-month-old infants' visual perception*. Thesis poster presented at the University of Toronto Scarborough, Toronto, Ontario.

Sivananthan, S., Snaith, B., Liang, J. (2019). *Gibberellin-induced Della recognition by the gibberellin receptor GID1*. Research article presented at the University of Toronto Scarborough, Toronto, Ontario.

Sivananthan, S., Abdulla, S., Talukder, L. (2019). *Neural compensation facilitates response inhibition in schizophrenia*. Poster presented at the University of Toronto Scarborough, Toronto, Ontario

Sivananthan, S., Fernandes, B. (2019). *How Coping Mechanism in Pathological Gamblers are Affected in High Stress Situations*. Awareness presentation presented at the University of Toronto Scarborough, Toronto, Ontario.

Sivananthan, S., Mirza, A., Pires, A., Zhang, A., To, M. (2018). *A potential preventative vaccine for HIV-1.* Awareness presentation presented at the University of Toronto Scarborough, Toronto, Ontario.

Sivananthan, S., Chang, Y., Chittambalam, M., Rajkumar, S., Sassaninejad, K., Sattar, I., Zakhary, M. (2018). *Domestication of dogs.* Poster presented at the University of Toronto Scarborough, Toronto, Ontario.

Sivananthan, S., Banik, S., Chen, K., Kananathalingam, A., Rizvi, A., Safaryan, A. (2017). *Caspase-3 Role in long- term depression*. Poster presented at the University of Toronto Scarborough, Toronto, Ontario.

Sivananthan, S. (2015). *The complications of ALS.* Poster presented at the Faculty of Medicine: Youth Summer Program at the University of Toronto St. George, Toronto, Ontario.

Sivananthan, S. (2013). *The effect of acid rain.* Poster presented at the Owens-Corning Fiberglass Symposium at Lester B. Pearson CI, Toronto, Ontario.

MEMBERSHIPS

2017 – 2018	Student member of S.E.E.D.S (Supporting Education, Empowerment, and Development, through Science) for youth education
2017 – 2019	Student member of the Future Black Physicians
2016 – 2019	Student member of the Global Youth Impact
2016 – 2019	Student member of the Psychology and Neuroscience Department Association

COURSE HIGHLIGHTS

Introduction to Epidemiology · Animal Development · Biochemistry · Immunology · Organic Chemistry · Organic Chemistry Laboratory · Animal Physiology · Human Development and Anatomy · Human Development and Anatomy Laboratory · Cell Biology · Molecular Aspects of Cellular and Genetic Processes · Statistics · Life on Earth: Unifying Principles · Life on Earth: Unifying Principles Laboratory · Life of Earth: Form, Function and Interactions · Life on Earth: Form, Function and Interactions Laboratory · Structure and Bonding · Structure and Bonding Laboratory · Reactions and Mechanisms · Reactions and Mechanisms Laboratory · Mitochondrial Medicine: Theory and Approaches · Molecular Biology of Human Diseases